Wind-induced flow noise in headphones

Christopher Haut, Tenzin Sonam Stelljes, Volker Mellert
Oldenburg University

study program Engineering Physics

(condensed version of the Bachelor Thesis of Tenzin Sonam Stelljes, April 2009)

supported by
SENNHEISER

Summary

Wind produces turbulent pressure fluctuations at the human ear, sensed as flow-noise and as (in general low-frequent) pressure fluctuations. Wearing headphones can reduce or enhance this sensation causing an unwanted back-ground noise for the perceived headphone signal. It is investigated how much noise is produced at the ear wearing different head- and earphones while being attacked by wind from about 2 to 8 m/s speed. 12 different models of head- and earphones are measured. The (turbulent and acoustic) pressure is picked up with a calibrated ear-microphone. The experiments are carried out in an acoustic wind tunnel with a dummy head and with test persons. Some preliminary set-ups with simple shielding are tested to reduce flow noise and turbulent pressure fluctuations. The "naked" ear produces already considerable flow noise. Most noise is measured for frontal wind exposure at the highest wind speed applied (about 8 m/s). Increasing the wind speed by approximately 2 m/s in the investigated range of wind velocity causes an increase of flow noise about 5-10 dB. The spectra of all flow noise measurements exhibit a maximum in the frequency range about 60-130 Hz, and then decay continuously to sound pressure levels of 20-30 dB at 20 kHz, which is the noise floor of the measurement set-up in the wind tunnel. Wind-induced tonal components are only observed in one case. The measurements are hampered by the fact that the reference microphone in the ear canal is often overloaded by the turbulent pressure. If possible, measurement sequences are selected for further analyses, in which no overload is noticed or heard. In principle it is not possible to distinguish between acoustic and turbulent pressure in the signal of the ear-microphone.

Content

List of Figures

1 Introductory remark

The following report is the condensed and revised version of the Bachelor Thesis of Tenzin Sonam Stelljes, which was performed with support by the Sennheiser electronic GmbH & Co. KG during the winter term 2008/ 2009 at Oldenburg University, Acoustics Group.

The report is given by Volker Mellert (supervisor of the Thesis of Tenzin Sonam Stelljes). An improved analysis of the measured signals and updated calculation is carried out by Christopher Haut (2nd supervisor of the Thesis).

The investigation was initiated by Sennheiser and aims at an often reported disturbance when wearing headphones outdoors: When listening to music via headphones, e.g. during leisure time in a windy area or while riding a bike the acoustic output is disturbed by flow noise and turbulent pressure fluctuations induced by the wind. The noise is generated by the air flow around the head, the outer ear and possibly the hardware of the headphone. The noise and the pressure fluctuations can reduce the dynamic range of or even mask the music or other audio files one is listening to. The aim of the Thesis is to determine magnitude and origin of the wind-generated flow noise for different types of headphones and to derive possible measures for reduction. The flow noise is measured under defined conditions in the acoustic wind tunnel of Oldenburg University with the help of a dummy head and also with real test persons. The flow noise is measured with a small microphone which is placed inside the ear canal.

The updated analysis of the microphone signals measured in the thesis revealed that the microphone was often overloaded by turbulent pressure fluctuations. The original thesis does not differentiate between acoustic and turbulent pressure. Since turbulent pressure reduces also the performance of the headphones some of the spectra from the original thesis are kept in this report, which is notified in the respective figure caption, even if the microphone membrane is overloaded. Christopher Haut identified by aural inspection time series, which show no overload. The updated analysis relates to these time frames. But of course, the microphone signal may still consist of flow-acoustic and of turbulent pressure fluctuations. Both are indistinguishable in the presented measurements.

All general aspects of physics and electroacoustics are dropped from the original Thesis, as these are known for the interested reader. The procedures for the calibration of wind-velocity, the MATLAB scripts for analysis of the measured signals, and photos of the headphones are also dropped from the original. Technical details like the transfer functions of the investigated models of headphones, as well as other subjects of intellectual properties are not included in this excerpt.

2 Introduction

2.1 Types of headphones

The headphones used for the flow-acoustic experiments are divided into four groups. The largest group are the ear buds which are placed in the concha. The second group is defined by supra-aural headphones. They have a soft pad which sits on top of the ear. The third type is a circumaural headphone which sits on the ear by a pad that surrounds the pinna completely. One headphone is designed like a circumaural headphone but is too small to surround the whole ear. For this reason it is counted as a supra-aural headphone. It includes an active noise cancelling mechanism. Only one type of in-ear headphone is investigated with respect to flow noise. Table 1 gives an overview of the investigated headphones.

type	**headphone**
Supra-aural	HD457
	PX100
Supra-aural, noise-canceling	PXC150
Circumaural	EH150
In-ear	CX500
Ear-bud	MXL70
	MXL560
	MX75
	MX260
	MX660
	OMX70
	LX70

Table 1: Sennheiser headphones used for measurements

2.2 Transfer functions

In order to estimate the decrease in performance or even masking effects of wind-induced flow-noise the transfer function of each headphone is measured.

A pseudo-random white noise signal (MLS noise) from a laptop is fed to the headphone, which is fitted on the dummy head. The cross correlation of the white noise and the output of a calibrated in-ear microphone (see next chapter) is measured and transformed by a FFT to the cross power spectral density, or transfer function, and the result is transferred to dB SPL (see Fig. 1).

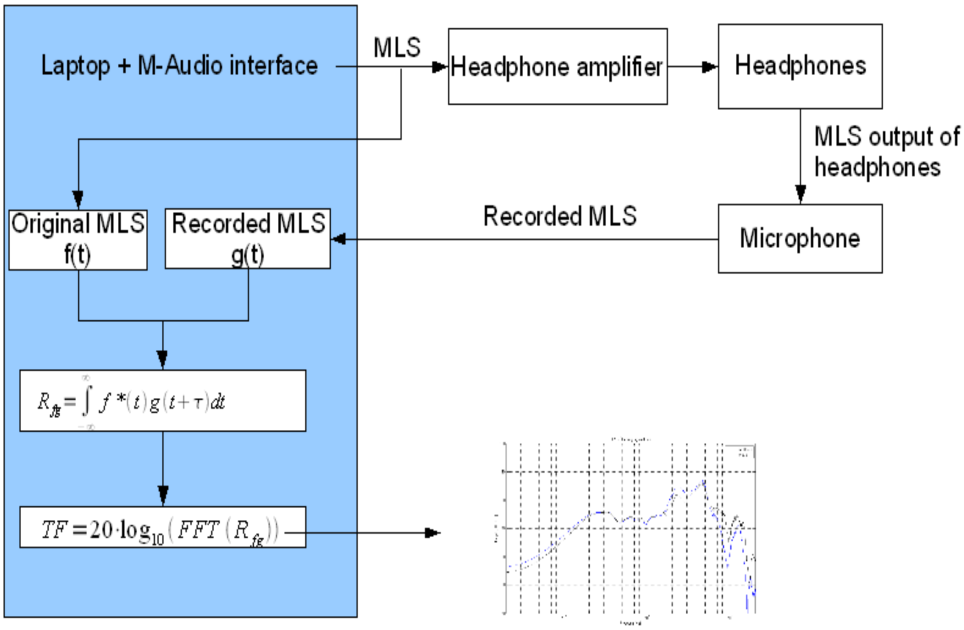

Figure 1: Measurement set-up for determination of the transfer function

The transfer functions are not presented in this report. They serve as reference to estimate the relative contribution of the flow noise compared to the wanted audio signal.

3 Calibration

3.1 Calibration of the measurement system

The measurement system is calibrated to obtain the (absolute) SPL in the ear in the following way. A dummy head with artificial ears is used, which was developed in the acoustic department of Oldenburg University [1], and has anthropomorphic measures collected on a diploma thesis [2]. The dummy head is modified with an ear canal of $3.5 \pm 0.1\,\mathrm{cm}$ length in which a WM61A microphone (Panasonic) is mounted in front of a thin foam absorber modelling the eardrum (Fig. 2).

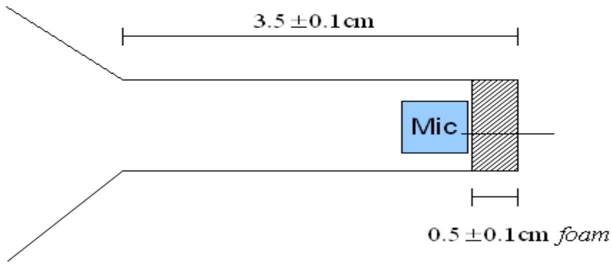

Figure 2: Scheme of ear canal of the dummy head with measurement microphone in front of an "ear drum"

The microphone signal is fed to an USB Audio interface (M-Audio Fast Track Pro) connected to a HP laptop evaluating the signal and plotting its frequency spectrum with a MATLAB script.

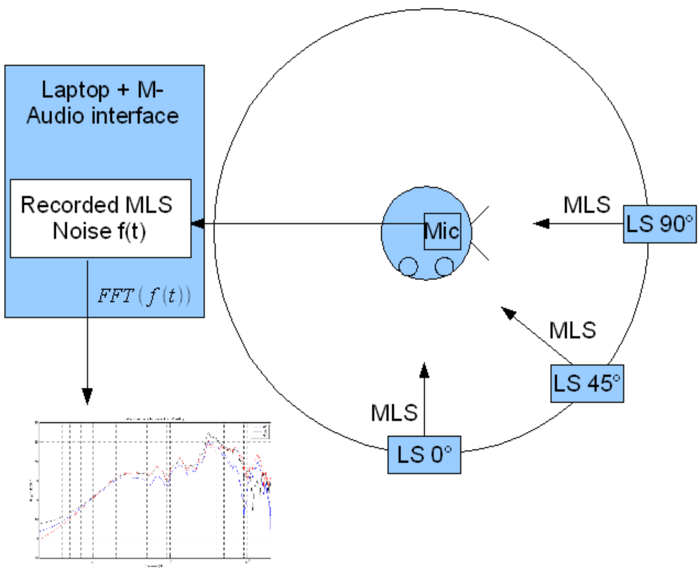

Figure 3: Measurement set-up with dummy head for free-field calibration of the measurement system

The reference measurement is carried out in the anechoic chamber. A MLS noise signal is radiated from a loudspeaker (Manger) at distance of 1.90 m to the dummy head under three different angles of incidence (0°, 45°, 90°) and is recorded with the WM61A ear-microphone, which is also used for the measurements with test subjects later on. Different angles of incidence are chosen because the flow noise at the dummy head is also to be measured under different angles of incidence (see Fig. 3).

The transfer function of the measurement system includes the frequency response of the loudspeaker, the microphone and the dummy head (see Fig. 4). A second reference measurement is done by only measuring the MLS signal with the microphone without the head (see Fig. 5). This transfer function includes the frequency response of the loudspeaker and the microphone. The assumption that the microphone has omnidirectional characteristic implies that one direction of measurement was sufficient. The transfer function in Fig. 5 reflects mainly the frequency characteristic of the loudspeaker as the microphone has nearly a flat frequency response (see Appendix 7.3).

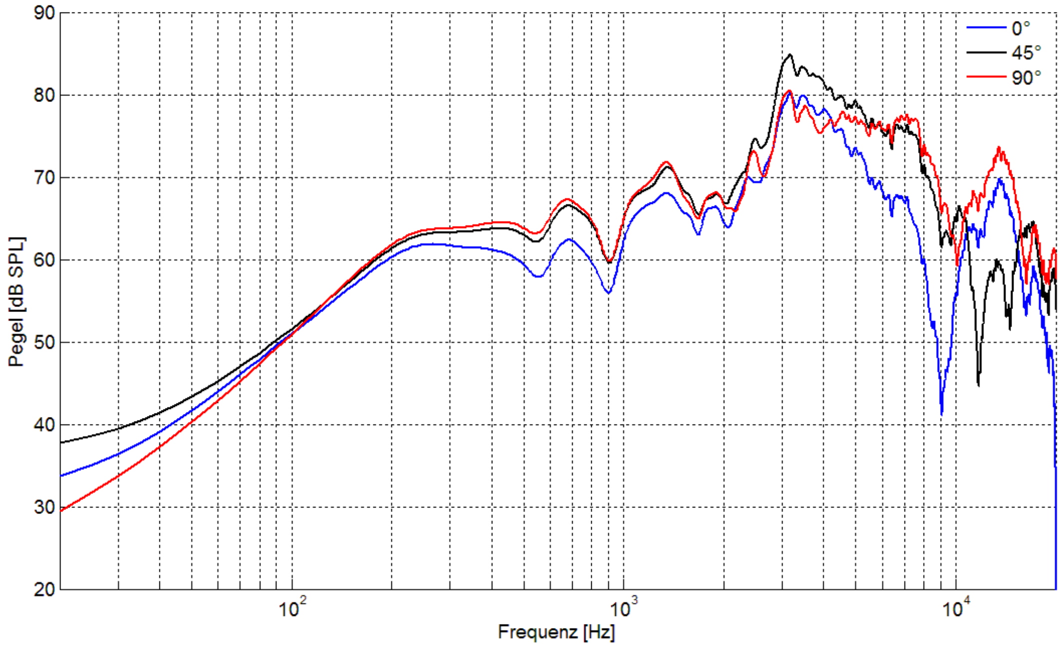

Figure 4: Reference measurement of the measurement system

Comparing Fig. 5 with Fig. 4 shows a different response of the microphone to the MLS-noise at low frequencies, when it is mounted in the ear of the dummy head, compared to the free space condition. The difference is clearly visible from Fig. 6. Differences above about 450 Hz are due to the dummy head and outer-ear diffraction of the sound field. The roll-off below 200 Hz and the fluctuations in the spectrum are caused by the loudspeaker and not the microphone.

The free-field transfer function to the dummy-head ear-microphone shows an additional roll-off at frequencies below about 450 Hz, which is largest at 90° angel of incidence.

The additional low-frequency roll-off of the ear-microphone is due to the arrangement of the microphone at the end of the mimicked ear-canal. In order to compensate for this low-frequency filtering, the difference visible in Fig. 6 is implemented to all measurements as a filter with amplitude characteristic in Fig 7, i.e. after each measurement, the frequency weight of Fig. 7 is simply added to the spectrum of the signal.

All measurements are carried out with a frequency solution of 5 Hz.

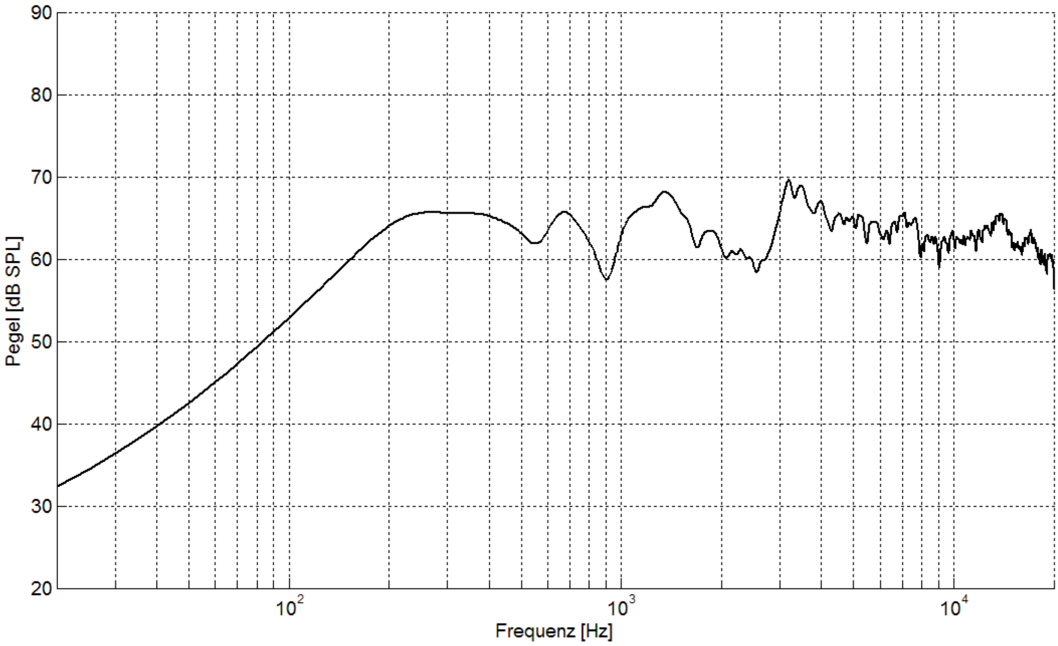

Figure 5: Reference measurement with the microphone alone (without dummy). The transfer function reflects the frequency response of the loudspeaker.

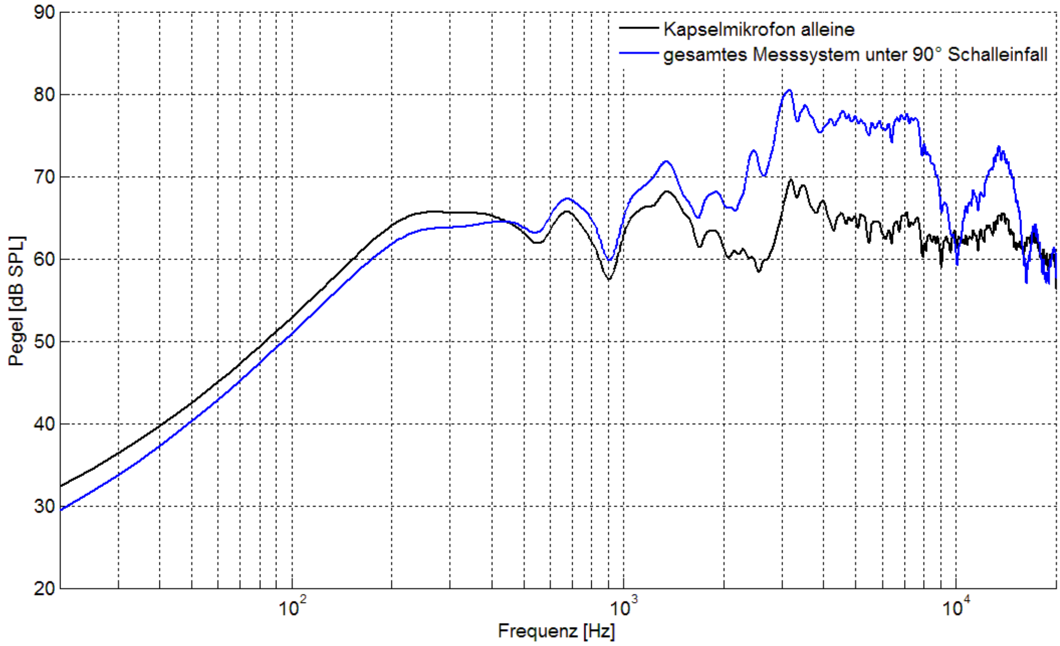

Figure 6: Comparison of microphone in free field alone (Fig. 5) and in ear canal under 90° free-field condition

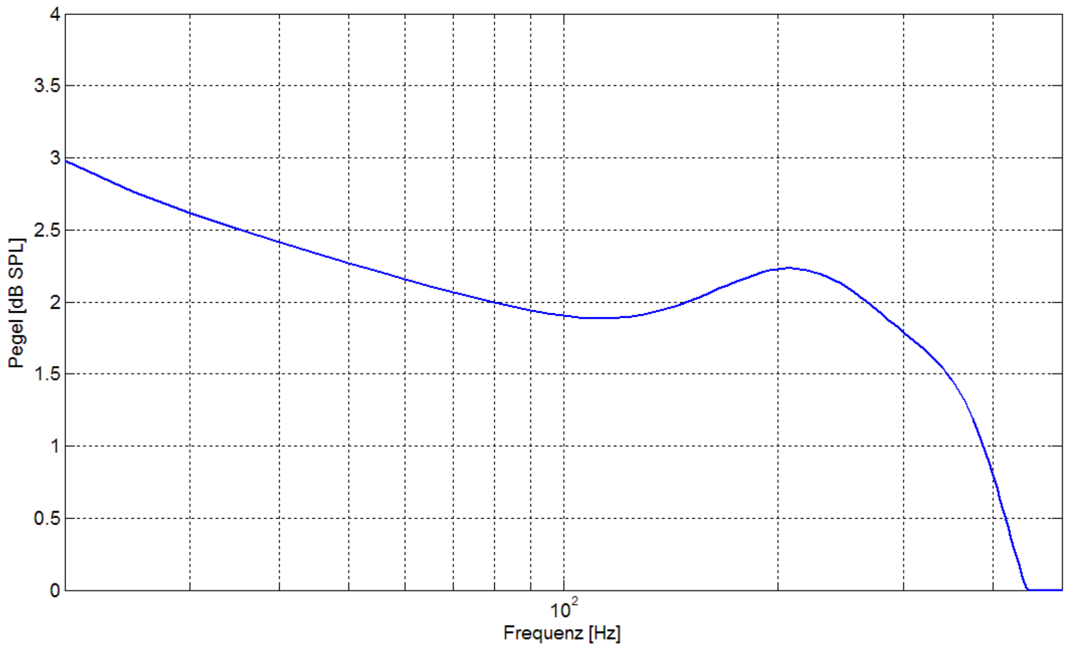

Figure 7: Spectral weighting in the frequency range from 20 Hz to 450 Hz, applied to all measurements

3.2 Transfer function of the headphones

The transfer function of the different headphones are measured in order to determine the reduction of dynamical range caused by flow noise generated by wind when wearing headphones. The set-up is the same as described in the reference measurement in the previous chapter:

A MLS signal is sent from the loudspeaker towards the dummy head. The ear-microphone WM61A records the signal and feeds it to a laptop which is programmed as a sound level meter, i.e. calculating the rms-value with A- or B-weighting. The laptop itself is calibrated with the WM61A - microphone in free field by adjusting the amplification with a correction factor C according to the parallel measurement with a calibrated sound level meter (see Fig. 8).

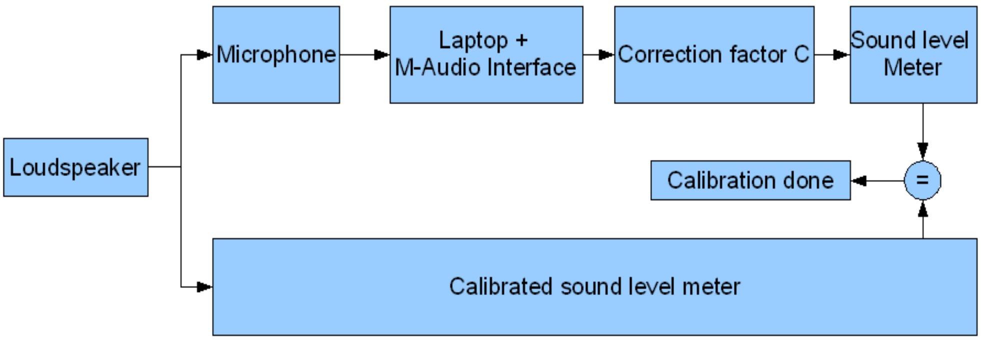

Figure 8: Calibration procedure of the measurement device (lap top with dummy head microphone)

Additionally it is investigated if A- or B-weighting affects the calibration measurement within the given accuracy. But due to the frequency weighting of the dummy head the difference between A- (attenuation of low frequencies) and B- (less attenuating low frequencies) weighted transfer functions is only about 1dB, which is negligible in the present investigation. In all following measurements of SPL the A-weighted dB scale is used to give a near-reality estimate of the sound level in the ear.

The loudspeaker is now replaced by headphones which are mounted directly on the dummy head. The same MLS signal used for the calibration measurement is sent to the headphones, recorded by the ear-microphone and analysed by the calibrated laptop sound level meter. All earphones are driven such that $72 \pm 1\, dB(A)$ is measured by the ear-microphone inside the dummy head. This level is chosen arbitrary but is meant to provide a loudness for a potential user well below 80 dB(A).

Additional measurements are carried out with headphones more tightly pressed onto the ears of the dummy head in order to enhance the low-frequency performance, which increases the SPL about 5 dB at 50 Hz. Also the dummy-head measurement is compared to the measurement with an artificial ear (Brüel & Kjaer 4153). Both measurements are in satisfactory agreement. Deviations are of course at higher frequencies due to the outer-ear resonances. Details of this investigation are discussed in the Thesis.

3.3 Calibration of the wind tunnel

The wind velocity in the measurement volume of the wind tunnel is determined with a calibrated Pitot tube [3]. In all measurements the velocity is chosen to be 4 m/s, 6 m/s and 8 m/s as denoted on the display of the control display, which corresponded to the true velocity of 3.3 m/s, 5,2 m/s and 7,1 m/s, respectively.

4 Measurements

4.1 Measurements of flow noise with the dummy head

4.1.1 Set-up

After determining the transfer functions of all headphones, the measurement of the flow noise contribution is carried out[1], which reduces the dynamic range and performance of the headphones and might even cause masking of the audio material: The dummy head is placed in the wind tunnel with headphones attached. The (calibrated) ear-microphone of the dummy head (see Fig. 2) measures the flow noise, which is recorded via the USB Audio interface on the (calibrated) laptop (same recording set-up as in Fig. 8). The time signal is controlled for overload from turbulent pressure fluctuations (but not always successfully). The frequency spectra of the flow noise are calculated with a MATLAB script, using the filter from 3.1(Fig. 7). Fig. 9 shows a photo and Fig. 10 the scheme of the experimental set-up. The measurements are carried out for the three different velocities 3.3 m/s, 5.2 m/s and 7.1 m/s (denoted 4 m/s, 6 m/s, and 8 m/s in the legends).

1 The term “flow noise” might include turbulent pressure fluctuations as mentioned in the introduction.

Two different angles of wind incidence were chosen (0°, 45°) for the following reason:

Preliminary experiments revealed that most flow-noise is generated at 0° wind attack (dummy head or test person facing the wind flow) and least noise at 45°. Sidewards "flow attack", i.e. 90° incidence was therefore not measured.

Figure 9: Photo of measurement set-up in wind tunnel. The nozzle is left (not to be seen); the dummy head faces the flow; the rectangular funnel on the right captures the free jet.

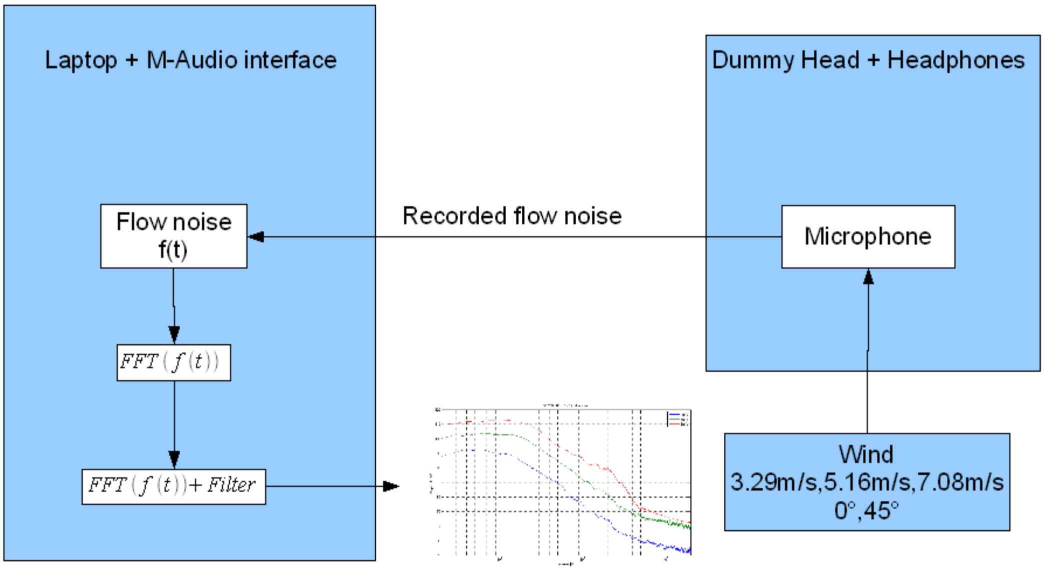

Figure 10: Scheme for measurement of flow noise with the dummy head

4.1.2 Measurements with directional microphones

In order to know how the dummy head itself causes flow-noise in the wind tunnel, measurements are carried out with a directional microphone outside the flow. The measurement set-up is practically the same as in 4.1.1, but instead of the ear-microphone inside the dummy head a directional microphone positioned outside the wind flow pointing towards the head is used to measure the flow noise..

The directional microphone used is a Sennheiser KE-6p interference tube in combination with a ME-67 microphone. The amplifier hardware, laptop and analysing script are the same as in 4.1.1.

However, before using the directional microphone for a quantitative measurement it has to be calibrated. For this purpose it is placed in an anechoic chamber and connected to the laptop running as sound level meter. The procedure is the same as in 3.2 (depicted in Fig. 8): A MLS signal is radiated from the loudspeaker at 1.9 m distance to the microphone, which points towards the loudspeaker. The correction factor C is adjusted until the MATLAB sound level meter displays the same sound pressure level as the calibrated sound level meter.

The flow-noise measurement is carried out under three different conditions. At first the directional microphone just points into the empty wind tunnel running with wind speed of 7.1 m/s. The second measurement is done placing the dummy head into the measurement volume of the tunnel. In a third step PCX150 headphones are attached to the dummy head. The results of the measurement are shown in Figure 11.

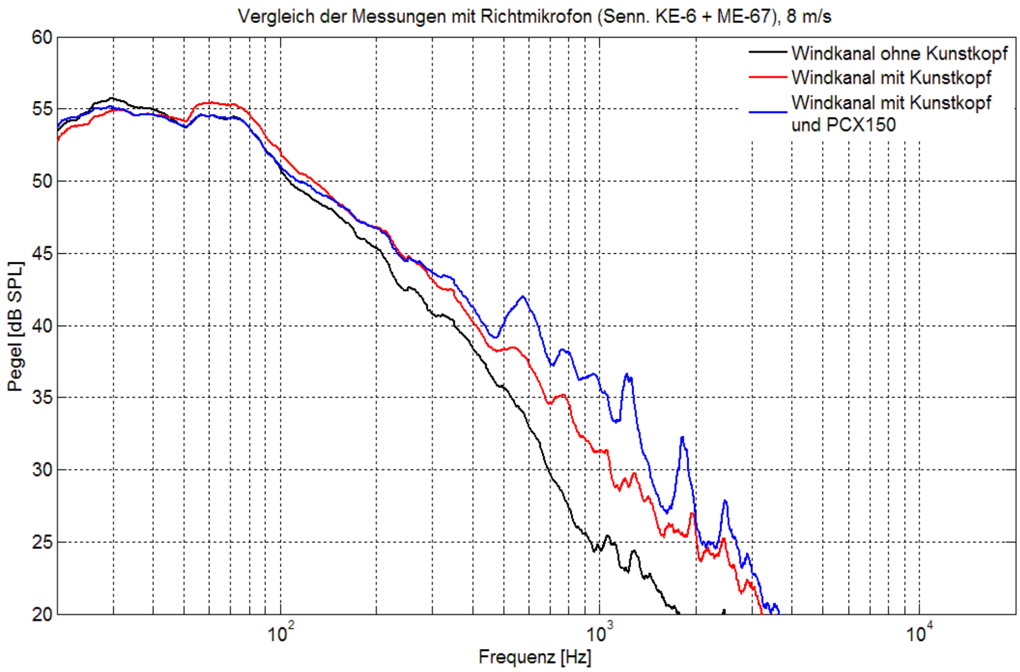

Figure 11: Measurements of "external" flow noise with directional microphone

The dummy head alone contributes to the overall noise above 500 Hz with an increase of 5-10 dB compared to the empty measurement section. The difference in sound pressure level without dummy head and with a dummy head with headphones applied to it is about 10 dB and more at frequencies above 500 Hz.. A sough of the wind around the headphones PCX150 can be heard and also seen in the peaks of the spectrum shown in Figure 11.

4.1.3 Results

The results of the measurements with the dummy wearing headphones in the wind tunnel are shown in the following section. Each pair of headphones has two plots for the wind incidence angles of 0° and 45°. The different wind velocities are marked by three different colours. The first measurement is carried out measuring flow noise in the ear of the dummy head without headphones in the wind tunnel as a reference (see Fig. 12

(0°) and Fig. 13 (45°)). Wind-generated flow-noise in the dummy head's ear without wearing headphones is loudest for 7.1 m/s wind speed and frontal wind incidence (Fig. 12). The maximum sound level of 110 dB is reached around 100 Hz. From there on, the spectra decay like all following ones down to sound pressure levels of about 20 dB (lowest speed) and 48 dB at 20 kHz. (The noise floor of the measurement system is about 20 dB). Noise generated under an angle of attack of 45° is 10 dB to 15 dB lower than under 0° wind incidence (see Fig. 13).

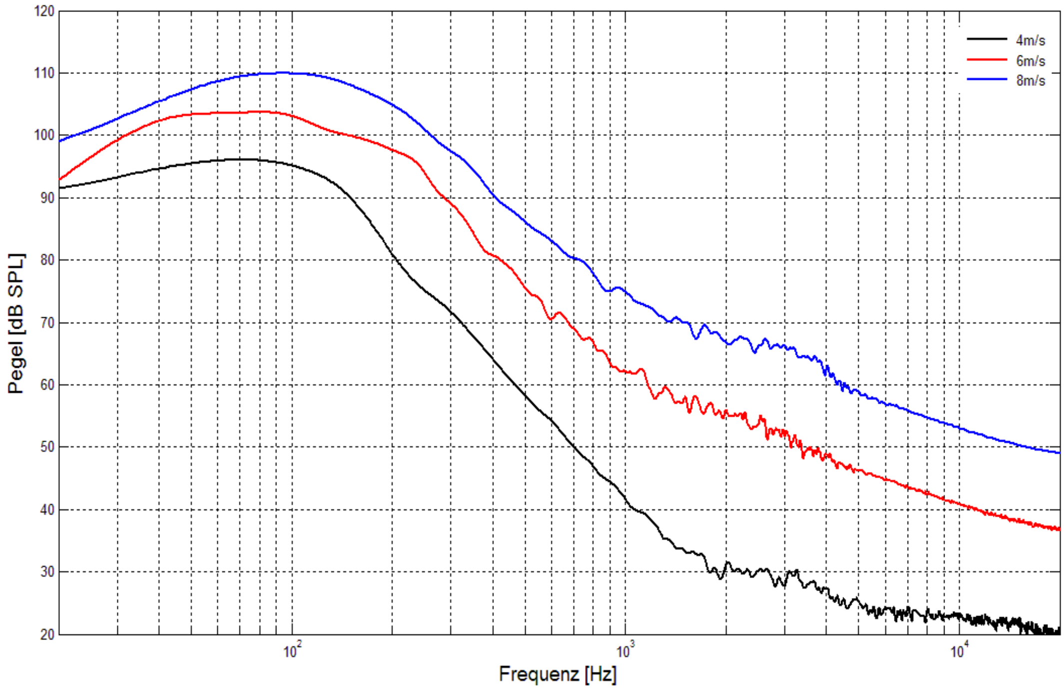

Figure 12: Reference measurement of wind generated noise in the ear of the dummy head for 0° wind attack without headphones

In general, ear buds induce more flow noise and the supra- and circumaural headphones reduce it compared to the “naked” ear.

The HD457 headphones (see Figs. 14, 15) seem to show “louder” high-frequent flow noise at 45° wind incidence for wind velocities of 5.2 m/s and 7.1 m/s, compared to 0° wind attack. But the lack of roll-off at higher frequencies (in particular for “6 m/s”) indicates that the measurement for 45° attack in Fig. 15 reflects overload from turbulent pressure fluctuations. However, the HD457 headphones reduce considerably flow noise for *frontal* wind exposure (Fig. 14)compared to the “naked” ear (Figs. 11, 12).

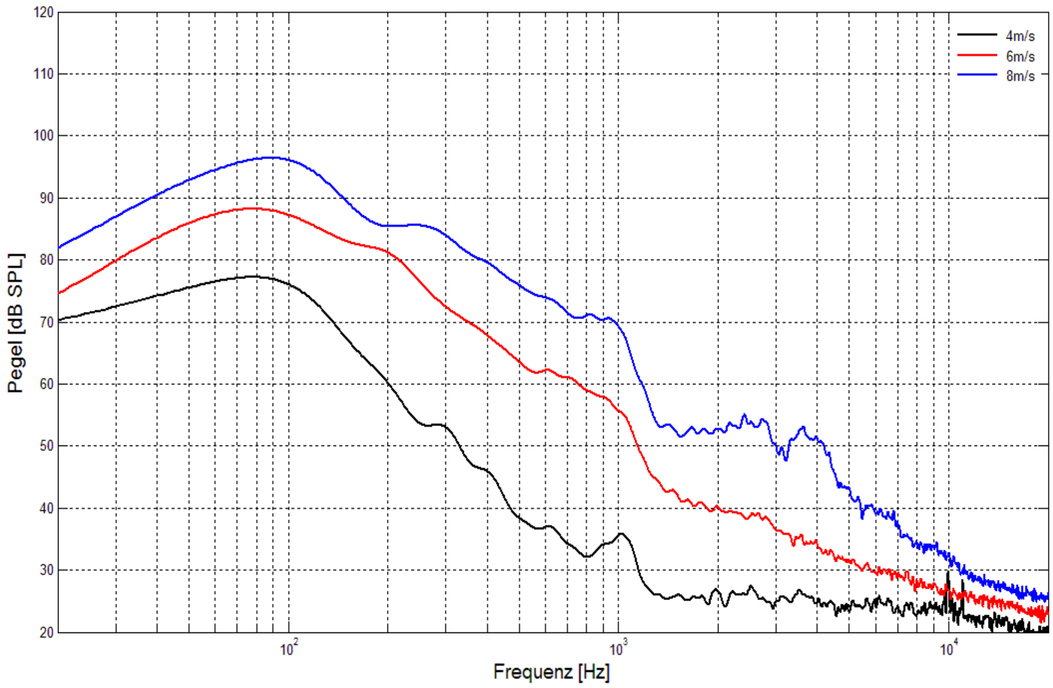

Figure 13: Reference measurement wind generated noise at dummy head 45° without headphones

For the eH150 headphones the highest sound pressure level of 105 dB for flow noise is found for an angle of wind incidence of 0° and wind speed of 7.1 m/s at a frequency about 60 Hz (see Fig. 16). Compared to frontal wind exposure, flow noise stays at high sound pressure level for a wider range of low frequencies (until 700 Hz) and then drops off rapidly under a wind incidence angle of 45° (see Fig. 17). The flow noise is increasing exponentially with wind velocity in the investigated range. Doubling the wind velocity from “4 m/s” to “8 m/s” enhances the noise level about 20 dB (mid frequencies). The eH150 model reduces flow noise in comparison to the “naked” ear only for 0° incidence and enhances flow noise for 45° attack.

A high level of flow noise of about 113 dB is observed at a frequency of about 90 Hz under an angle of wind incidence of 0° and 7.1 m/s wind velocity for the LX70 headphones (Fig. 18). The measurement under 45° wind incidence (Fig. 19) seems again (as in Fig. 15) to reflect turbulent pressure fluctuations, which give rise to high-frequency components by overload of the microphone membrane.

Applying modelling clay to the LX70 headphones (see Figs. 20, 21) realise a “ tight-fit” condition and decrease flow noise about 5-10 dB below 400 Hz for 0° wind attack and 7.1 m/s wind speed. This is presumably due to the fact that flow noise is produced outside the ear entrance and is now blocked out of the ear canal by the modelling clay. No reduction is observed for 45° wind attack, but tonal noise at higher frequencies is induced wearing a "tight-fit" LX70 (Fig. 21).

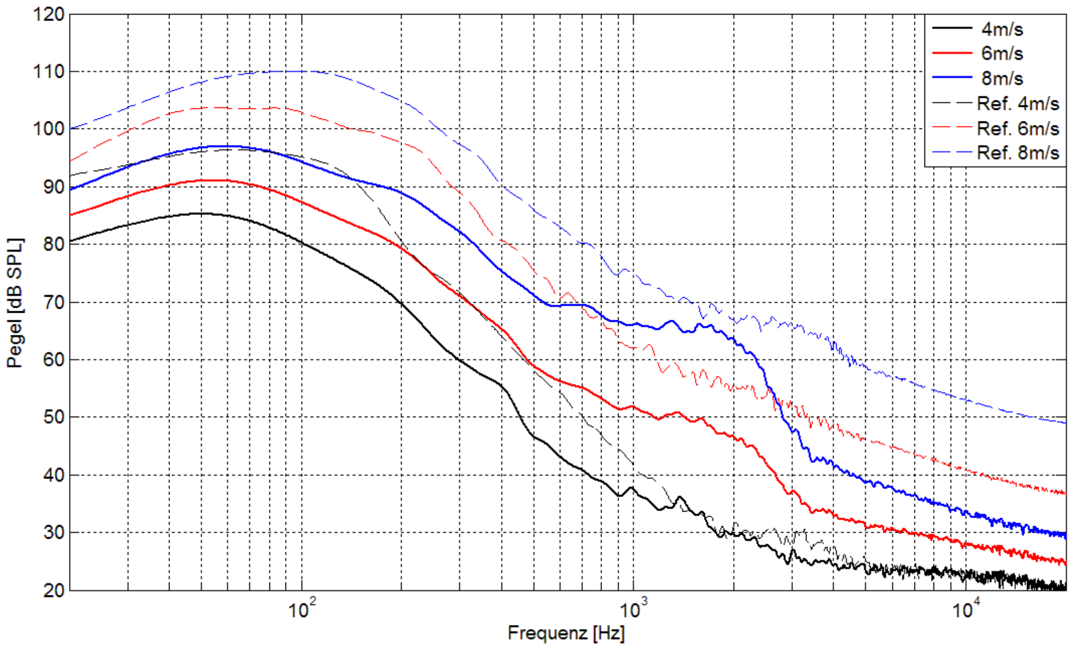

Figure 14: HD457 – flow noise in dummy head's ear at 0° wind attack

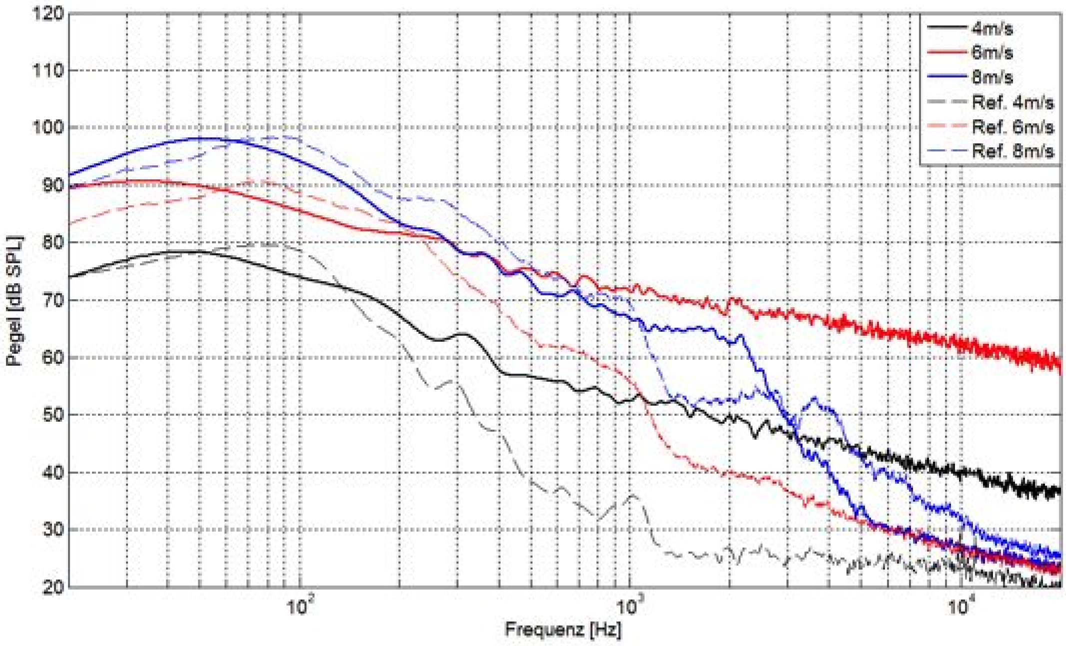

Figure 15: HD457 - flow noise in dummy head's ear at 45° wind attack. The spectra indicate microphone overload by turbulent pressure fluctuations

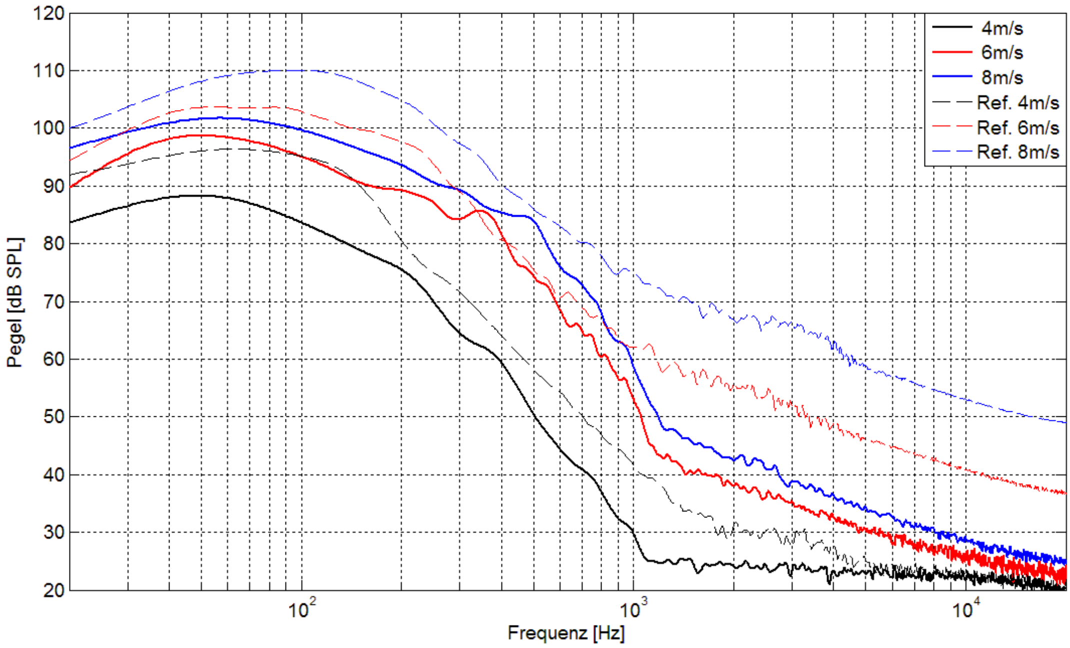

Figure 16: eH150 - flow noise in dummy head's ear at 0° wind attack

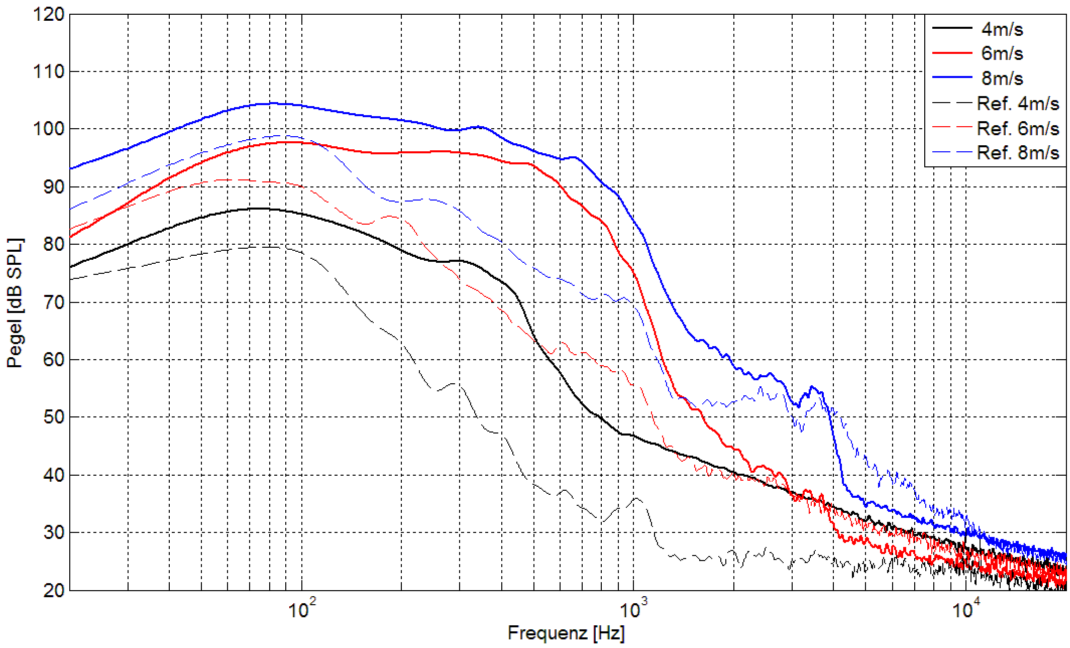

Figure 17: eH150 - flow noise in dummy head's ear at 45° wind attack

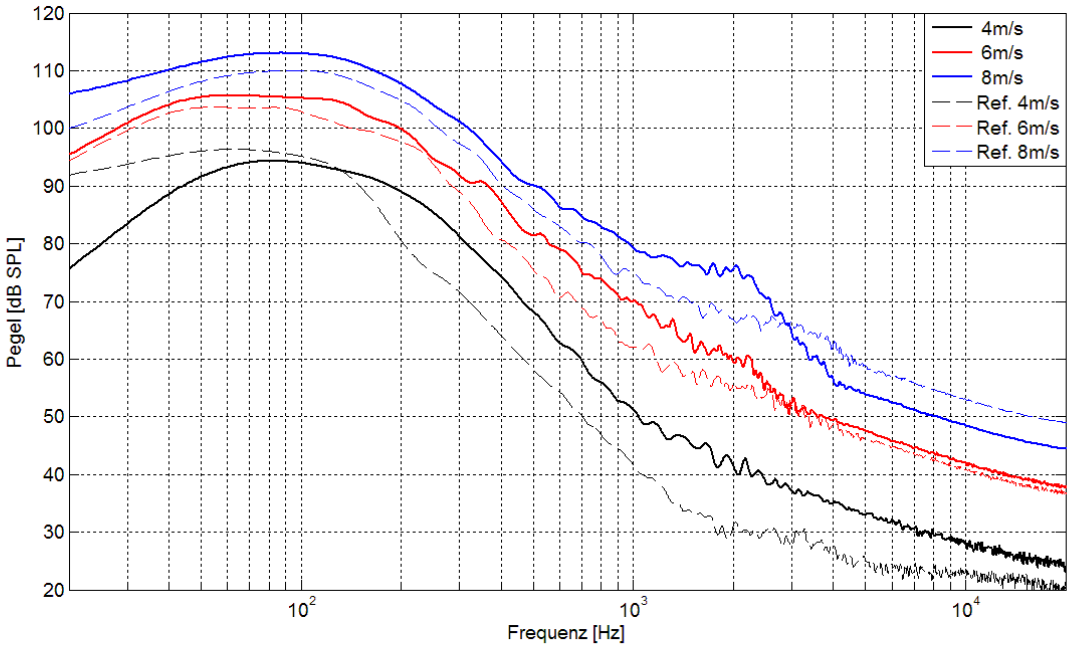

Figure 18: LX70 - flow noise in dummy head's ear at 0° wind attack

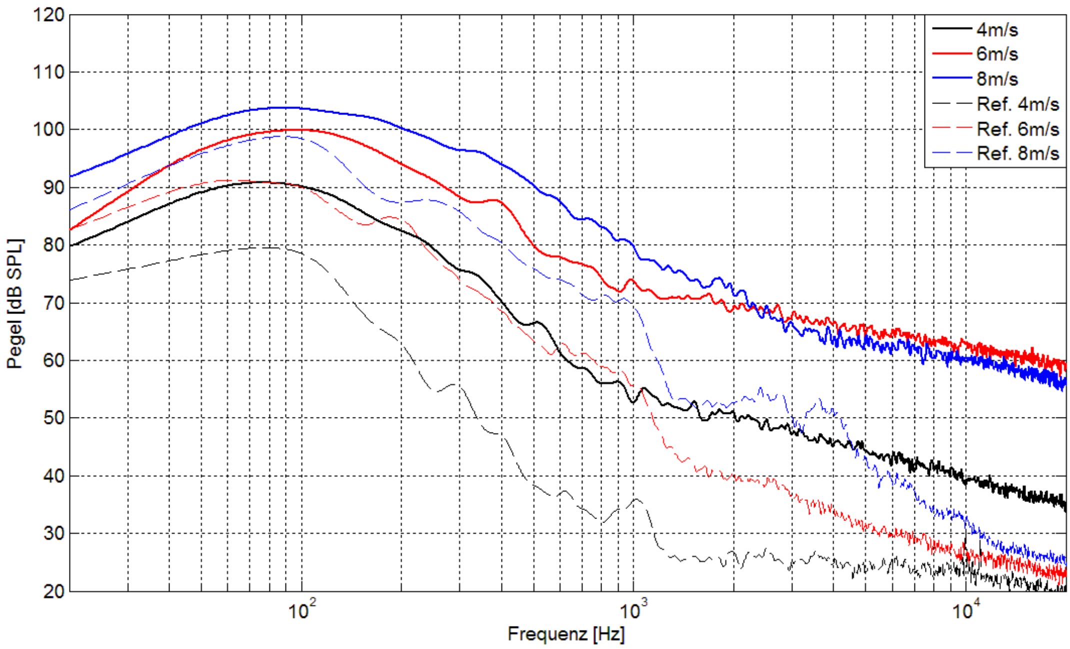

Figure 19: LX70 - flow noise in dummy head's ear at 45° wind attack. The spectra indicate overload of the microphone by turbulent pressure fluctuations (lack of high-frequency roll-off)

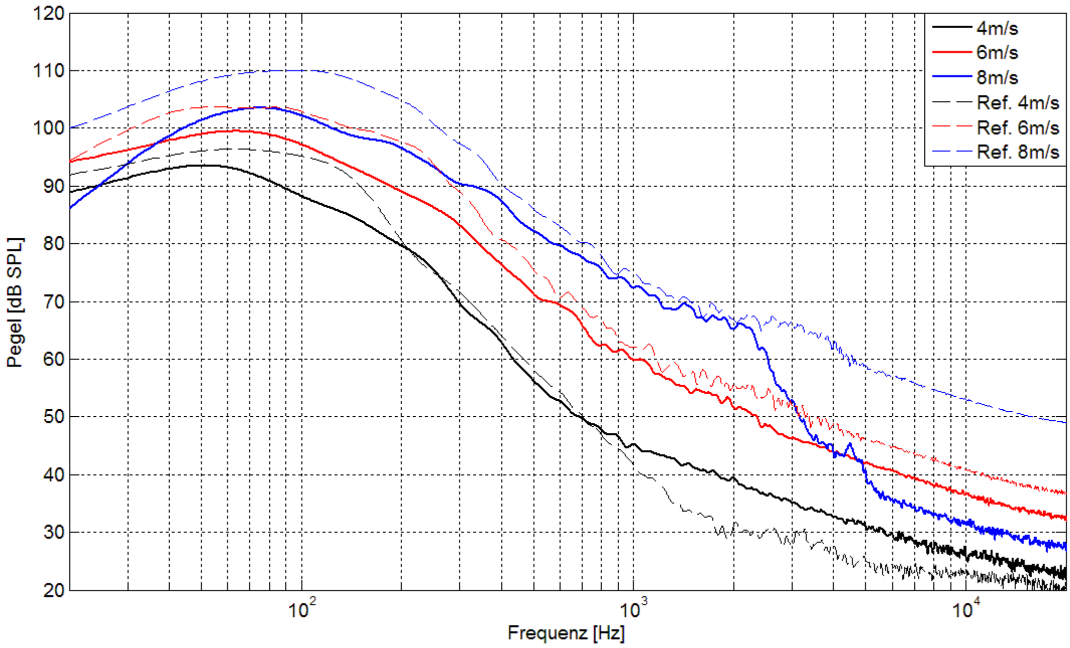

Figure 20: LX70 with clay - flow noise in dummy head's ear at 0° wind attack

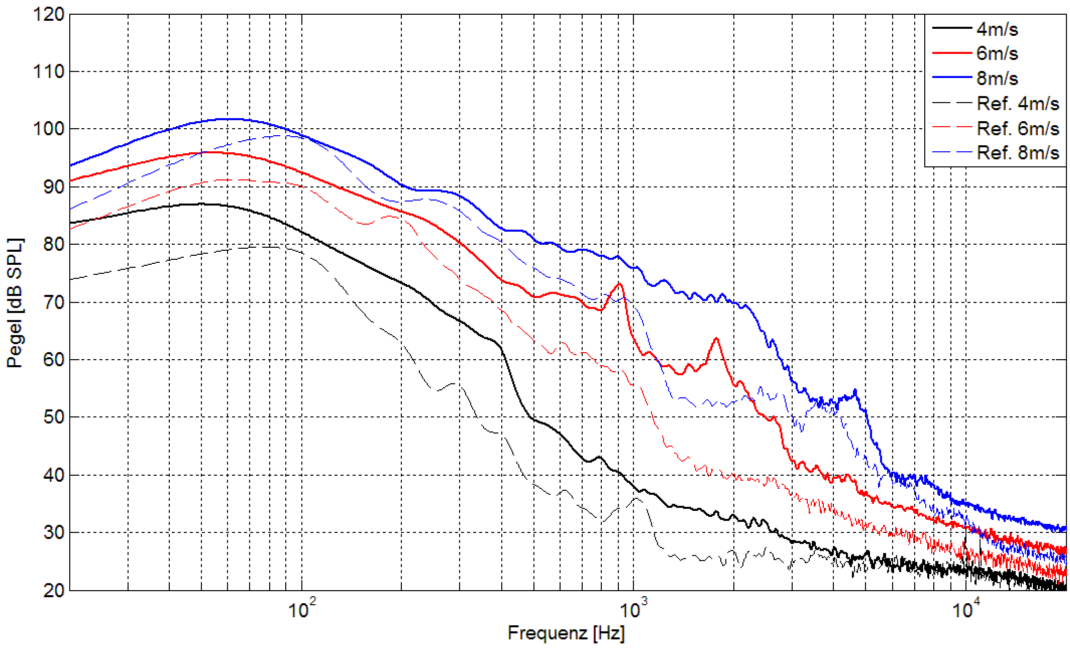

Figure 21: LX70 with clay - flow noise in dummy head's ear at 45° wind attack

For the MX75 earphones the highest flow-noise sound pressure level of 110 dB is measured at a frequency of about 80 Hz (see Fig. 22) for an angle of wind attack of 0° and wind speed of 7.1 m/s. The flow noise is slightly higher compared to the "naked" ear. Lack of roll-off at high frequencies is again an indicator for microphone overload by turbulent pressure during the measurements of 45° angle of wind incidence (see Fig. 23). Flow noise is increased by by wearing the MX75.

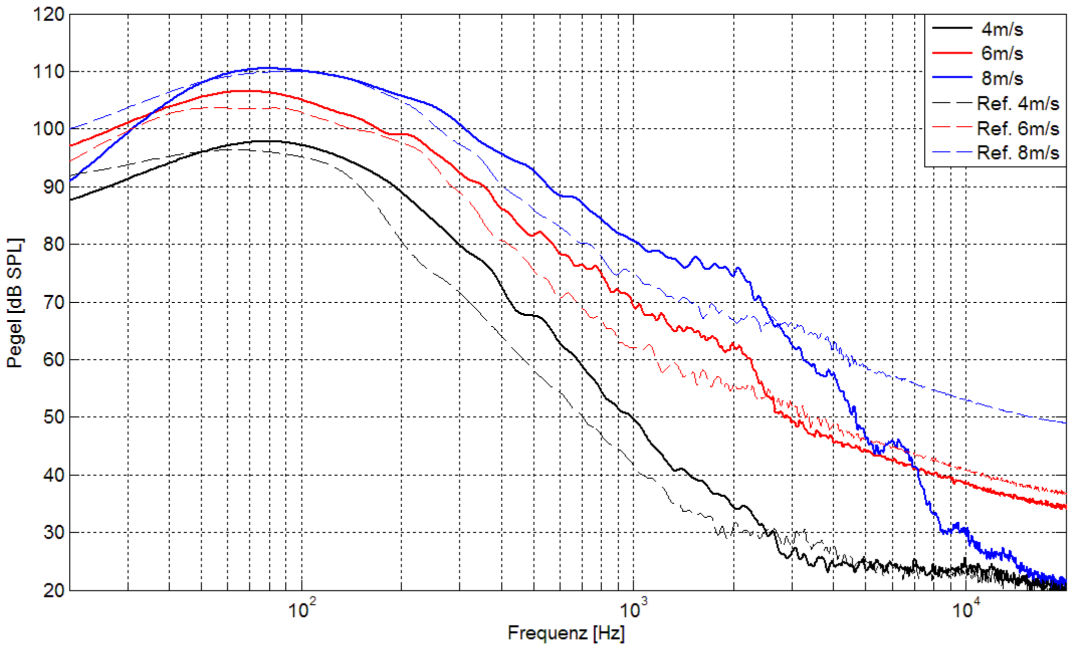

Figure 22: MX75 - flow noise in dummy head's ear at 0° wind attack

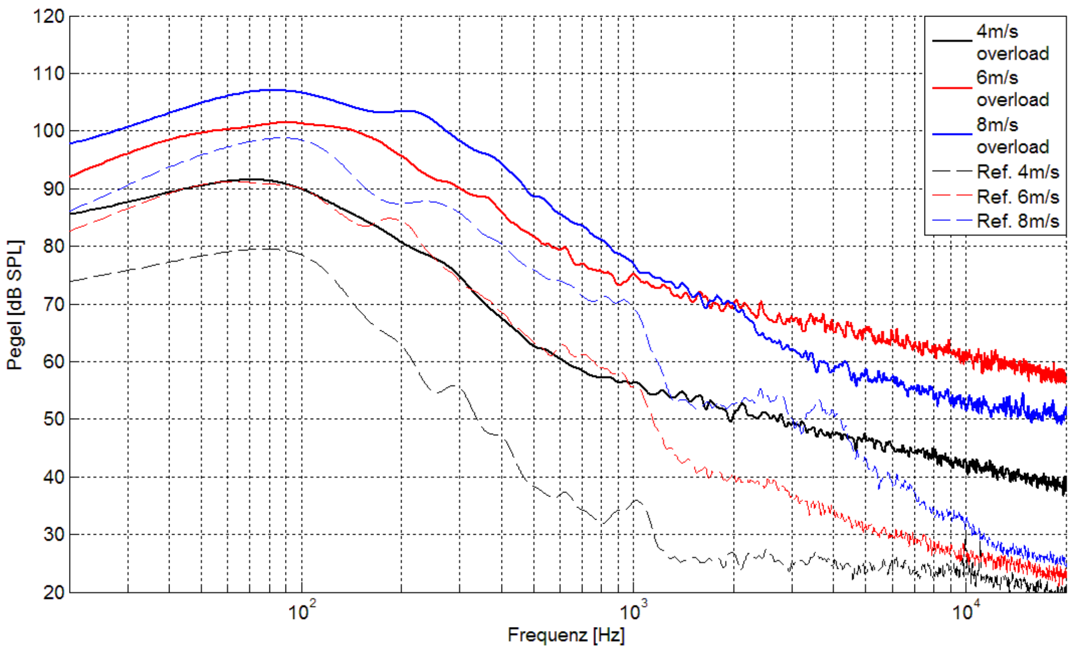

Figure 23: MX75 - flow noise in dummy head's ear at 45° wind attack. All spectra indicate microphone overload due to turbulent pressure fluctuations causing high-frequent spectral components.

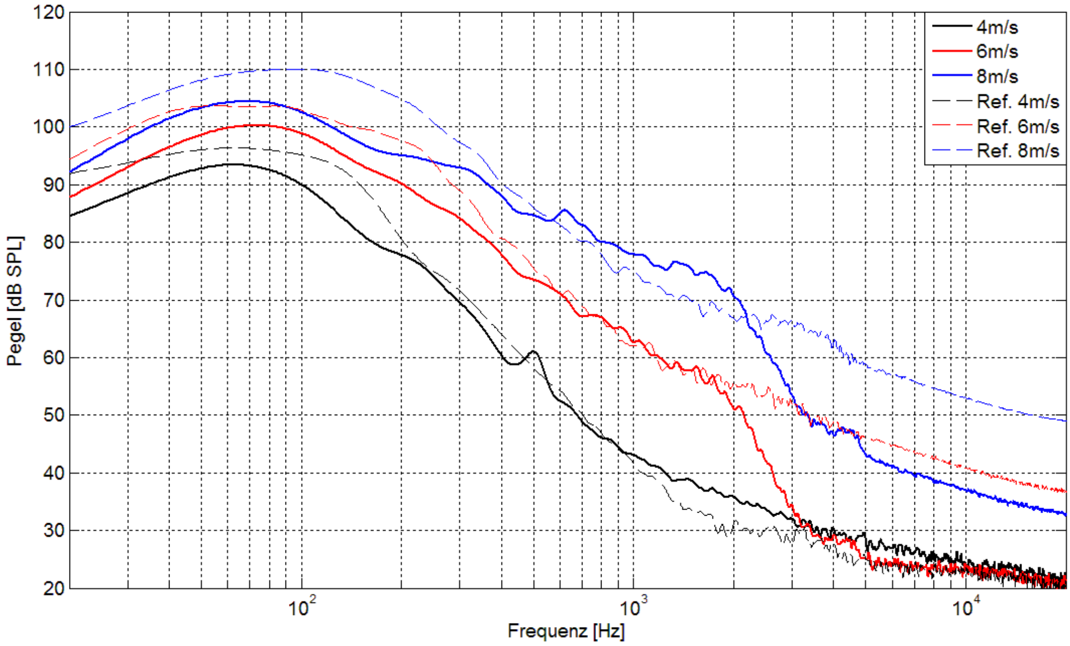

Figure 24: MX75 with clay - flow noise in dummy head's ear at 0° wind attack

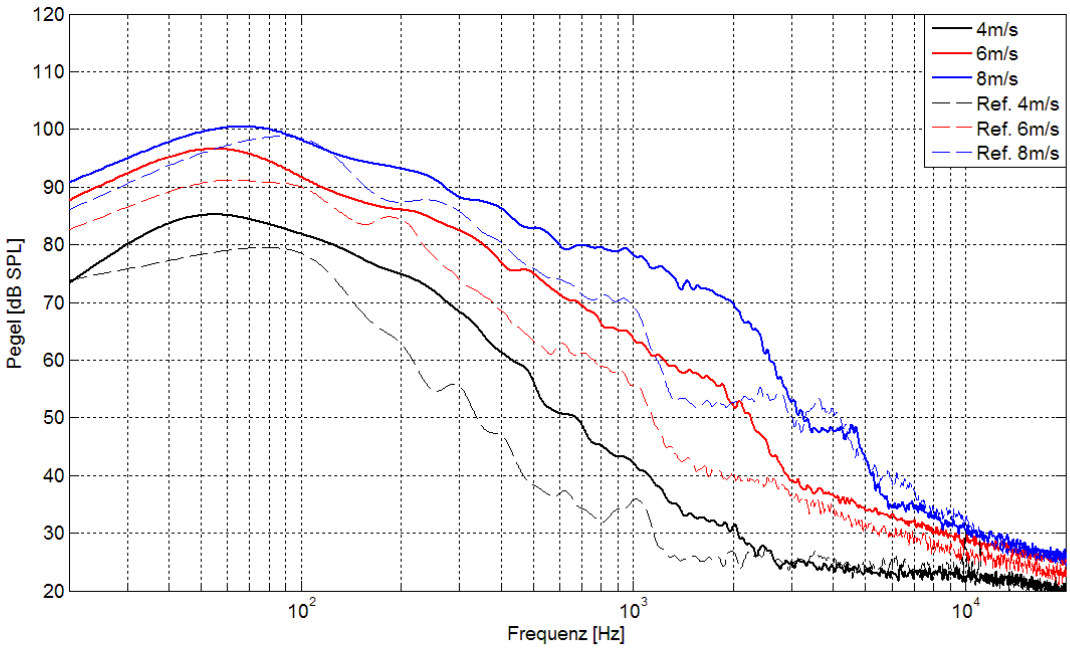

Figure 25: MX75 with clay - flow noise in dummy head's ear at 45° wind attack

Applying modelling clay to the MX75 earphones (“tight-fit” condition) lowers the flow noise about 5-10dB for 0° wind attack, and above 3 kHz even down to the measurement noise floor of about 20 dB (Fig. 24) - avoiding overload of the microphone membrane. No significant noise reduction is measured at 45° wind attack (Fig. 25).

For the MX260 headphones, highest sound pressure level of 113 dB is found at about 90 Hz for an angle of wind attack of 0° (see Fig. 26). The flow noise is larger compared to the naked ear up to 3 kHz. At 45° wind flow incidence, only the 7.1 m/s measurement is without turbulent overload, and is therefore the only spectrum drawn in Fig. 27. The flow noise at 45° is about 6 dB less than the noise measured for 0° wind incidence.

Applying modelling clay to the MX260 earphones (see Figs. 28, 29) reduces the noise below 600 Hz up to about 5-10 dB for frontal incidence. The reduction in noise for 45° is not significantly compared to the naked ear, and it is even enhanced for the mid-frequency range. The enhancement is striking for the low flow-velocity of “4 m/s”.

Applying a foam cover to the MX 260 ear buds has only minor effects for 0° wind incidence (Fig. 30) but an adverse effect at 45° incidence: Enhancement of flow noise of more than 10 dB is observed (Fig. 31).

The flow noise for wearing MX660 headphones is again highest at about 100 Hz with 112 dB and 0° wind attack, and shows some enhancement of flow noise compared to the naked ear (Fig. 32). However, the flow noise at 45° flow incidence is considerably increased (see Fig. 33). Turbulence prohibits at “4 m/s” and “6 m/s” a valid acoustic measurement.

Again, applying modelling clay to the MX660 headphones reduces drastically the flow noise for frontal incidence over a broad frequency range (Fig. 34). For 45° wind incidence (see Fig. 35), at least a reduction is achieved for low frequencies such that the flow noise is comparable with the naked ear condition. But it is increased above about 200 Hz.

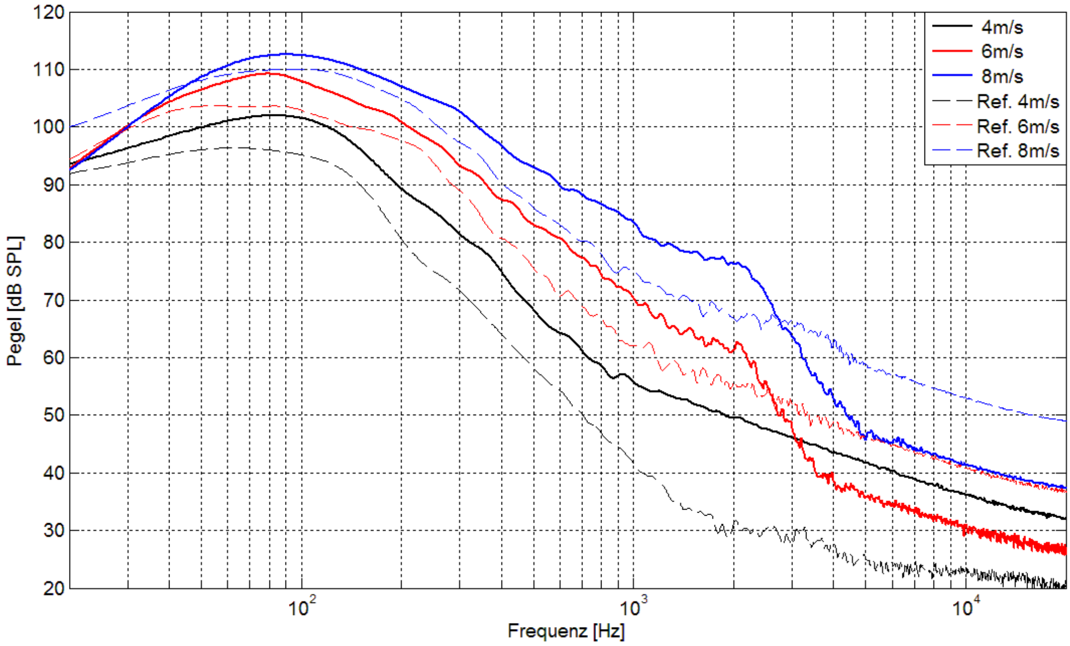

Figure 26: MX260 - flow noise in dummy head's ear at 0° wind attack

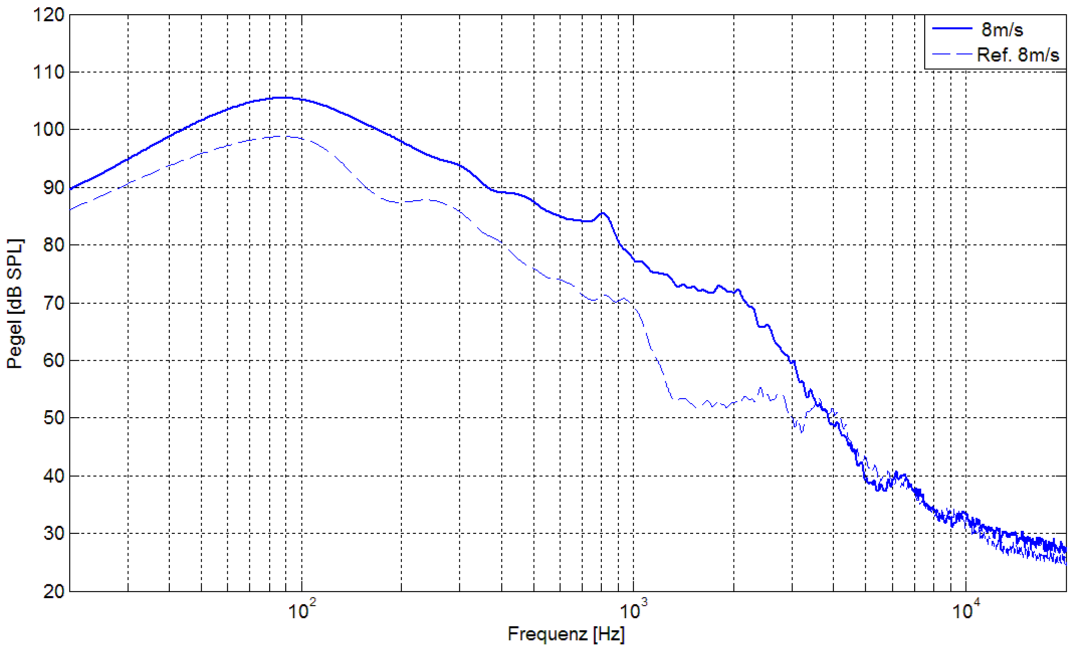

Figure 27: MX260 - flow noise in dummy head's ear at 45° wind attack. Microphone signals for 4 m/s and 6 m/s show strong overload due to turbulent pressure fluctuations – spectra are therefore not shown.

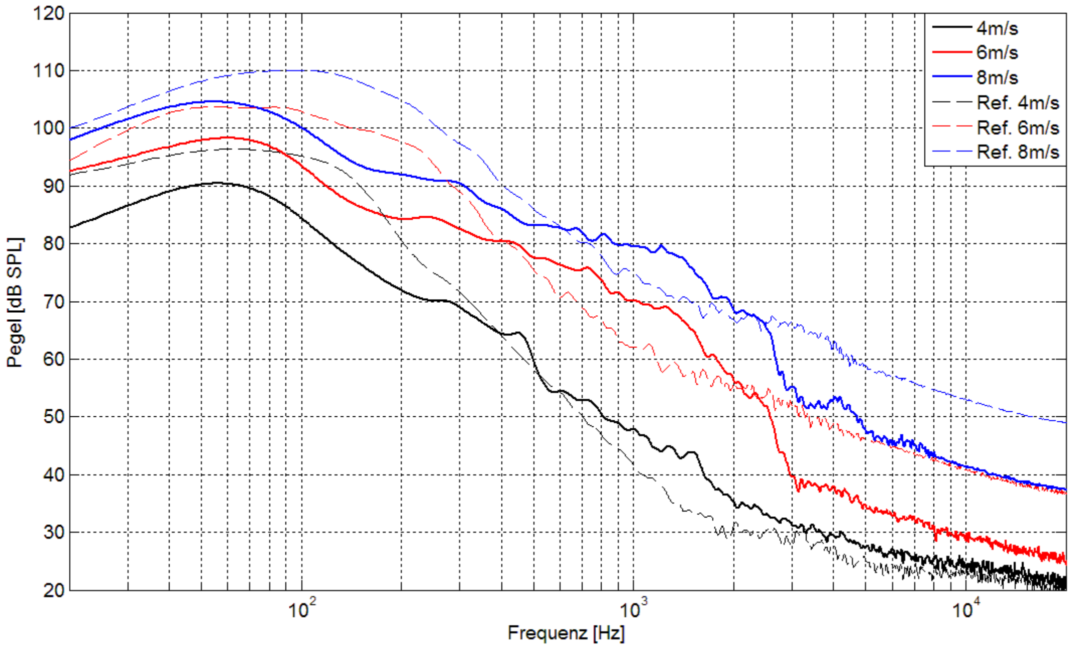

Figure 28: MX260 with clay - flow noise in dummy head's ear at 0° wind attack

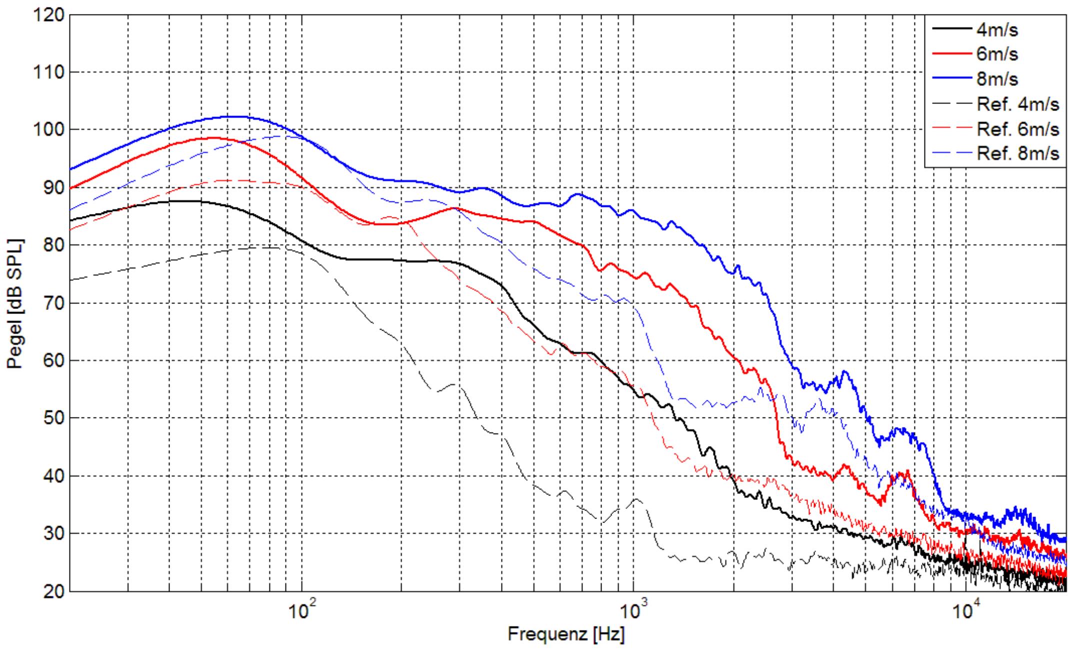

Figure 29: MX260 with clay - flow noise in dummy head's ear at 45° wind attack

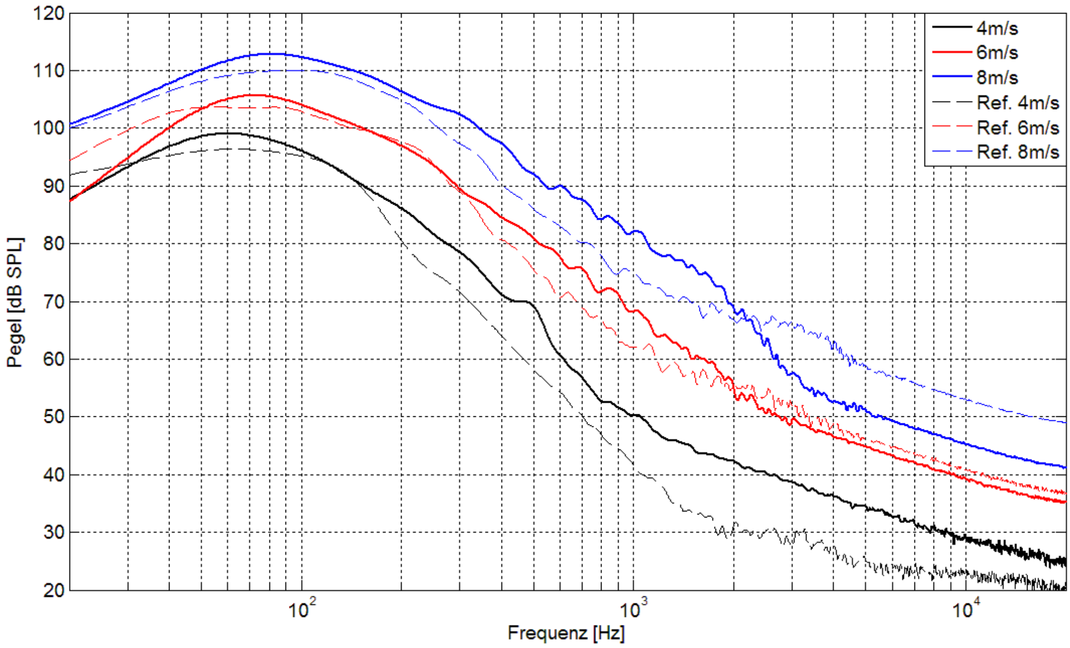

Figure 30: MX260 with foam - flow noise in dummy head's ear at 0° wind attack

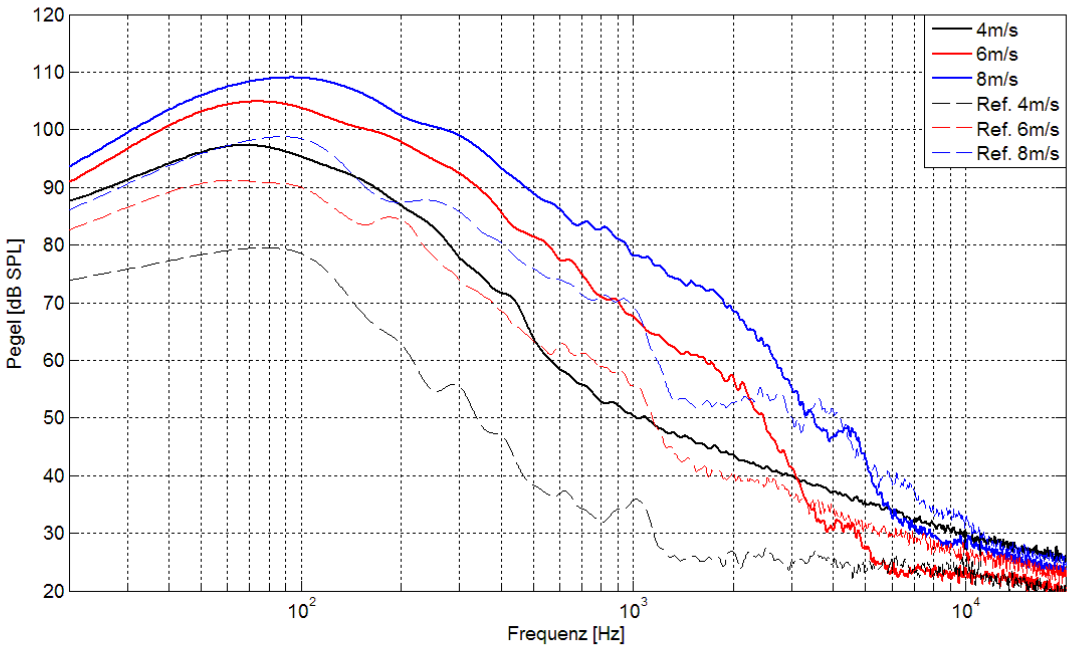

Figure 31: MX260 with foam - flow noise in dummy head's ear at 45° wind attack

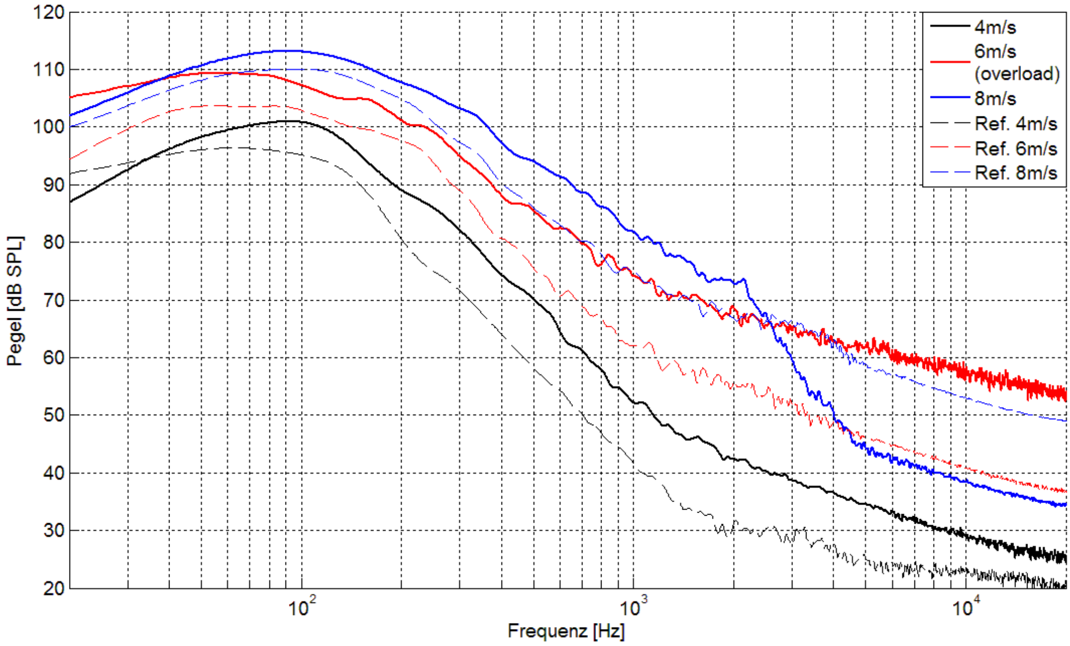

Figure 32: MX660 - flow noise in dummy head's ear at 0° wind attack. Microphone signal for 6 m/s shows overload due to turbulent pressure fluctuations.

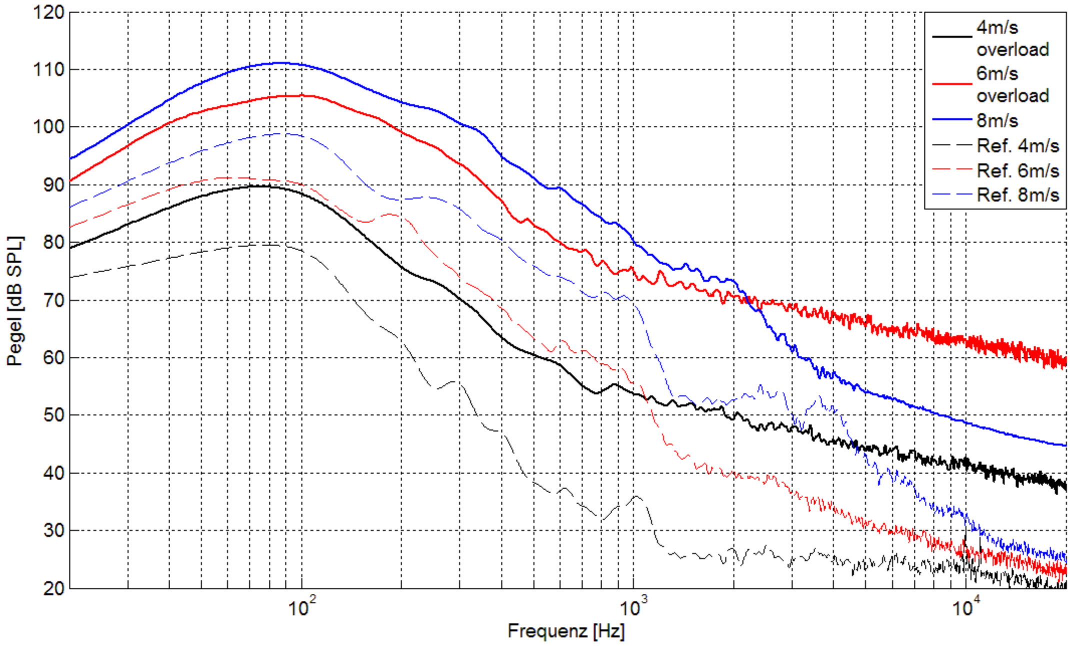

Figure 33: MX660 - flow noise in dummy head's ear at 45° wind attack. Microphone signals for 4 m/s and 6 m/s show overload due to turbulent pressure fluctuations.

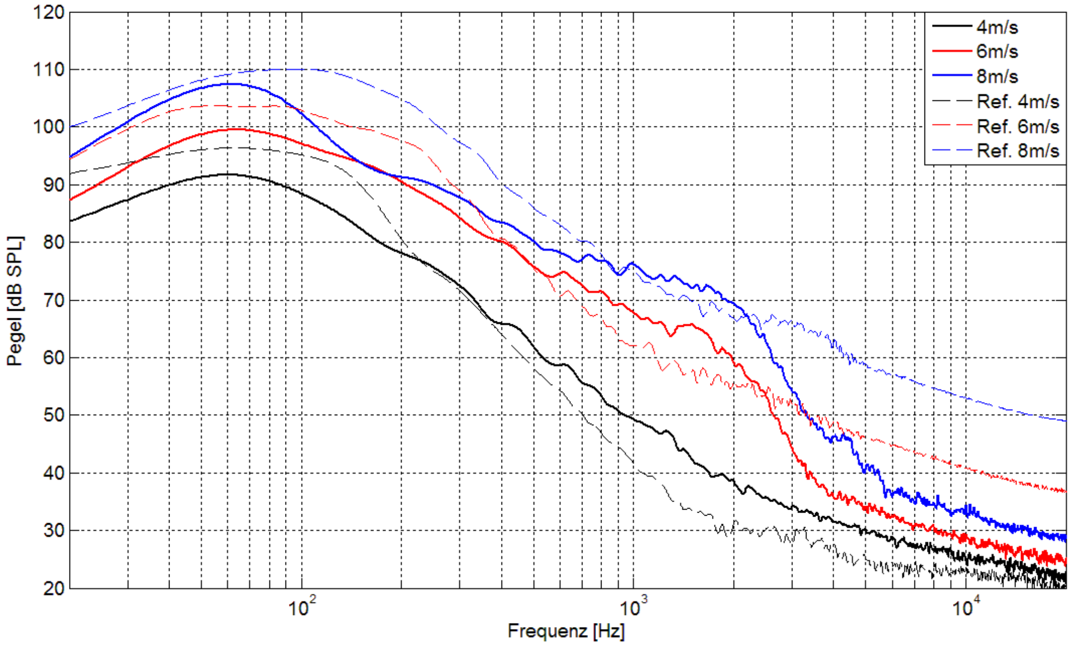

Figure 34: MX660 with clay - flow noise in dummy head's ear at 0° wind attack

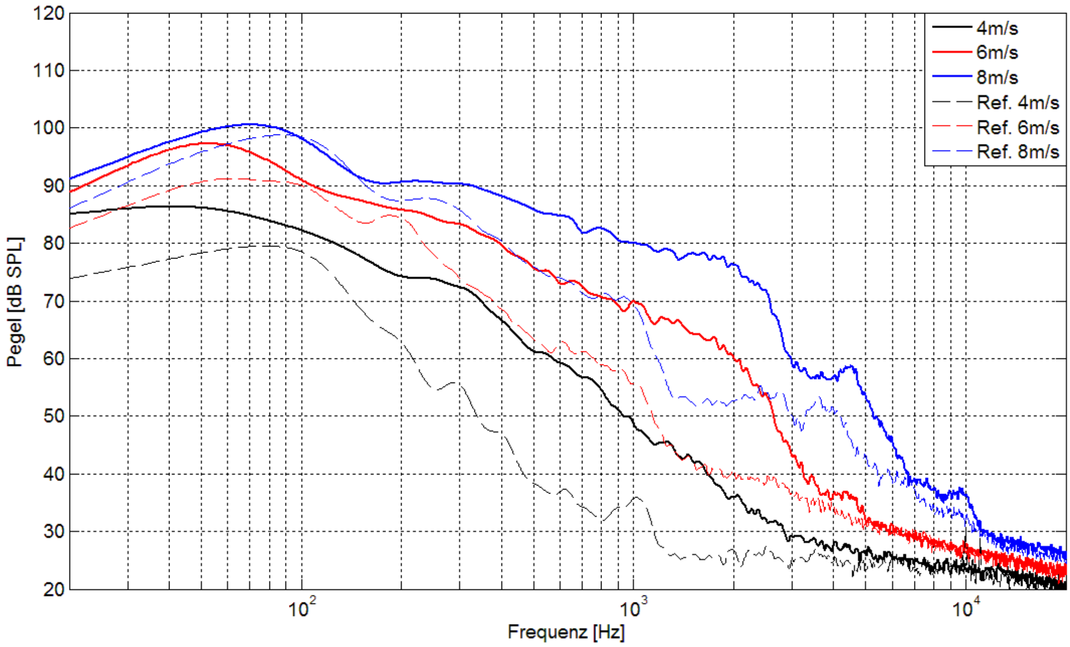

Figure 35: MX660 with clay - flow noise in dummy head's ear at 45° wind attack

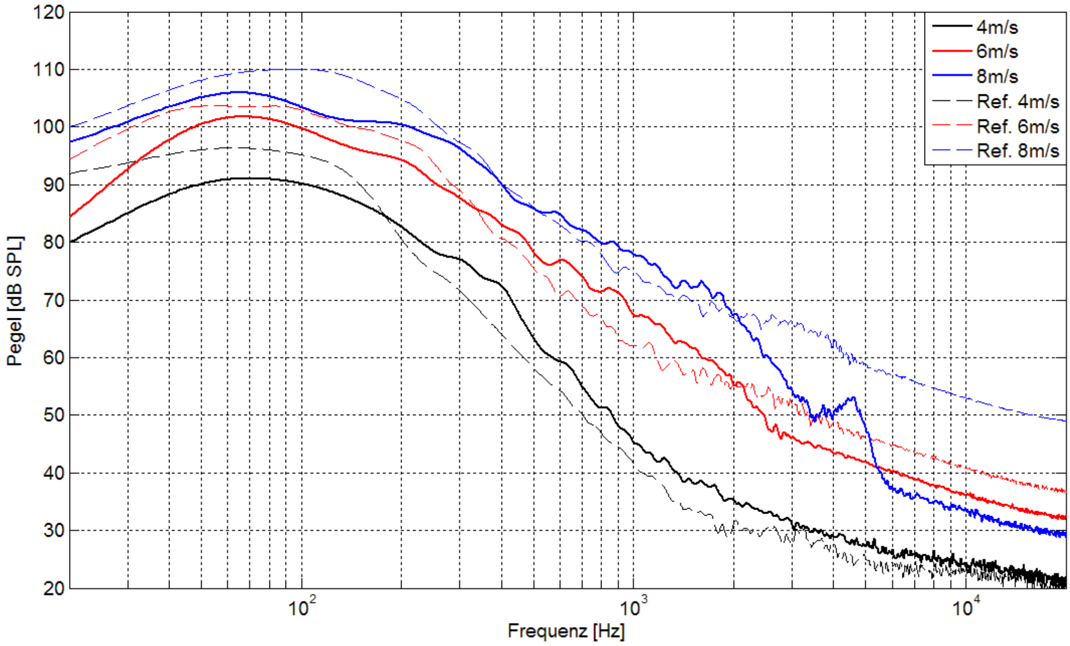

Figure 36: MX660 with foam - flow noise in dummy head's ear at 0° wind attack

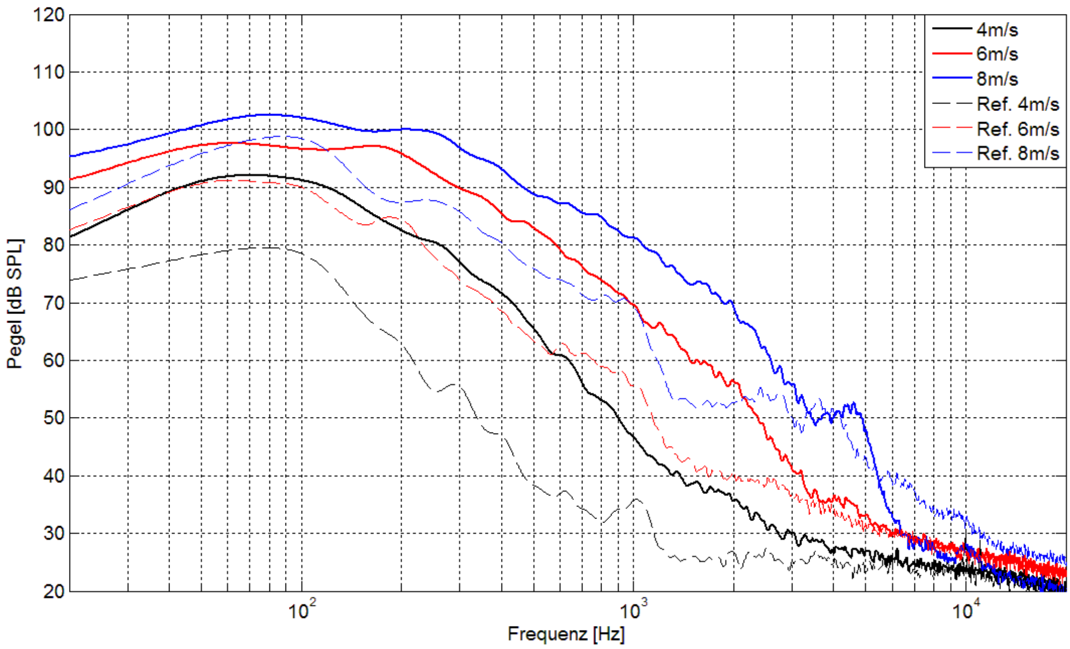

Figure 37: MX660 with foam - flow noise in dummy head's ear at 45° wind attack

Applying a foam cover to the MX660 headphones reduces the flow noise slightly for frontal wind attack compared to the naked ear (Fig. 36). For 45° wind incidence no improvement is observed, but flow noise is increased (Fig. 37), in particular for low wind speed.

Flow noise is only slightly increased by wearing MXL70 headphones, even at 45° wind attack (see Figs. 38 and 39).

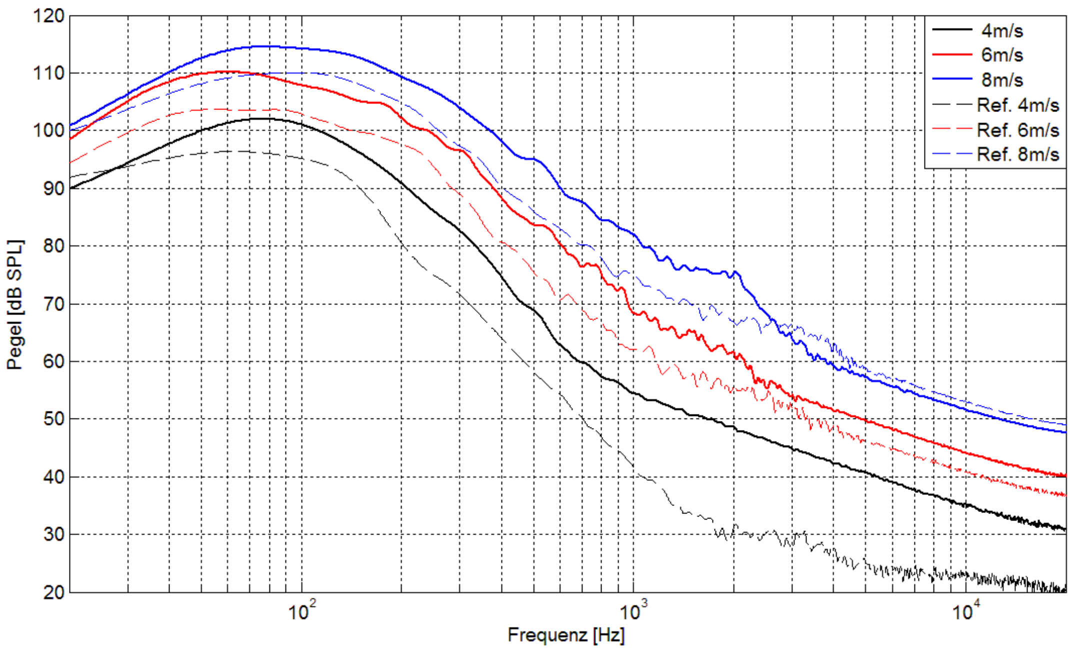

Figure 38: MXL70 - flow noise in dummy head's ear at 0° wind attack

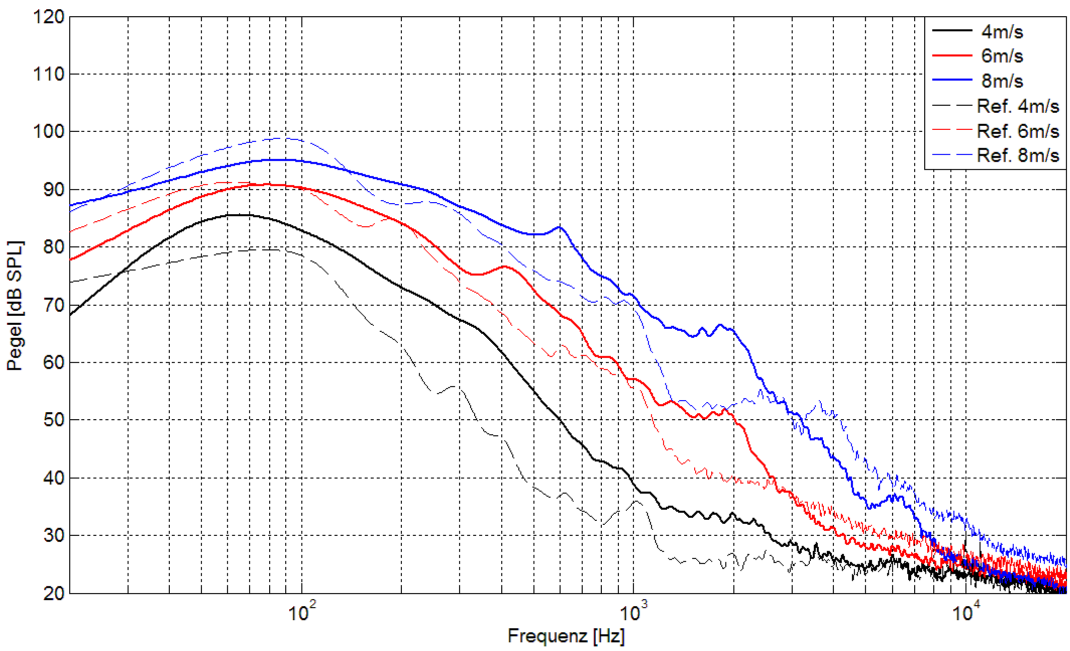

Figure 39: MXL70 - flow noise in dummy head's ear at 45° wind attack

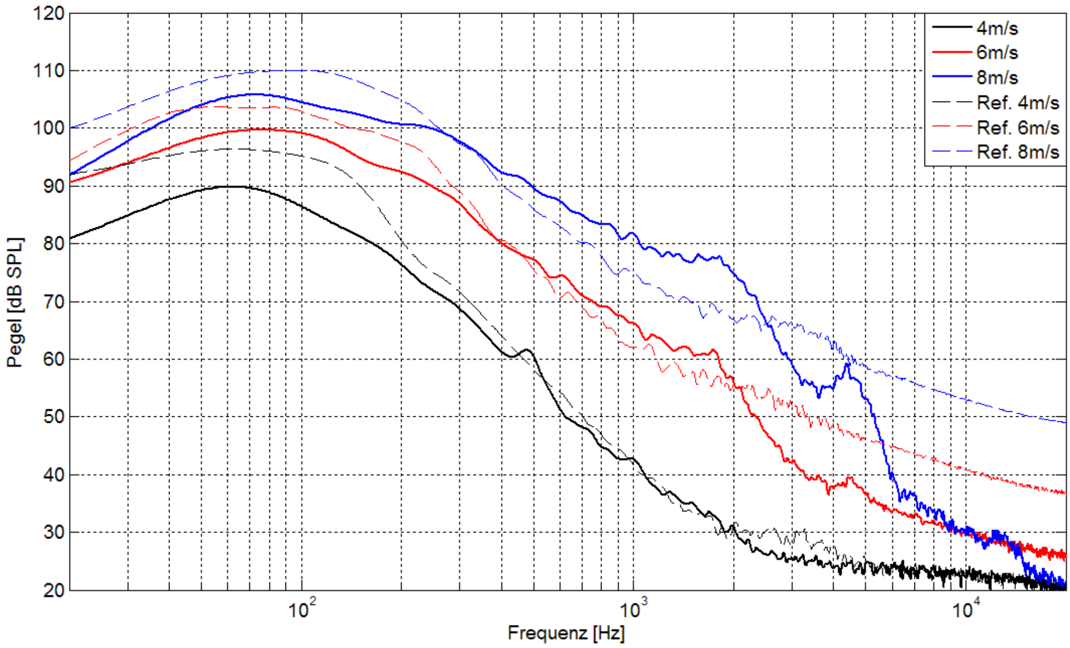

Figure 40: MXL70 with clay - flow noise in dummy head's ear at 0° wind attack

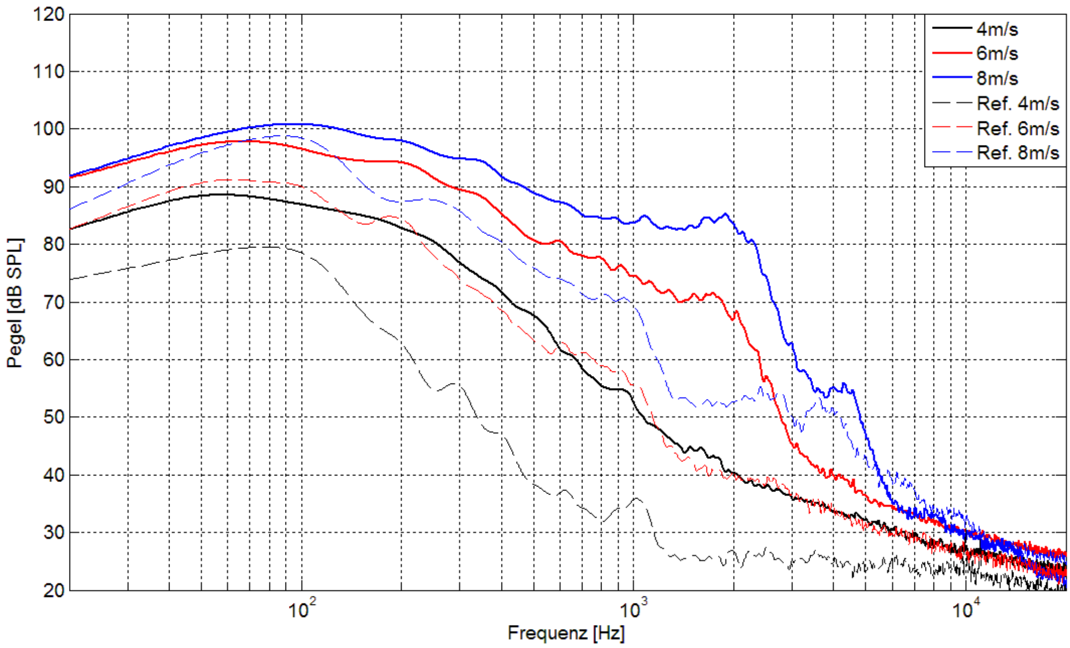

Figure 41: MXL70 with clay - flow noise in dummy head's ear at 45° wind attack

Applying modelling clay to the MXL70 headphones to achieve a "tight-fit" condition decreases flow noise for 0° wind incidence about 10 dB at the maximum level around 70 - 80 Hz and lowers flow noise at low wind speed considerably (Fig. 40). Even at high frequencies flow noise is reduced compared to the naked ear. But a tonal noise between 4 kHz and 5 kHz is observed (and maybe heard) at "8 m/s" wind speed. At 45°

wind attack flow noise is increased, again significantly for low wind speed, and the coloration of the noise is enhanced by spectral components at about 2 kHz (Fig. 41).

A high sound pressure level of 113 dB at at frequency about 80 Hz is observed with the MXL560 headphones for frontal wind incidence and 7.1 m/s wind speed (Fig. 42). For a wind incidence angle of 45° (Fig. 43) all measurements show a little bit less flow noise, but turbulent pressure fluctuations give rise to some microphone overload and thus to the observed spectral increase at high frequencies in the “4 m/s” and “6 m/s” measurements. Sealing with clay reduces the noise in the 100 Hz – 200 Hz region considerably: About 10 dB and more for “6 m/s” and “8 m/s” wind speed compared to the naked ear. However, turbulence is induced causing microphone overload (Fig. 44). At 45° wind attack flow noise is increased in the mid-frequency range, even at 4 m/s. Additionally, microphone overload is observed at “8 m/s” (Fig. 45).

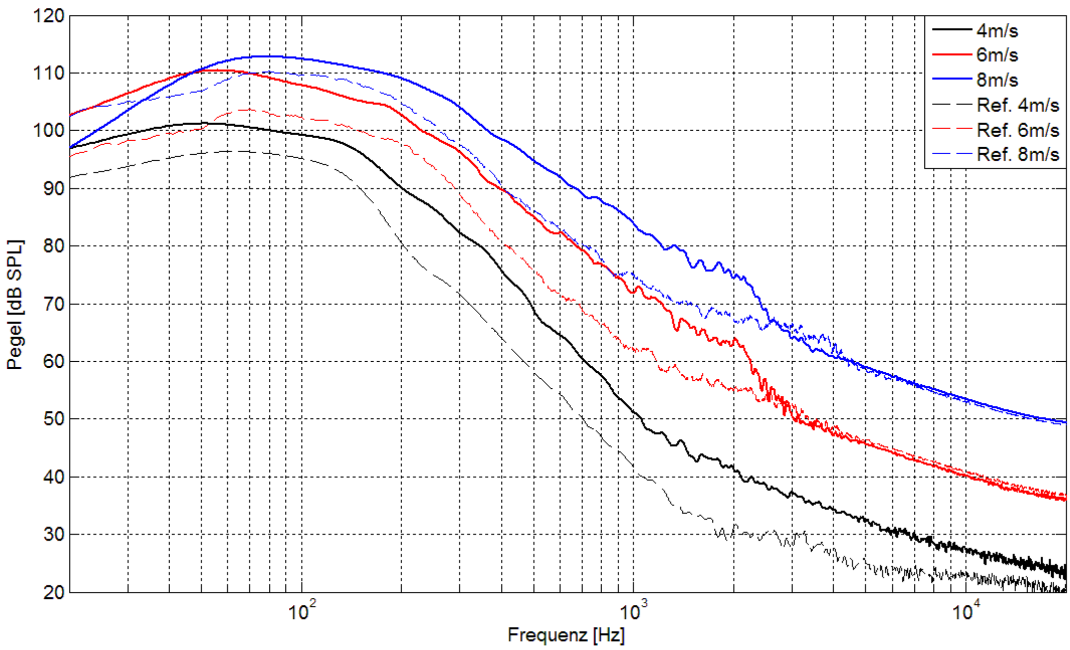

Figure 42: MXL560 - flow noise in dummy head's ear at 0° wind attack

The CX500 generate nearly no additional flow noise, except for a distinct tonal sound around 600 Hz at low wind speed. The source was not identified (Fig. 46). The same noise is heard at 45° flow incidence, too. But compared to the naked ear, the flow noise is increased at this angle (Fig. 47).

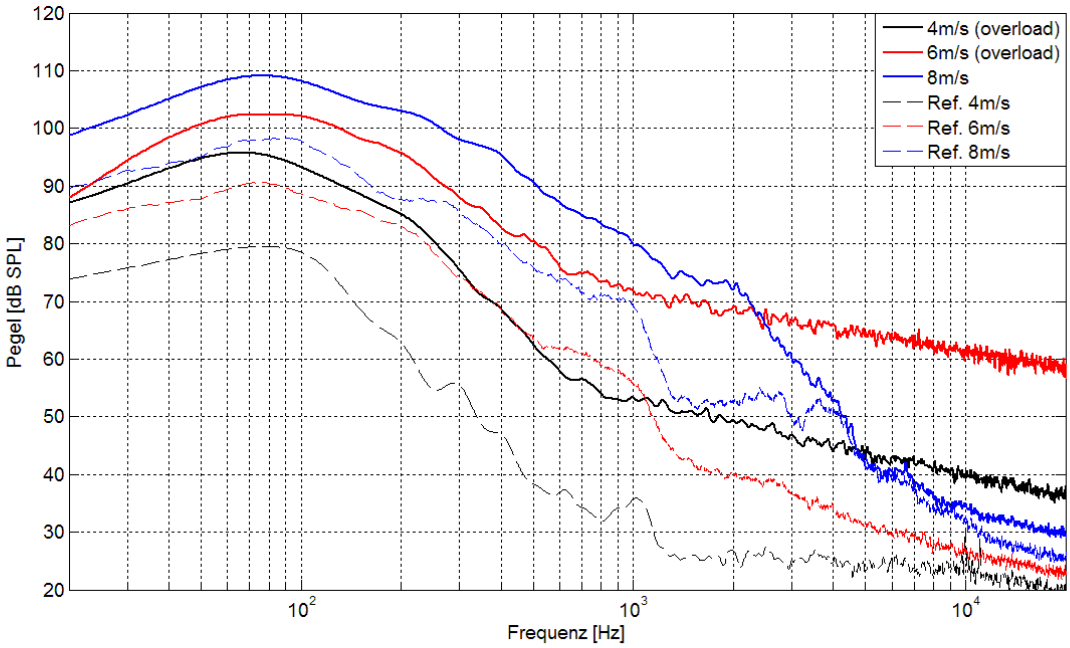

Figure 43: MXL560 - flow noise in dummy head's ear at 45° wind attack.

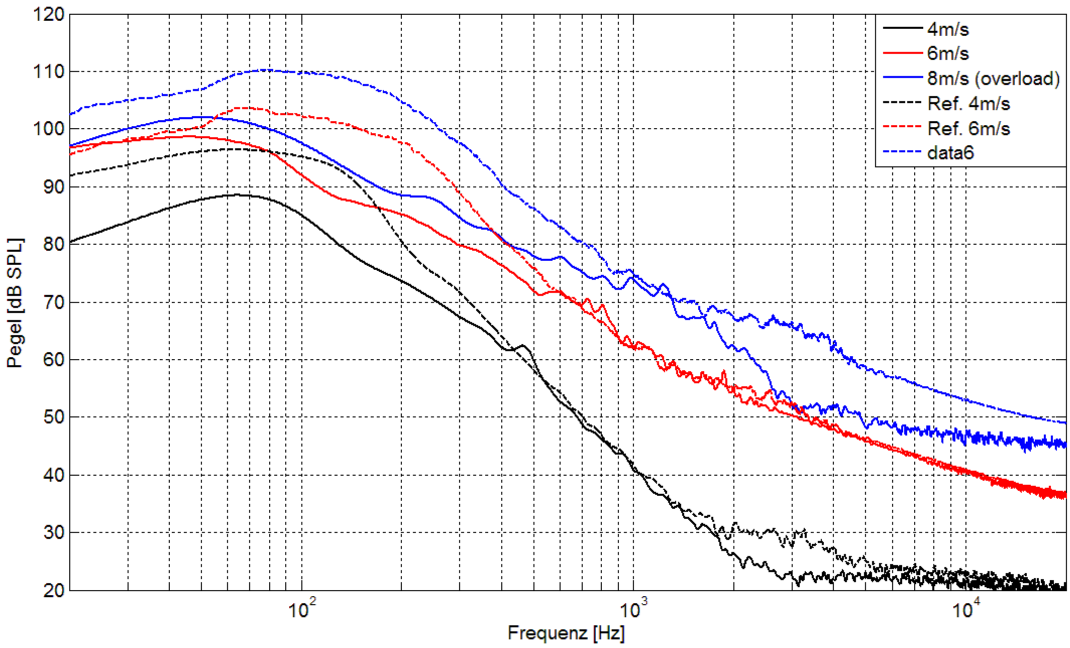

Figure 44: MXL560 with clay - flow noise in dummy head's ear at 0° wind attack

Wearing OMX70 headphones increase flow noise up to about 5 to 10 dB in for higher frequencies (> 100 to 200 Hz, Fig. 48). Considerable increase in turbulent pressure fluctuations is observed for 45° wind incidence with this headphone (Fig. 49).

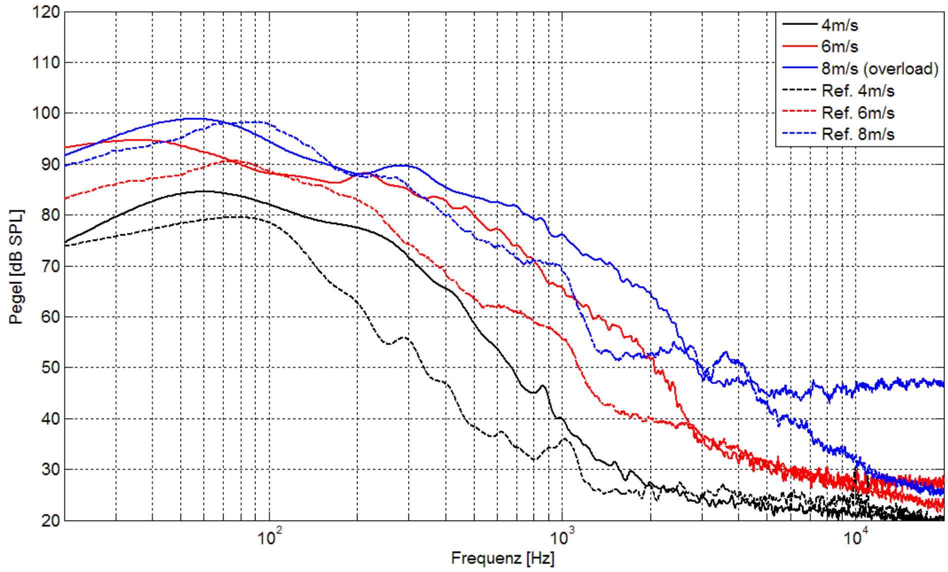

Figure 45: MXL560 with clay - flow noise in dummy head's ear at 45° wind attack

In a more "tight condition" with modelling clay the OMX70 headphones exhibit no additional flow noise compared to the naked ear. At "4 m/s" the flow noise is even reduced at low frequencies (Fig. 50). This is not the case for 45° wind attack. Flow noise is larger than in the naked-ear case (Fig. 51).

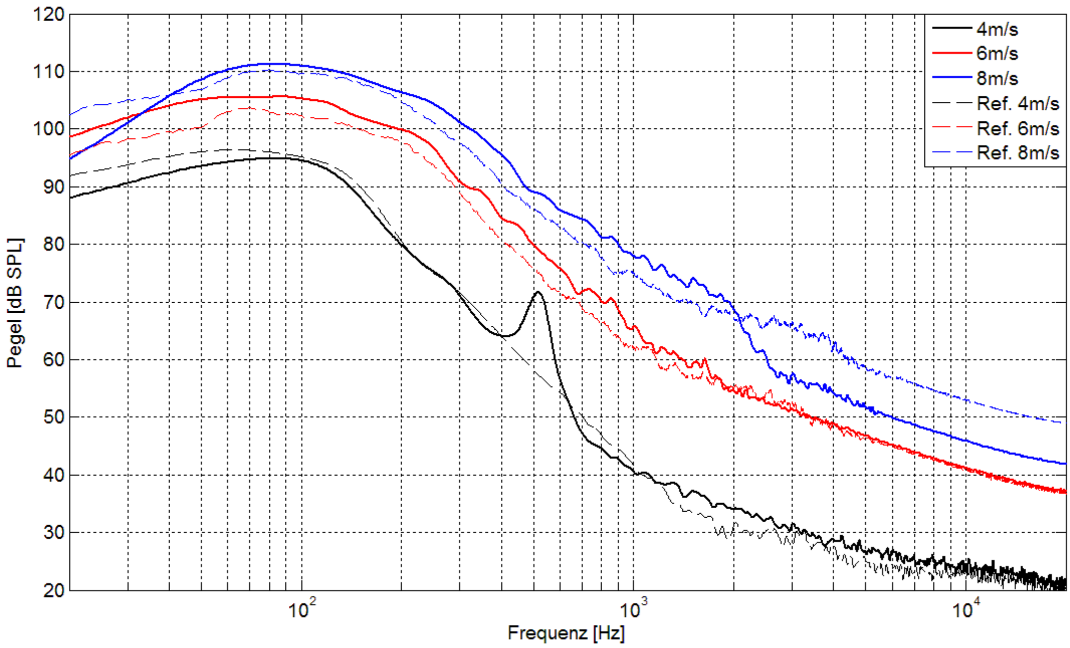

Figure 46: CX500 - flow noise in dummy head's ear at 0° wind attack

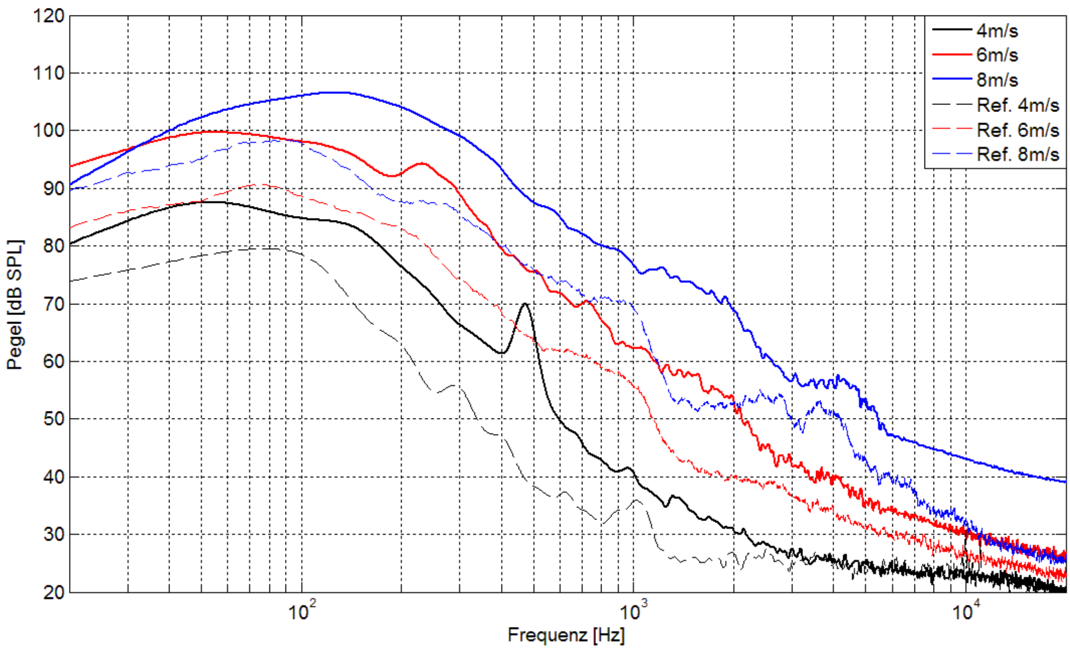

Figure 47: CX500 - flow noise in dummy head's ear at 45° wind attack

The PX100 supra-aural headphones are one of the most quiet headphones producing 103 dB flow noise at about 90-100 Hz for 7.1 m/s wind and frontal exposure, which is about 7 dB below the noise from the “naked” ear (Fig. 52). For 45° wind attack, the flow noise below about 130 Hz is slightly less compared to wearing no headphone, and slightly enhanced above 130 Hz (Fig. 53).

The PX150 showed results similar to the PX100 headphones. The flow noise reduction is even higher at 0° wind attack with 10 dB in the low-frequency range and even more for high frequencies (Fig. 54). For 45° the reduction of flow noise is a little less effective compared to the PX100 (Fig. 55). Both headphones exhibit a slight coloration of the flow noise for the 45° wind incidence. The PX150 allows for active noise control (ANC) to compensate for exposure by external noise. Therefore, the measurements are repeated with the ANC turned on (Figs. 56 and 57). For frontal wind incidence, the reduction is significant over the whole frequency range. For 45° wind attack, there is a certain reduction at least for very low frequencies. Compared to the ANC switched off (Fig. 55), the flow noise is a few dB less with the “active” PX150 in the whole frequency range, and is comparable for “6 m/s” and “8 m/s” with the noise produced at the “naked” ear.

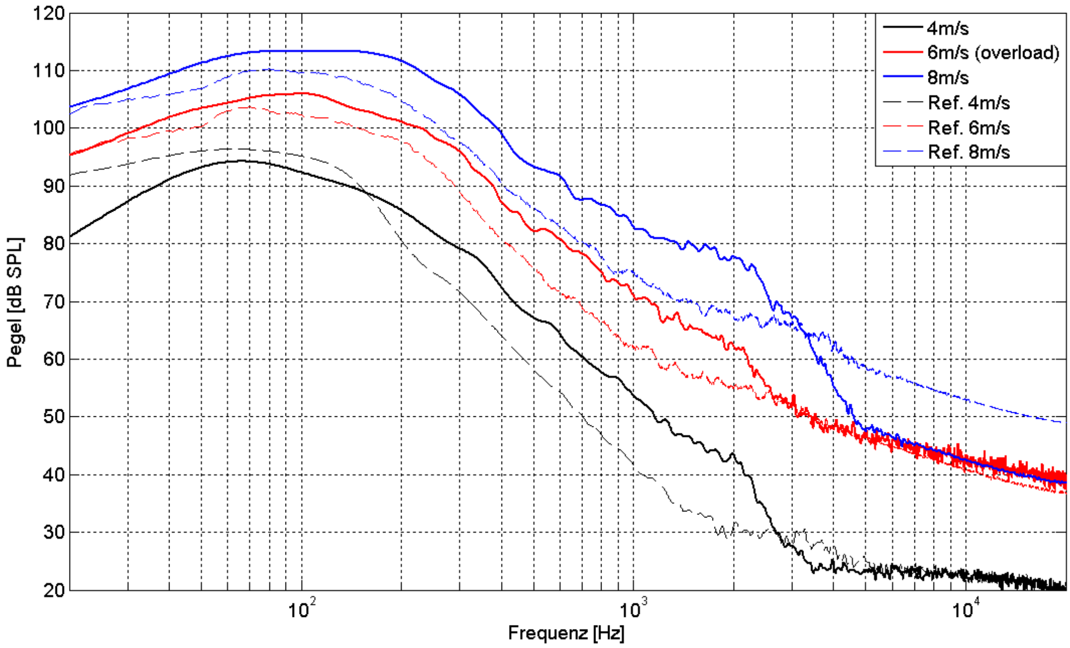

Figure 48: OMX70 - flow noise in dummy head's ear at 0° wind attack

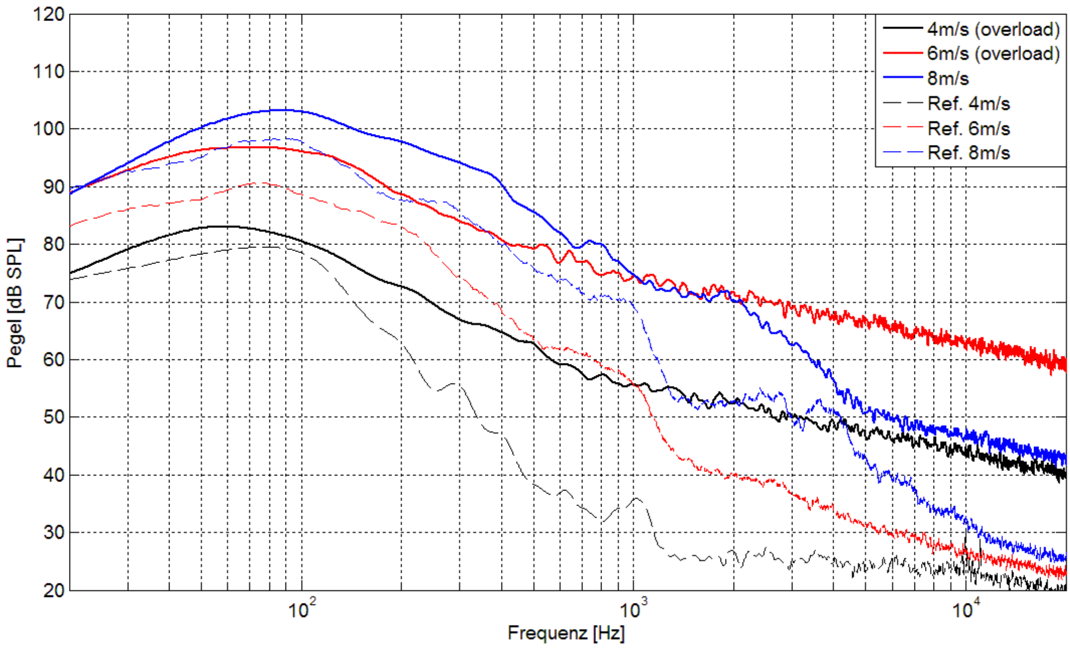

Figure 49: OMX70 - flow noise in dummy head's ear at 45° wind attack

The headphones with lowest flow noise at the dummy head are the supra- and circum-aural ones (PX100, HD457, PXC150), all having maximum sound pressure level of approximately 100 dB or less (HD457) for 0° wind incidence and 7.1 m/s wind speed. Only exception is the eH150 headphone which are a little bit louder regarding flow noise but nevertheless still more quiet than the ear-buds and the in-ear headphone.

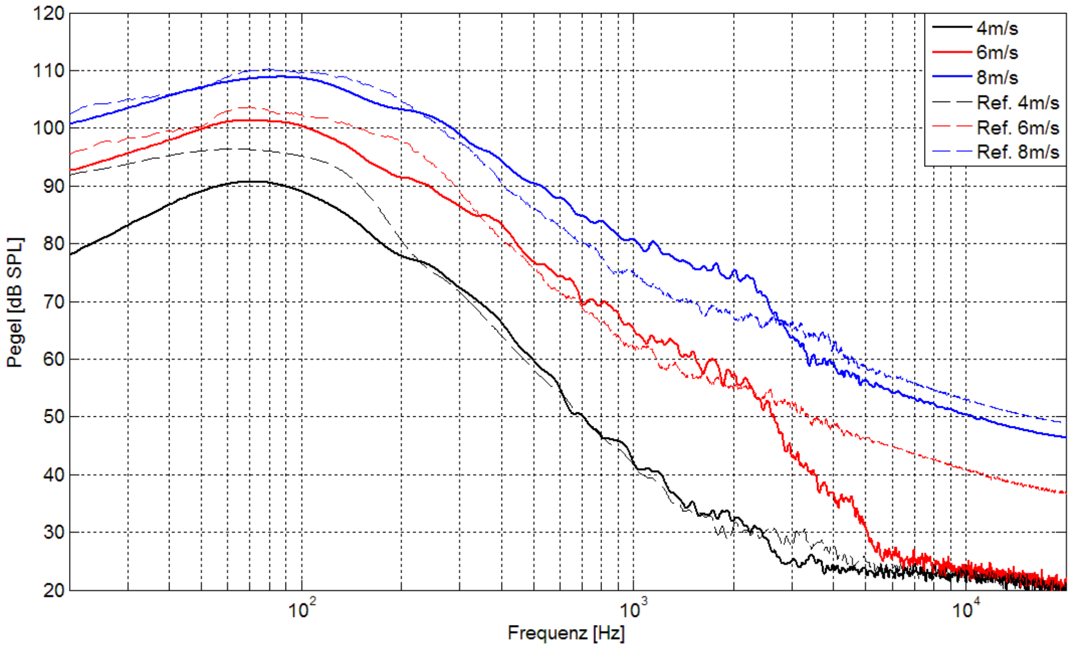

Figure 50: OMX70 with clay - flow noise in dummy head's ear at 0° wind attack

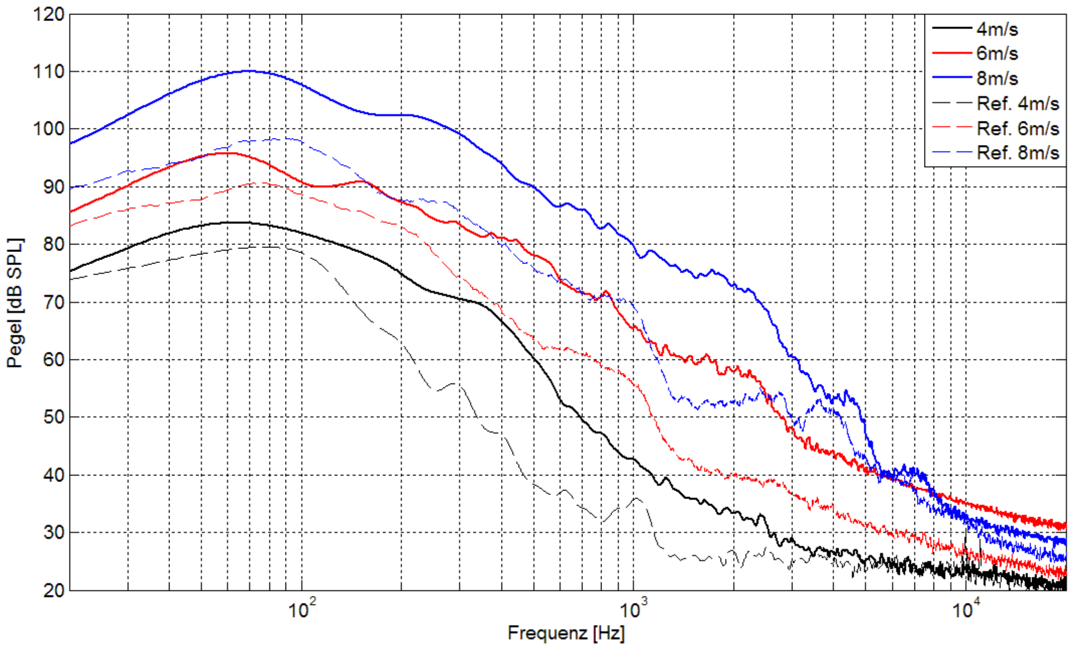

Figure 51: OMX70 with clay - flow noise in dummy head's ear at 45° wind attack

The circum- and supra-aural headphones reduce the flow noise for frontal wind incidence at least to the case of not-wearing a headphone, and sometimes even more, in particular in case of the HD457. But when changing the wind attack to 45° all headphones induce more noise than the reference measurement (no headphone) with exception of the PX100 model, which produces noise comparable to the naked ear. All ear buds increase flow noise compared to the naked ear.

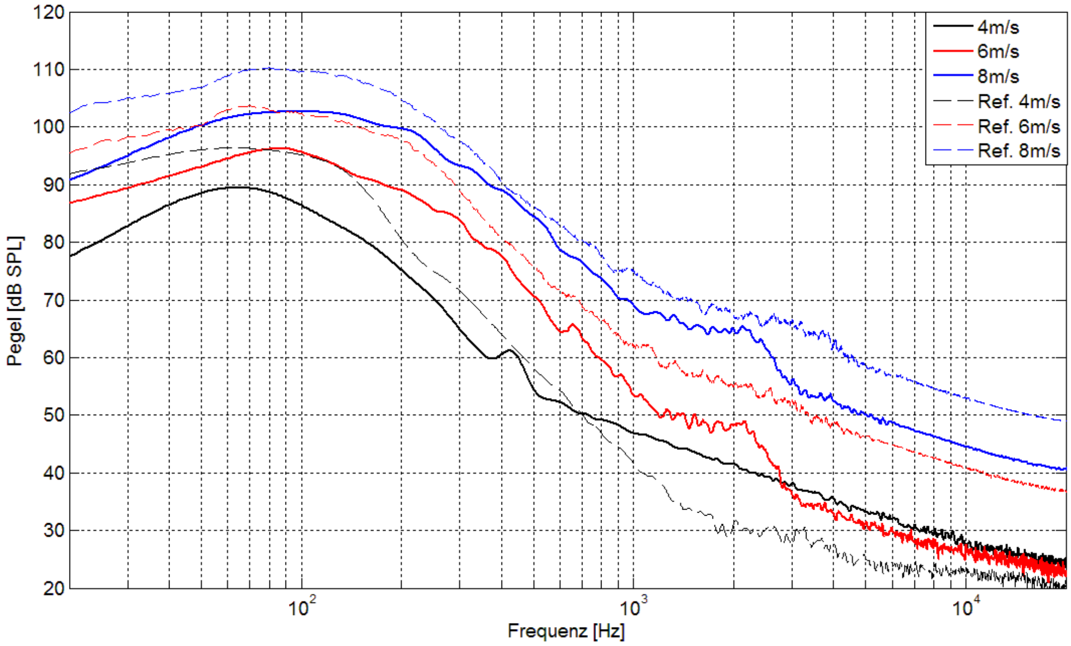

Figure 52: PX100 - flow noise in dummy head's ear at 0° wind attack

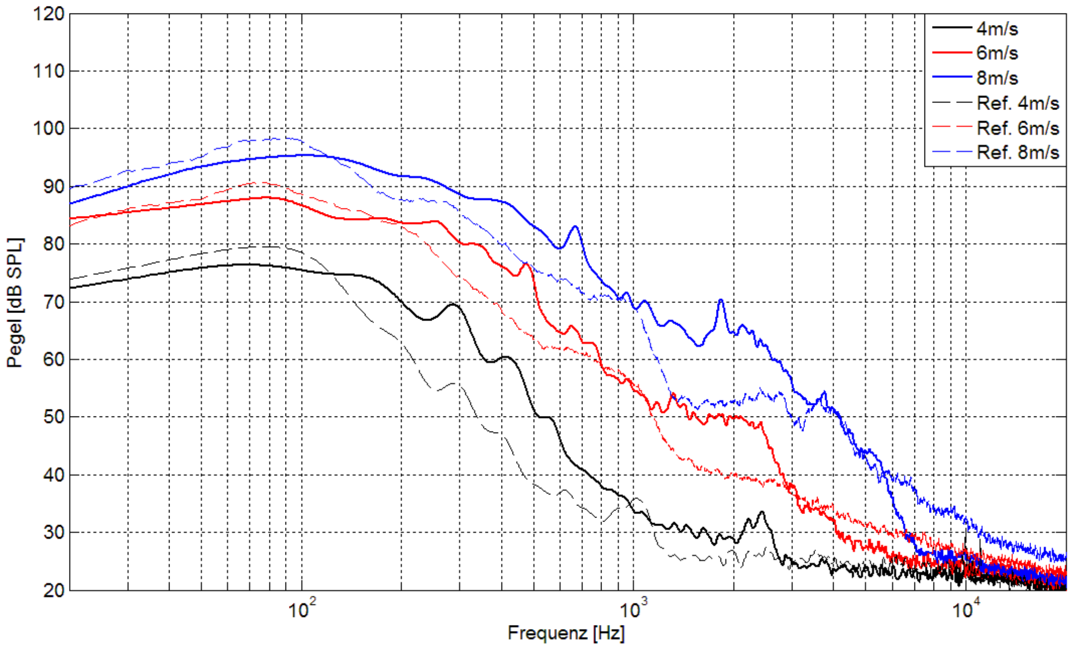

Figure 53: PX100 - flow noise in dummy head's ear at 45° wind attack

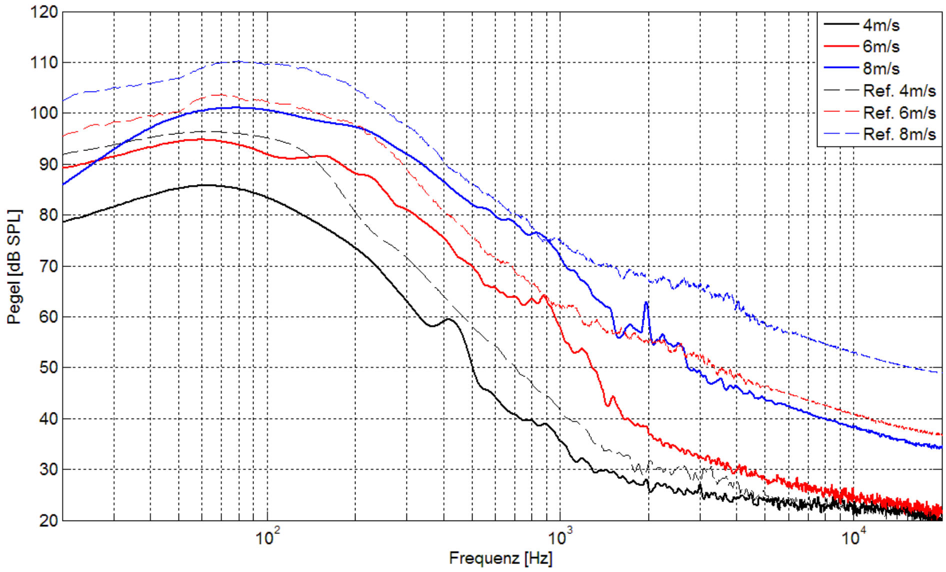

Figure 54: PX150 - flow noise in dummy head's ear at 0° wind attack

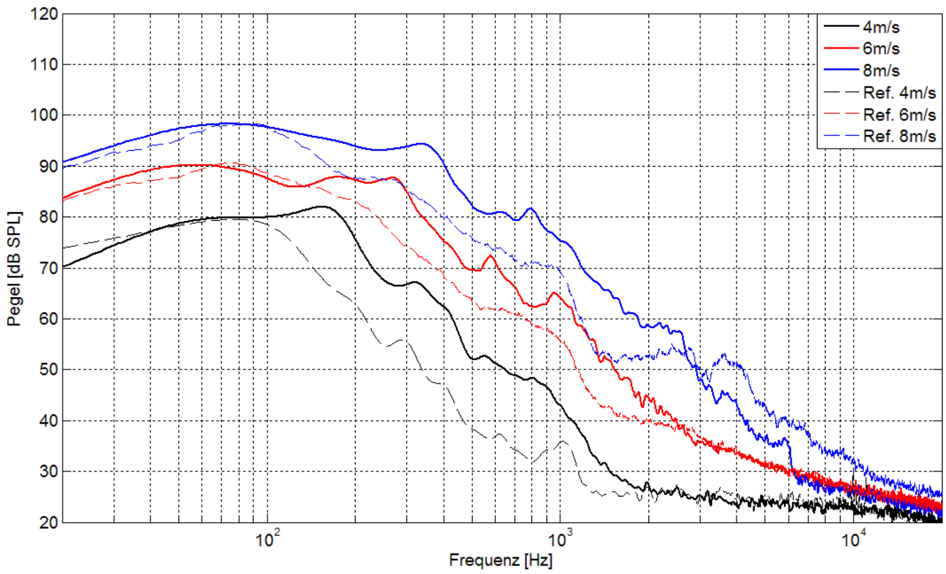

Figure 55: PX150 - flow noise in dummy head's ear at 45° wind attack

The large group of ear-buds and in-ear headphones produced quite similar results for flow-noise with maximum sound pressure levels of 110 dB and more in the frequency range from 80-120 Hz. The headphone with highest flow noise in this group is the OMX70 model at 45° wind incidence. Most earphones reduce the "natural" flow noise, in particular under the condition of a "tight" fit (clay, foam), some under 0°, some under 45° wind impact (MX660, PX100, MXL560, MXL70, MX75, LX70, eH150, PX150).

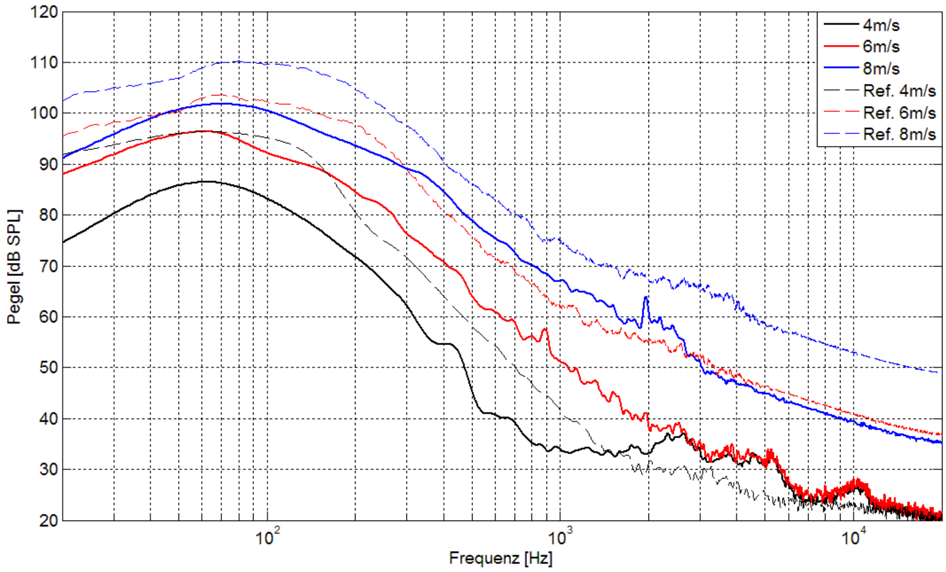

Figure 56: PX150 with ANC - flow noise in dummy head's ear at 0° wind attack

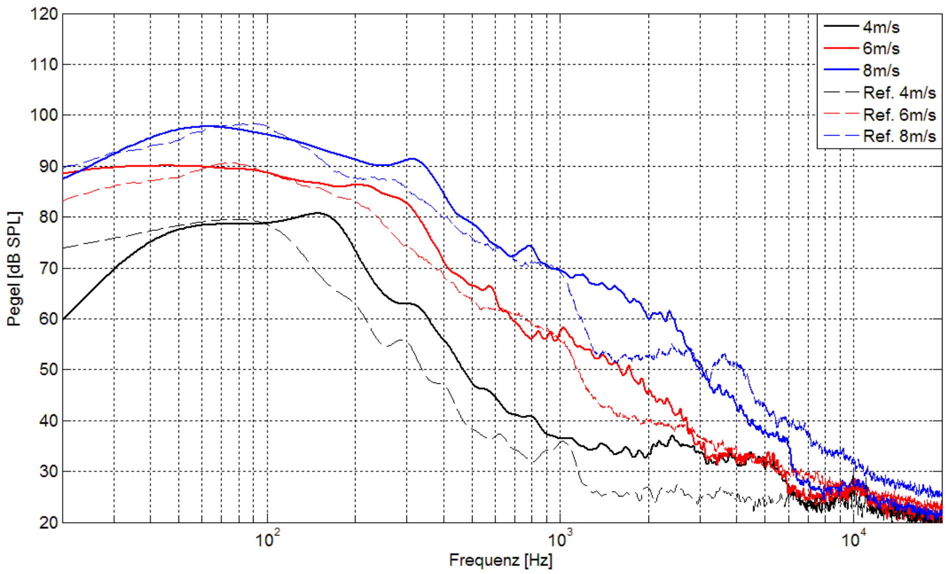

Figure 57: PX150 with ANC - flow noise in dummy head's ear at 45° wind attack

As a rule of thumb an increase of wind velocity by approximately 2 m/s results in an increase of flow noise about 5-10 dB for most headphones.

Applying clay and foam coating to the ear-buds reduced the flow noise by 5-10 dB.

4.2 Measurements with test subjects

Additionally to the dummy head measurements a test series is carried out with 10 subjects wearing the investigated headphones and sitting in the wind tunnel.

4.2.1 Set-up

The same WM61-A microphones which are used for the dummy head measurements are positioned in both ear canals of a test subjects with a foam rubber applied to the microphone in order to fix it in the ear canal (Fig. 58). The ear microphones are calibrated in the same way as described in 3.2 (see Fig. 8). The connecting wire is chosen to be very thin so that the test person is able to wear earphones like in normal usage. The only headphones for which flow noise with test persons is not investigated are the CX500. Due to the fact that they are in-ear headphones the microphones would have been pushed too far inside the ear canal of the test subjects when measuring flow noise.

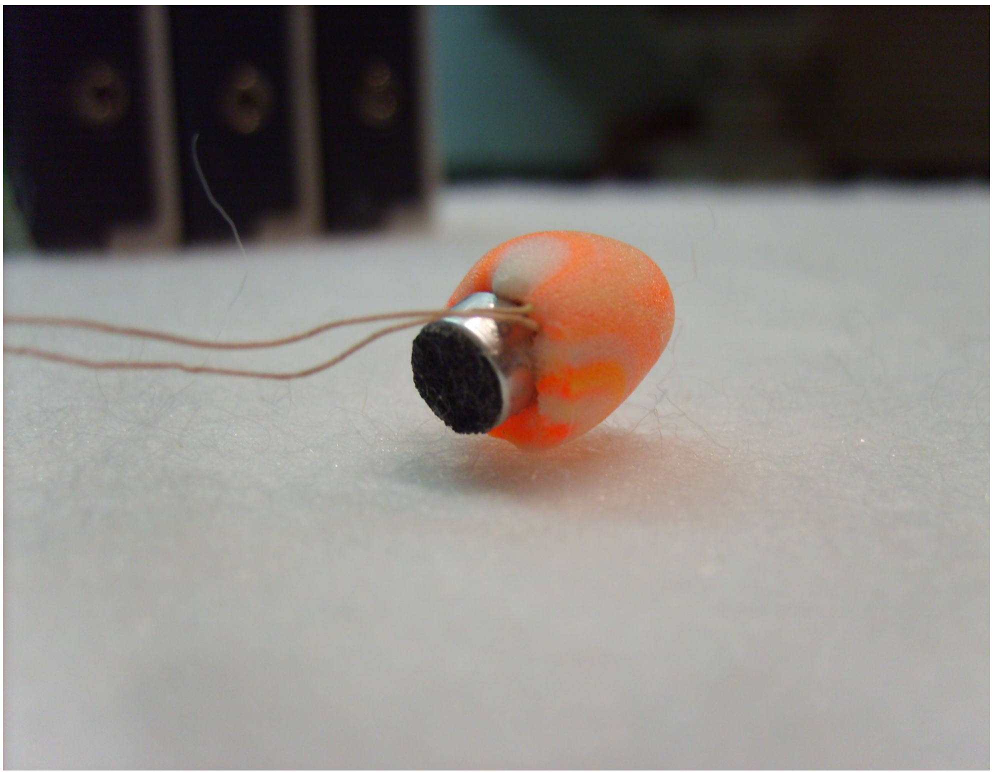

Figure 58: In-ear microphone for measurement with test subjects. The WM-61A is embedded in a soft ear-plug

The set-up is the same as described in 4.1.1 except the fact that two microphones, one in the left and one in the right ear canal of the subjects, are measuring flow noise simultaneously. Because of the limited time available for measurements in the wind tunnel and with respect to the test persons' comfort only the louder angle of wind incidence 0° is chosen for the measurements at a constant wind speed of 5.2 m/s. Assuming that the WM-61A microphones in the test subjects' ear canals show a similar drop-off at low frequencies as in the ear of the dummy head, the spectral weight in Fig. 7 is also applied.

4.2.2 Results

The results of the measurements with test persons are presented as an average of all individual measurements of the individual ears. A few measurement results are omitted due to background noise, and again due to turbulent pressure fluctuations. Therefore, the average flow noise measurements represent a slightly varying ensemble.

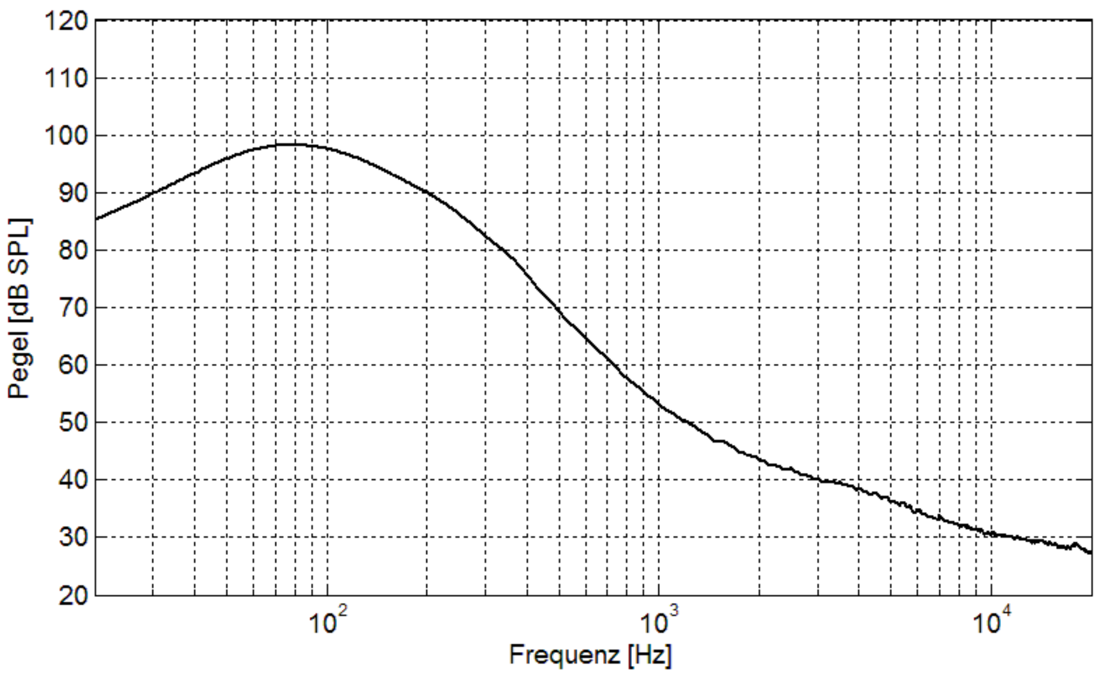

Figure 59: Reference measurement - test subjects (frontal wind impact of 5.2 m/s)

Fig. 29 Shows the basic flow noise measurement (average) for 0° wind attack with test subjects in the wind tunnel wearing *no* headphones. Compared to the measurement with the dummy head (Fig. 12) the flow noise is about 7 dB lower with a maximal level of about 98 dB around 80 Hz. The drop-off at high frequencies reaches 27 dB at 20 kHz.

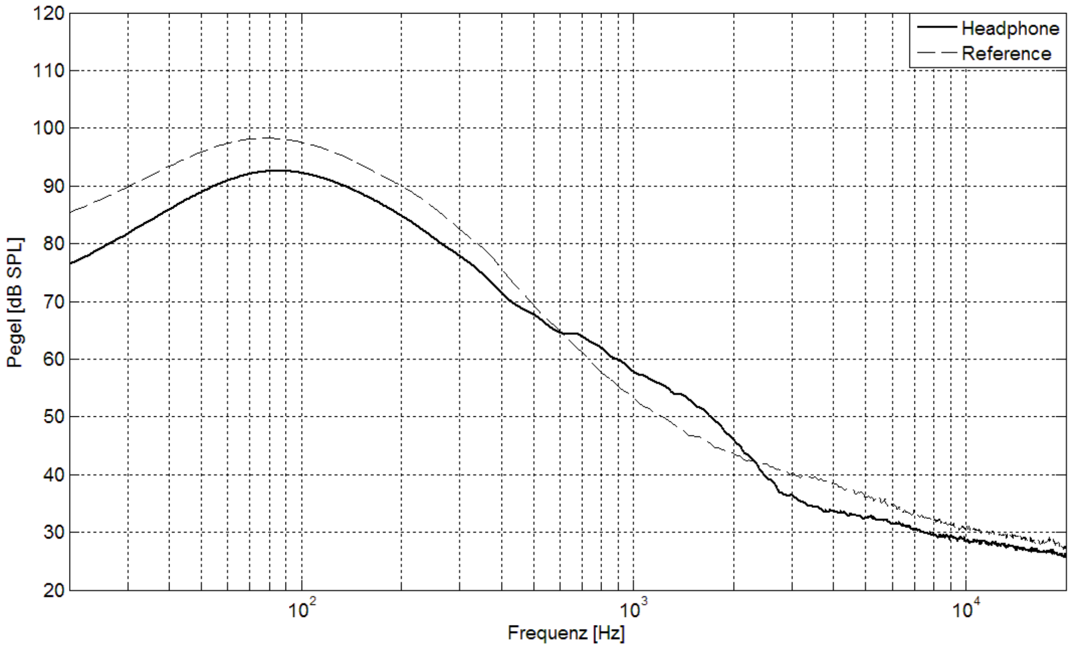

Figure 60: HD457 - test subjects

Wearing HD457 headphones reduces the flow noise at the “naked” ear up to 10 dB (at low frequencies), and has no additional effect above about 500 Hz (Fig. 60).

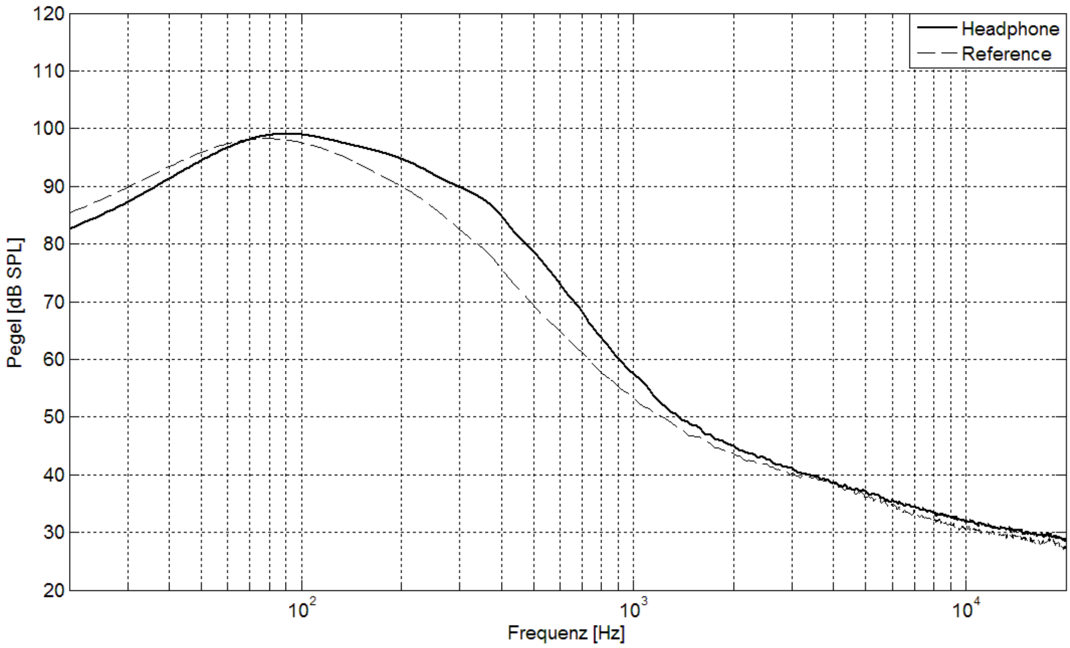

Figure 61: eH150 - test subjects

The eH150 headphones increase slightly the flow noise level from 100 Hz to 1 kHz up to 10 dB (Fig. 61).

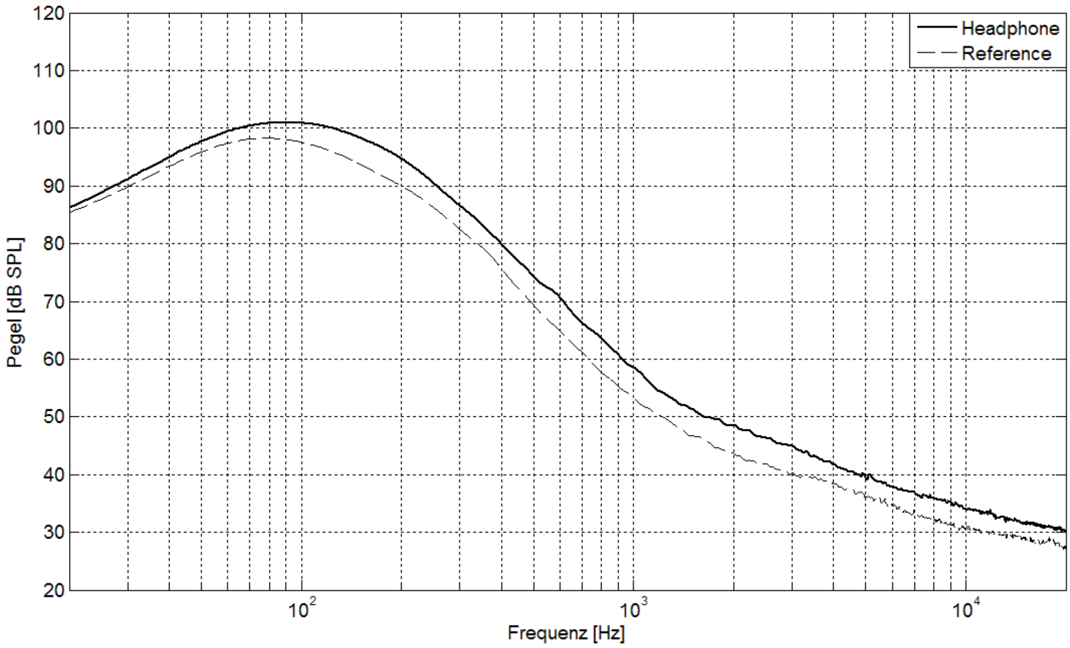

Figure 62: LX70 - test subjects

Also, the LX70 headphones increase slightly the flow noise about 5 dB over nearly the whole frequency range (Fig. 62).

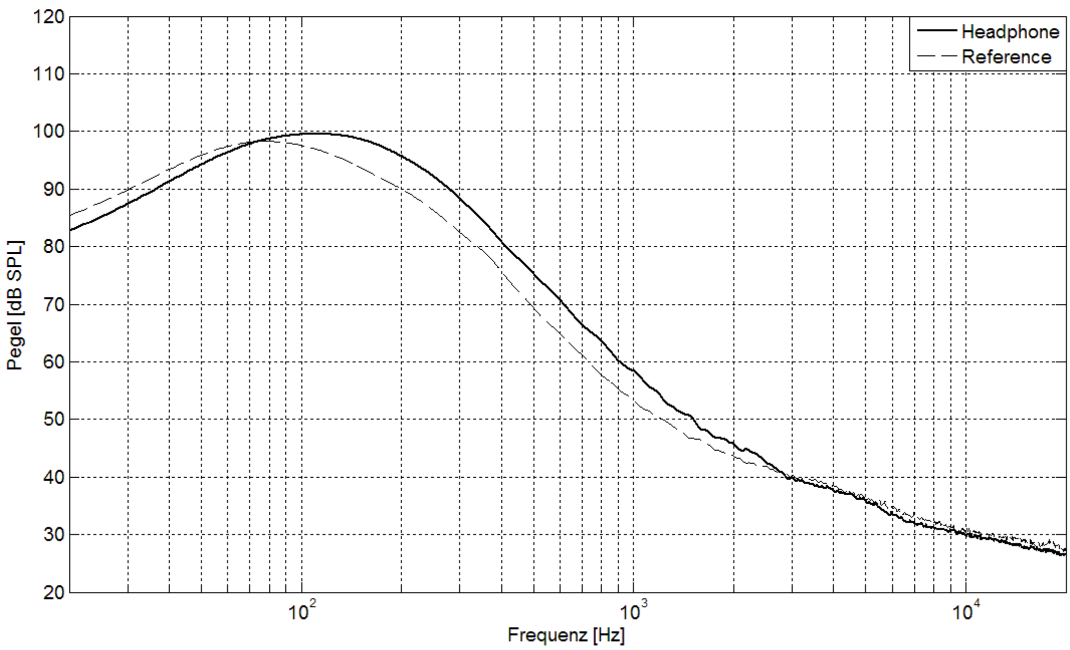

Figure 63: MX75 - test subjects

Compared to the LX70, less increase of flow noise is measured with the MX75 between 100 Hz and 3 kHz and a slight improvement at low frequencies (Fig. 63).

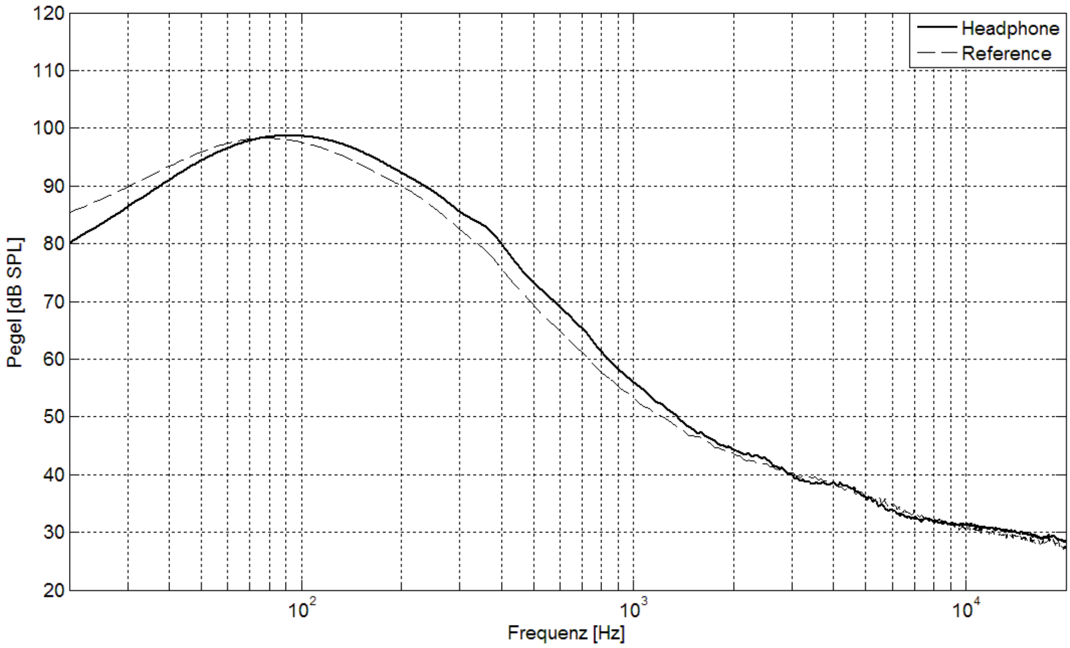

Figure 64: MX260 - test subjects

The MX260 show a similar behaviour as the MX75, but with less deviation from the flow noise measurement at the “naked” ear (Fig. 64).

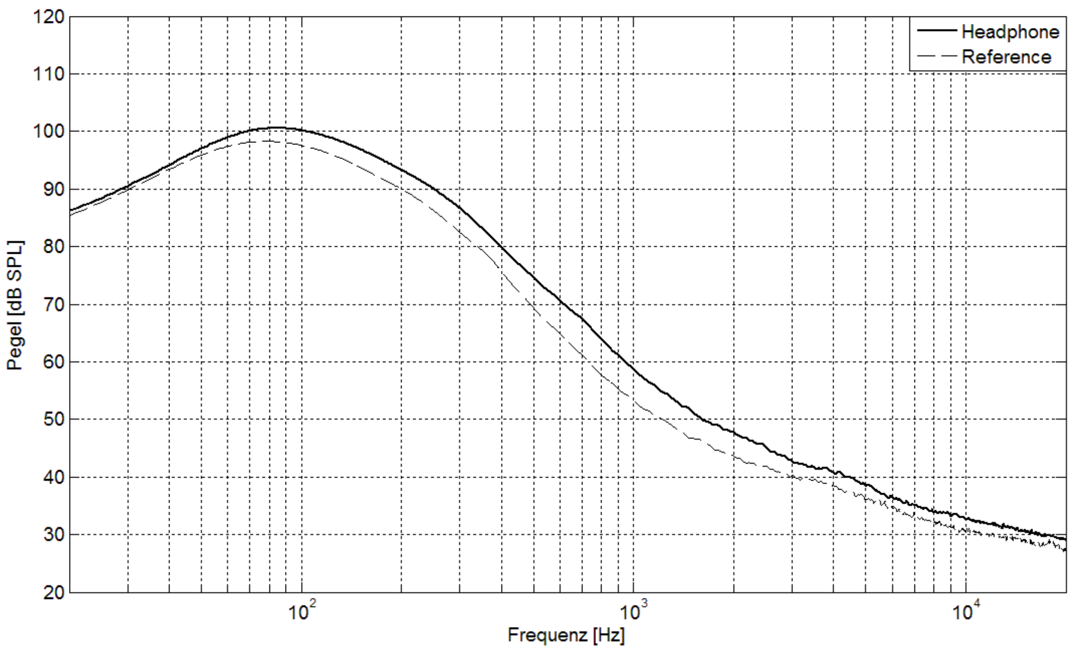

Figure 65: MX660 - test subject

MX660 headphones increase the flow noise level over nearly the whole frequency range - in the mid-frequency range up to 5 dB (Fig. 65).

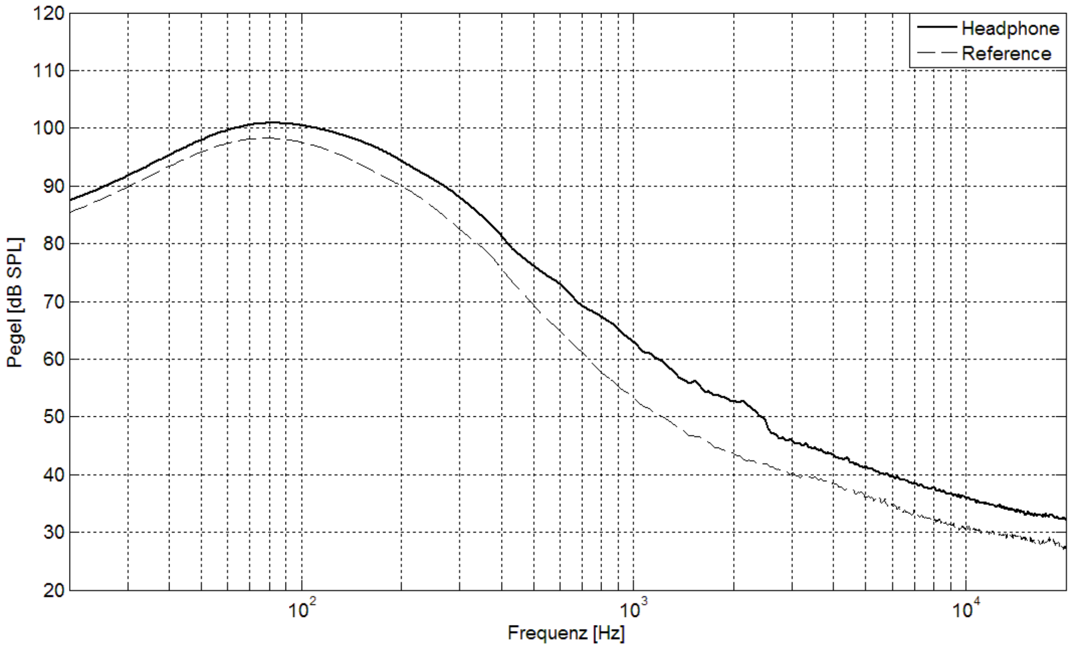

Figure 66: MXL70 - test subjects

The MXL70 measurement show a comparable large and broad-band increase of the flow noise level, in particular in the range of 1 to 3 kHz of more than 10 dB (Fig. 66).

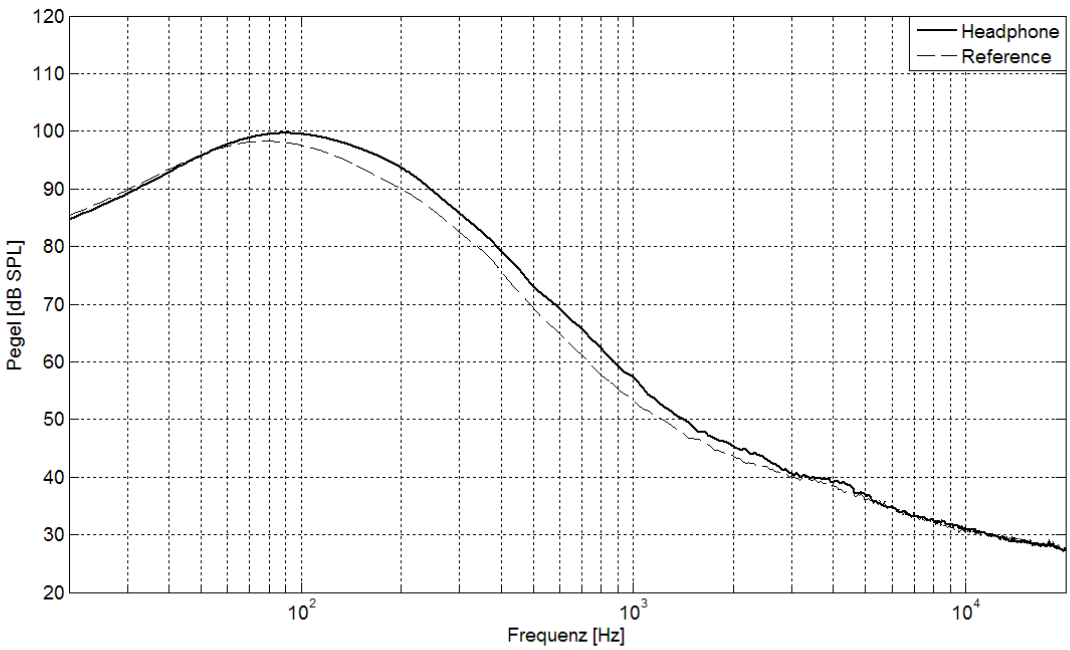

Figure 67: MXL560 - test subjects

The MXL560 headphones give only a slight increase in the flow noise between 80 Hz and 3 kHz (Fig. 67).

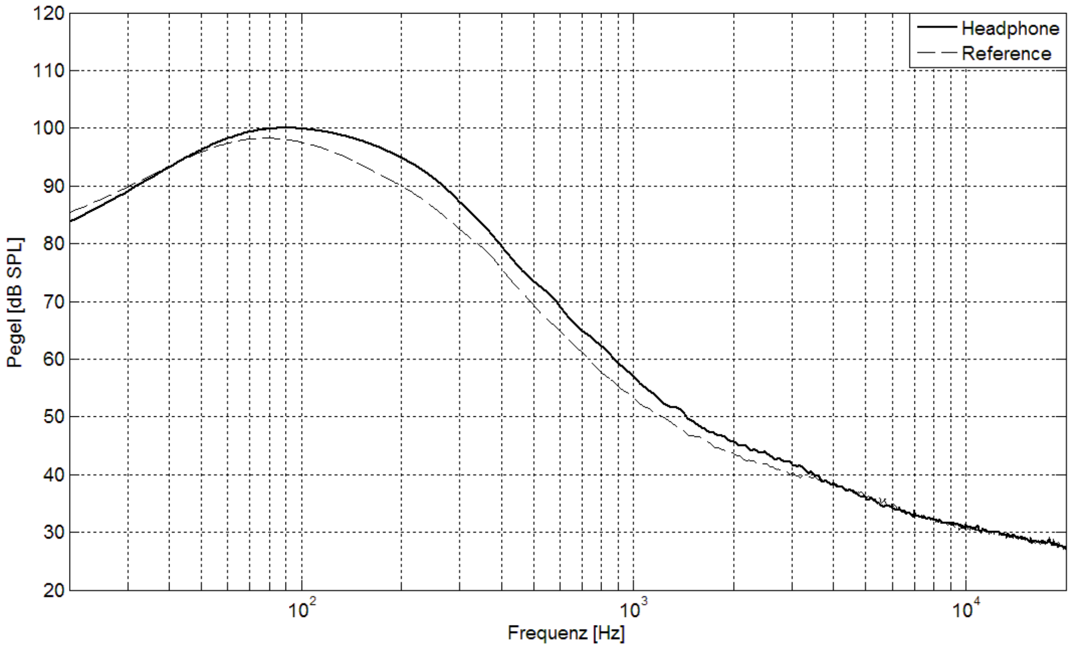

Figure 68: OMX70 - test subjects

The OMX70 headphones generate a slightly higher flow noise than the MXL560 in about the same frequency range (Fig. 68).

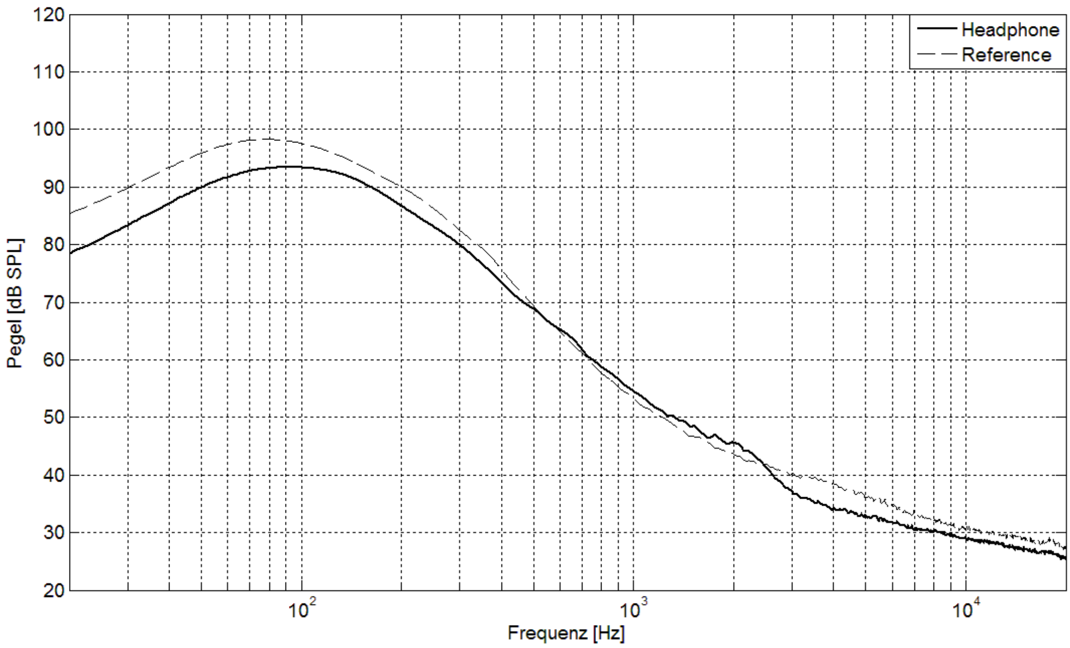

Figure 69: PX100 - test subjects

The PX100 headphone exhibit only at lower frequencies an increase in flow noise of maximal 7 dB (Fig. 69)

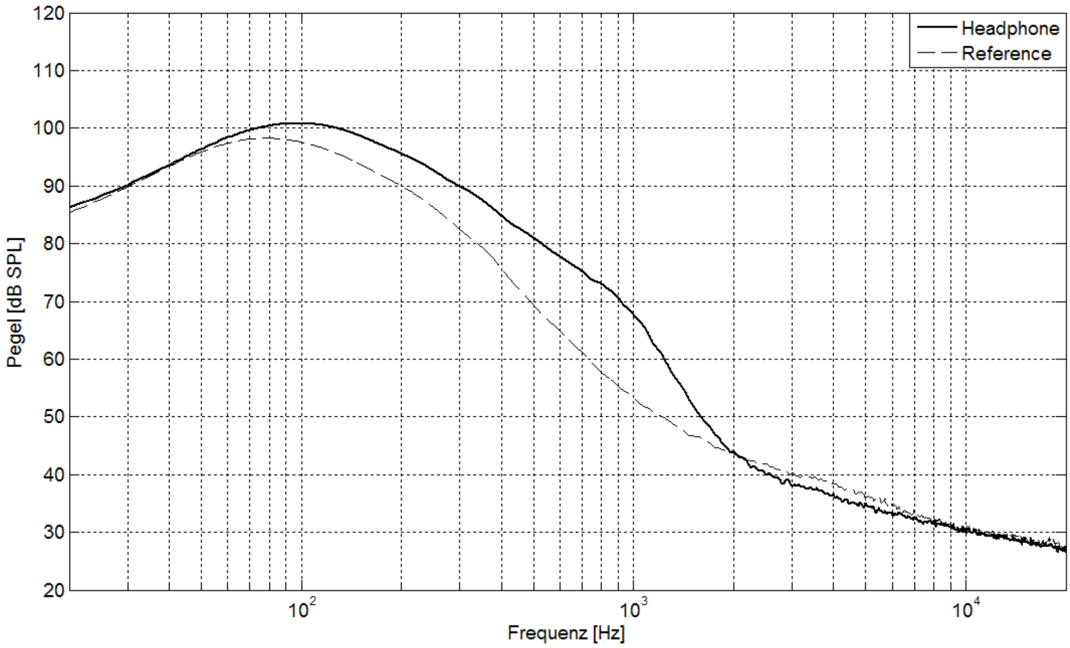

Figure 70: PXC150 - test subjects

The PXC150 (without ANC) give a considerable increase of flow noise in the mid-frequency range of up to 15 dB (Fig. 70).

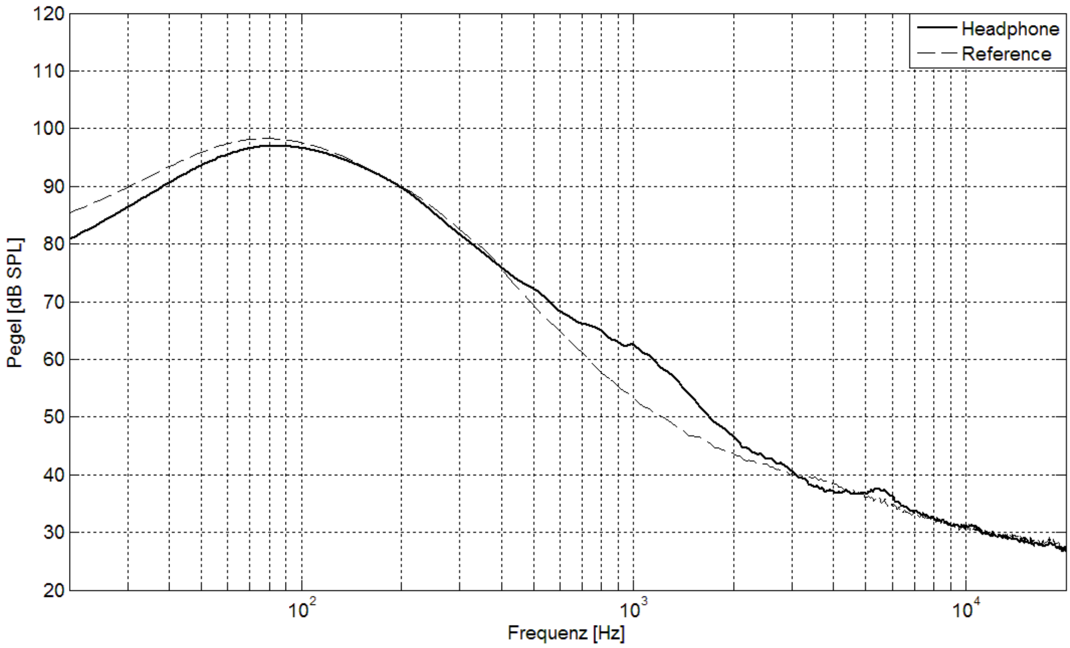

Figure 71: PXC150 ANC - test subjects

Turning on the ANC of the PXC150 reduced flow noise, partly to the condition of the "naked" ear, but still with a band-limited increase around 1 kHz (Fig. 71).

In general, the measurement of flow noise in the test persons' ears show a significant reduced flow noise compared to the dummy head measurements.

The only headphone which reduces flow noise compared to the test person wearing no headphone is the model HD457. The MX260, MXL560 and OMX70 give only small increase in flow noise, the PX100 only at low frequencies. But compared to the measurements in the dummy head's ear all headphones give rise to a more or less increase of flow noise. This could be due to the observation that the flow noise at the "naked" ear of a test person is significantly lower than the noise measured in the dummy head's ear.

4.3 Optimization

In order to investigate possible steps to reduce wind induced flow noise three headphones investigated. They are equipped with a small plastic shielding with the intention to "by-pass" the wind from the headphone. Measurements are made for 0° wind incidence and 5.2 m/s wind speed. The shielding is fixed to the headphones with modelling clay.

Fig. 70 shows the application for an eH150 headphone.

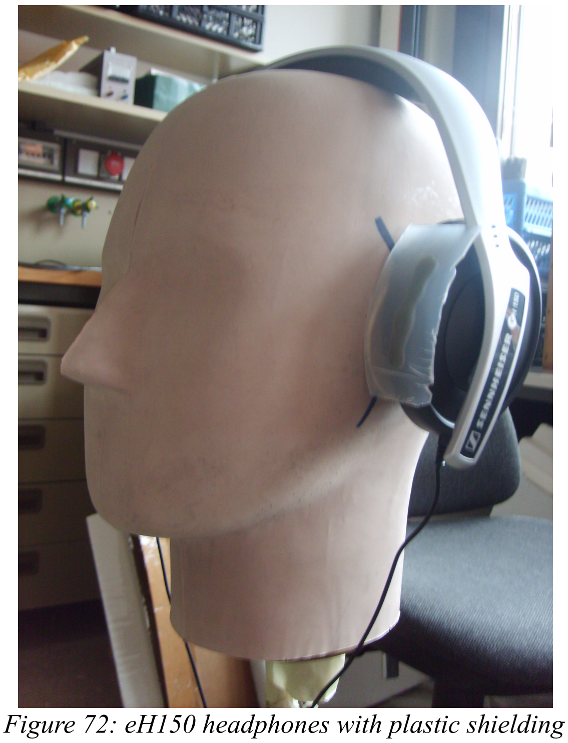

Figure 72: eH150 headphones with plastic shielding

The simple shielding yields in this configuration a considerable reduction of flow noise (Fig. 73).

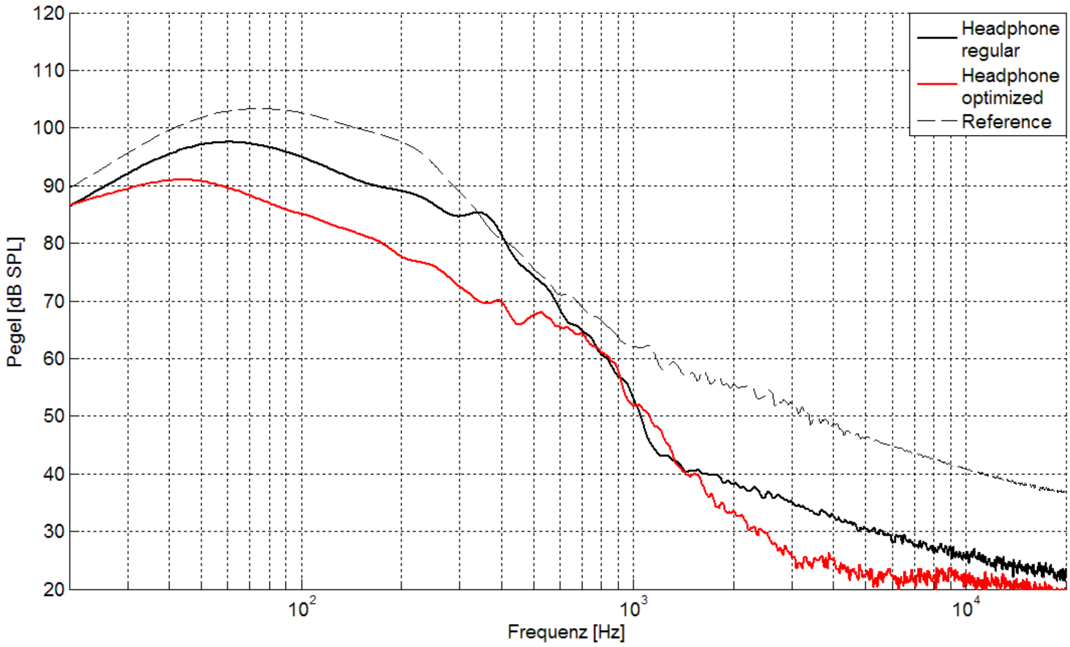

Figure 73: Flow noise for eH150 with and without shielding

The shielding of the eH150 lowers wind induced flow noise about 10-15 dB in the frequency range from 50 Hz to 700 Hz, and up to 10 dB above 2 kHz (meeting the noise floor of the measurement device).

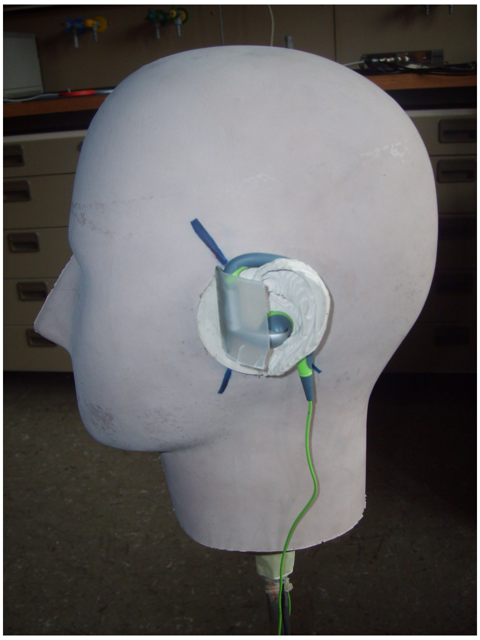

Figure 74: OMX70 headphones with plastic shielding

A second approach with shielding is applied for the OMX70 headphones (Fig. 74). The shielding is fixed with respect to the wind in a 90° and a 135° position.

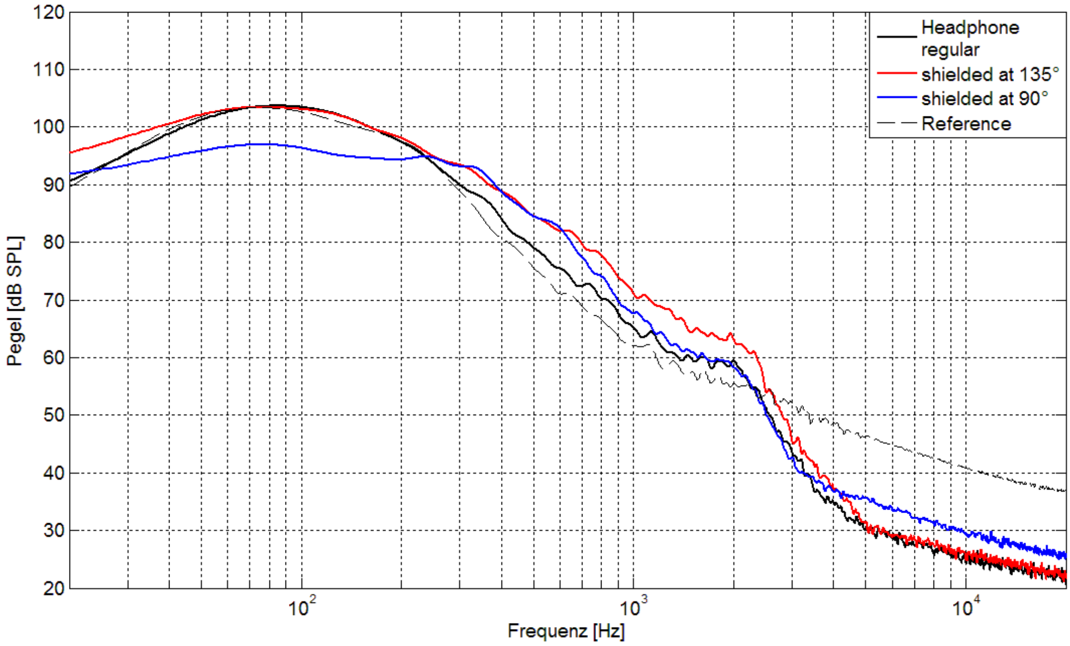

Figure 75: Flow noise for OMX70 with and without shielding

Fig. 75 Shows that only at 90° direction flow noise is reduced, about 5 dB for frequencies below 200 Hz. All configurations show an increase of noise above 200 Hz. It seems that turbulent pressure fluctuations are reduced by the shielding as the spectra decrease above 3 kHz down to the background noise floor.

Figure 76: MX660 headphones with plastic shielding

The third headphones measured with shielding are the MX660 (Fig. 76). The shielding is positioned such that it directly overlies the ear of the dummy head.

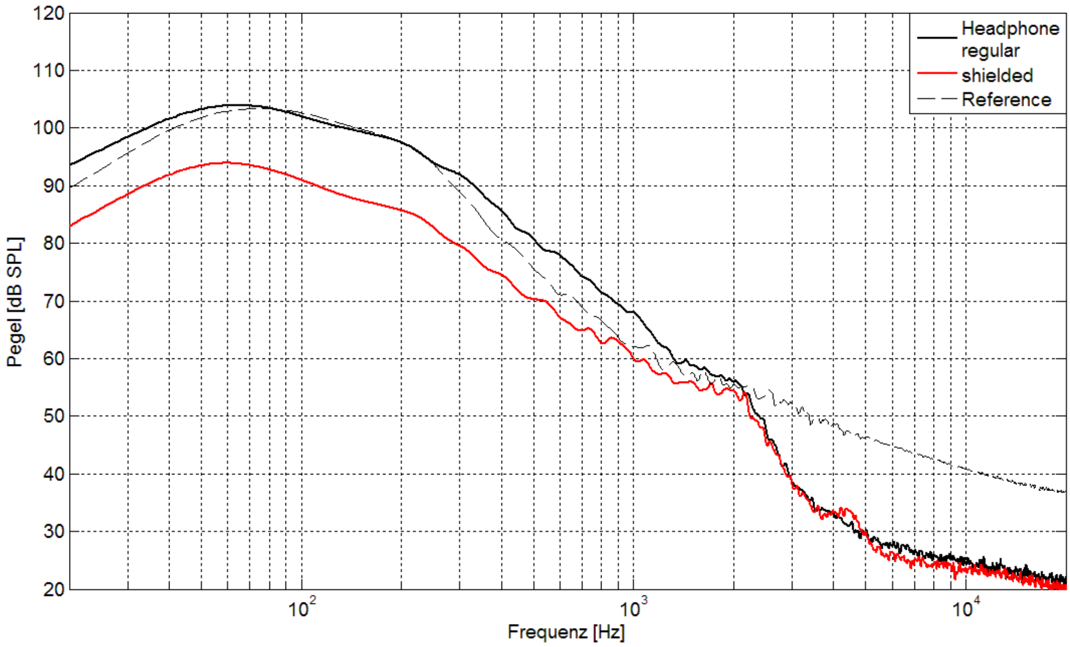

Figure 77: Flow noise for MX660 with and without shielding

The shielding reduces flow noise around the MX660 headphones by more than 10 dB in the low-frequency range (90 Hz to 200 Hz, Fig. 77). Note, that compared to Fig. 32 (MX660, "6 m/s" - measurement) the spectrum exhibits no overload from turbulent pressure fluctuations.

4.4 Subjective impressions of headphones found in the Internet

The Internet has become one major platform for formal and informal communication. A lot of bulletin boards and online stores give people the chance to share their experiences with certain products and evaluate them with respect to comfort, quality, price etc..

Some headphones reviews have been found in the Internet which will be summarized in this section.

The first review found is for the eH150 headphones [4]. The customer is disappointed that the headphones do not fit over his whole ear and he does not consider them as supra-aural headphones even though they are designed in such a way. The same problem occurred during the measurements where smaller artificial ears have to be attached to the dummy's head so that the eH150 covers the whole pinna. The sound quality is reviewed to be good (another customer even: “awesome”) but the headphones insufficiently block out the ambient noise which might be caused by the small size of the ear cups. Nothing is referred about flow-induced noise.

The next reviews are found for the PXC250 headphones a further developed version of the PXC150 headphones ([5], [6]), also having active noise control integrated. Both customers bought the noise cancelling headphones to lower the engine noise while travelling by plane. As reported, the noise is reduced quite well while travelling except for propeller driven air planes, and when sitting behind the turbines in a plane. By pressing the headphones to the ear and by wearing them a long time until the foam of the headphones becomes softer the noise is further reduced, the reviewers say. Nevertheless the low frequent hum of the engine is still audible. With ANC turned off the sound quality is reduced significantly.

The MX75 headphones are too noisy for a customer when wind is producing flow noise, as reported in [7].

The OMX70 earphones are rated quite positive by numerous customers saying that these model blocks out ambient noise quite well [8]. Additionally, it is reported that the OMX70 reduces “wind noise” while jogging. This is in slight contradiction to the measurement results: The dummy head measurements show a small increase of flow noise with the OMX70 headphones for 0° wind impact (Fig. 48) and some more for 45° attack (Fig. 49), which is reduced in a “tight-fit” condition (Figs. 50, 51). Test-person measurements produce a small increase of flow noise (Fig. 68). Shielding reduces flow noise a little bit for this model (Fig. 75).

5 Discussion & summary

All investigated headphones show a low-frequency roll-off. This drop is due to the near-field situation and the compromise to take advantage from the “free-field” performance of an open earphone system compared to a pressure-chamber reproduction. The best bass production is found for the HD457 headphone which has also the biggest dimension and is supra-aural. The lack of low-frequency reproduction gives rise to a considerably reduced dynamical range and even masking effect under a wind-flow noise condition. In the appendix (Chapt. 7.4), the (spectral) difference between the headphone transfer function and the respective flow noise measurement is listed for the dummy-head measurements. All headphones show “negative” dB values at low frequencies, indicating that the wind-induced flow-noise exceeds the sound level produced by the ear-phone. Note, that the transfer function refers to a reproduction level of 72 dB(A) (see Chapt. 3.2).

Noise produced by wind when wearing headphones depends on the angle of wind incidence and on wind speed. Noise becomes loud for frontal wind exposure and high wind speed. Increasing the wind speed by approximately 2 m/s causes an increase of flow noise about 5-10 dB in the investigated range of wind velocity (2 – 8 m/s).

The spectra of all flow noise measurements exhibit a maximum in the frequency range from 60-130 Hz and then decay continuously to sound pressure levels of 20-30 dB at 20 kHz, which is about the noise floor of the measurement set-up in the wind tunnel. Wind-induced tonal components are only observed in one case.

When applying some (simple plastic) shielding to various headphones the wind induced flow noise is reduced by approximately 10 dB. Problem with a shielding is to implement them in such a way that a good appearance of the headphones is maintained. Further investigation could help to find an optimum between noise reduction and nice appearance.

6 References

[1] Weber, R., and V. Mellert (1978). Ein Kunstkopf mit "ebenem" Frequenzgang. DAGA '78, Bochum, Deutschland, 1978. ISBN: (3-8007-1147-8), pp. 645-648. VDE-Verlag GmbH.

[2] Trampe, Ulrich (1988), Akustische Übertragung des durchschnittlichen anthropomorphen Außenohres. Diplomarbeit. Universität Oldenburg, Arbeitsgruppe Akustik

[3] http://www.spiraxsarco.com/images/resources/steam-engineering-tutorials/4/3/fig4.3.18.gif

[4] http://www.amazon.com/review/product/B00067OF80/ref=cm_cr_pr_hist_2?%5Fencoding=UTF8&filterBy=addTwoStar

[5] http://www.ciao.de/Sennheiser_PXC_250__Test_2595208

[6] http://www.amazon.com/review/product/B000089GN2?showViewpoints=1

[7] http://www.amazon.com/review/R1QAZPNHAQPFXR

[8] http://www.amazon.de/gp/product/B000FJEZ0C

7 Appendix

7.1 Pictures of headphones

HD457

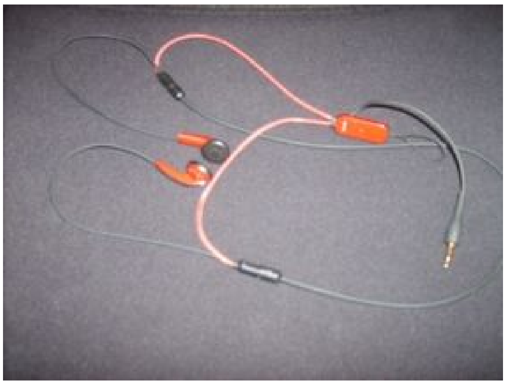

MXl560

MX660

OMX70

MX260

MXl70

eH150

PXC150

MX75

LX70

CX500 taken from
http://www.sanalmarketim.com/_prod/_img/l/d8ec9d1c0f_cx500white.jpg

PX100 taken from
http://www.discountdiscs.co.uk/Merchant2/graphics/00000002/PX100W.jpg

7.2 Matlab scripts

```
%-- file for measuring transfer functions of headphones with MLS noise
--

% This routine calls: pa_wavplayrecord.m, GetIR_xcorr.m, GetIR_wind.m,
clear all;
clc;
load('MLS'); %MLS signal
load Entzerr4.mat; %Filter


fft_size = 9600;                % leads to freq-resol. of 5 Hz at
48kHz f_s
fs=48000;
Fs=fs;
bin_breite = fs/fft_size;       % 5 Hz per sample

% -- just for display later---
for bin = 1:fft_size/2+1
    v_freq(bin) = bin*5;
end

record_ = pa_wavplayrecord(0.004*MLS,0,fs,0,1,1,0,['asio']) %recording
save Kopfhörer_Messungen\checkamplitude_HD457_2 record_



IR=GetIR_xcorr(record_, MLS, 10); %cross correlation

IR_short= GetIR_wind(IR,500, 1000, 495, 505); %short cross correlation

FFT_of_IR = fft((IR_short), fft_size); %FFT of cross correlation

magnitude1 = 20*log10(abs(FFT_of_IR(1:fft_size/2+1)));%transformation
to dB


% Adding the filter to the spectrum
for n=1:4801
magnitude1(n)=magnitude1(n)+Entzerr4(n);
end

%Plotting the spectrum
%+85 caused by the correction factor C=68, of the microphone which was
%added afterwards in this case
semilogx(v_freq, magnitude1+85,'b')
title('CX500 - Übertragungsfunktion')
xlabel('Frequenz [Hz]')
ylabel('Pegel [dB SPL]')
axis([20 20*10^3 40 100])
grid
```

```
% -- file for measuring the spectrum of wind induced flow noise
% -- just FFT and smoothing with an additional correction-Therm for
the mic
%
 clear all;
 clc;
 load Entzerr4.mat %Filter


fft_size    = 9600;        % leads to freq-resol. of 5 Hz at 48kHz
f_s
fs          = 48000;
rec_time    = 10;
bin_breite  = fs/fft_size;  % 5 Hz
C           = 68;           % Korrekturfaktor für Panasonic-kapsel,
mittels B&K-Levelmeter ermittelt

% -- just for display later---
v_freq = 0:(fs/fft_size):(fs/2);


% ---------------------------------------------------------

record_1 = pa_wavrecord(1,1,rec_time*fs,fs,0,['asio']);  %recording
save Windkanal_Messungen\Testmessungen\record_LX70knete_8mpros_0;
% ---------------------------------------------------------



FFT_record1 = fft((record_1(15:rec_time*fs)),(fft_size)); %FFT
magnitude1 = 20*log10(abs(FFT_record1(1:(fft_size/2+1))))+C;
%transformation to dB
smooth_magnitude1=moving_average(magnitude1,20); % planing the
spectrum

% Adding the Filter
for n=1:4801
    smooth_magnitude1(n)=smooth_magnitude1(n)+Entzerr4(n);
end

%Plotting the resulting spectrum
figure()
plot(v_freq,smooth_magnitude1)
title('CX500 - 0° - 10s Mittelungszeit')
xlabel('Frequenz [Hz]')
ylabel('Pegel [dB SPL]')
legend('4m/s')
axis([20 20*10^3 20 120])
grid
```

7.3 Frequency response of WM-61A microphone

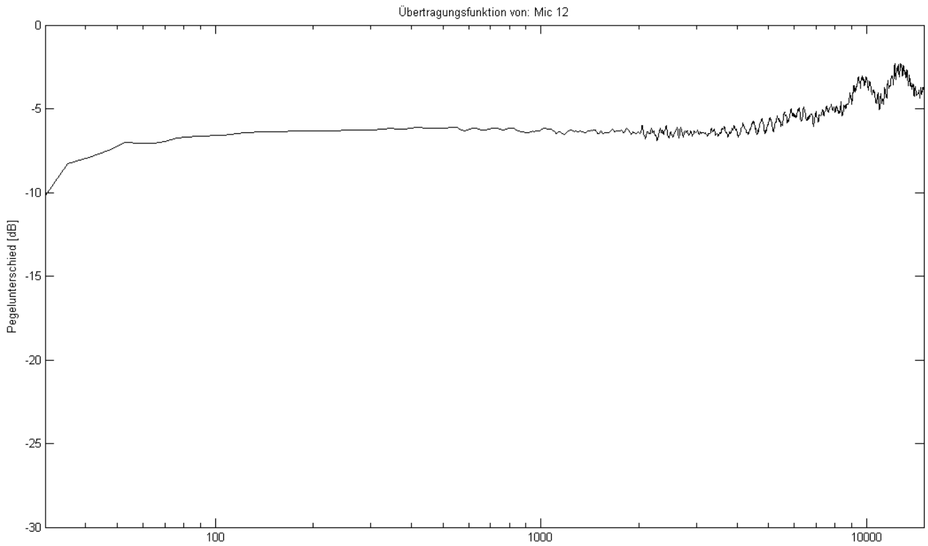

Deviation of WM-61A microphone from ideal linear frequency response

7.4 Difference between transfer function and flow noise

Transfer function is measured at a level of 72 dB(A) (cf. Chapt. 3.2).

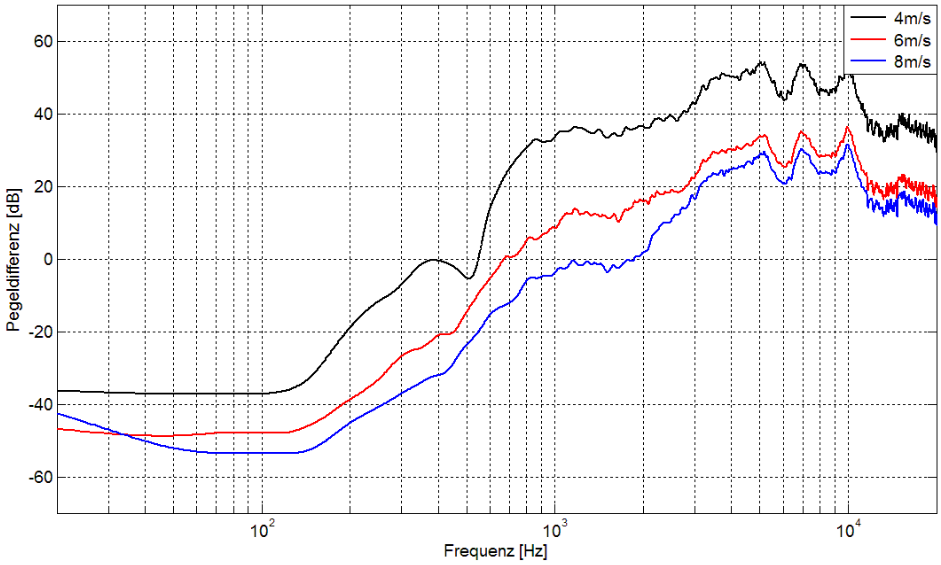

Dynamic of CX500 at 0° wind attack

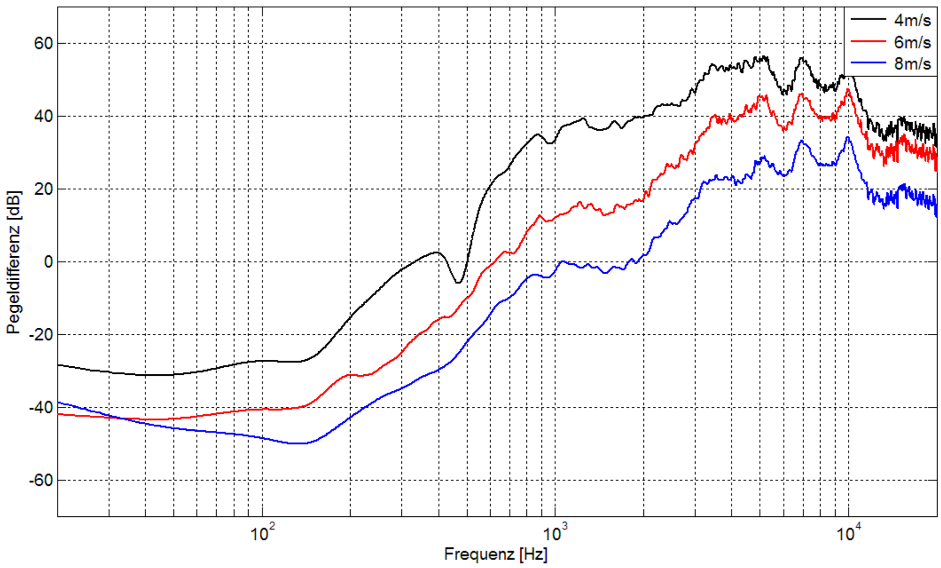

Dynamic of CX500 at 45° wind attack

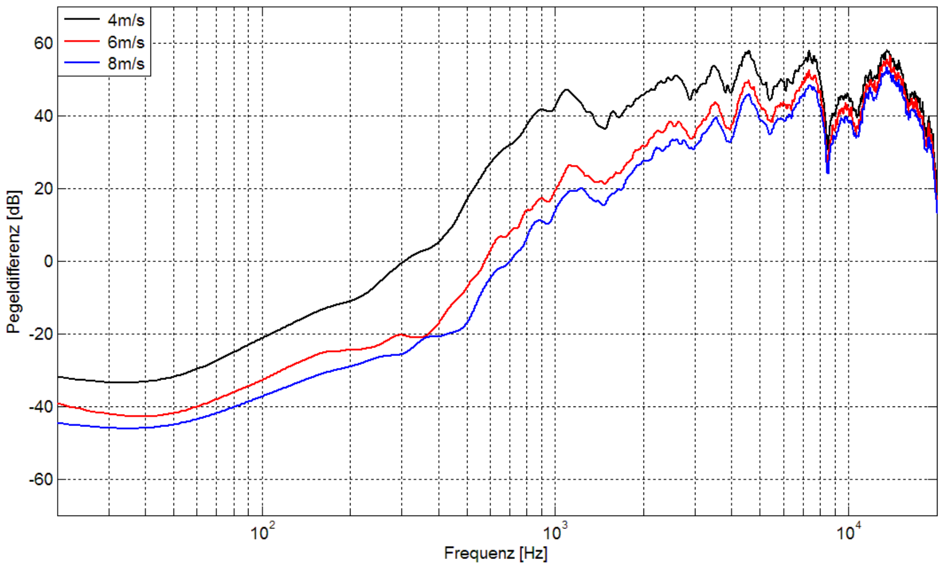

Dynamic of eH150 at 0° wind attack

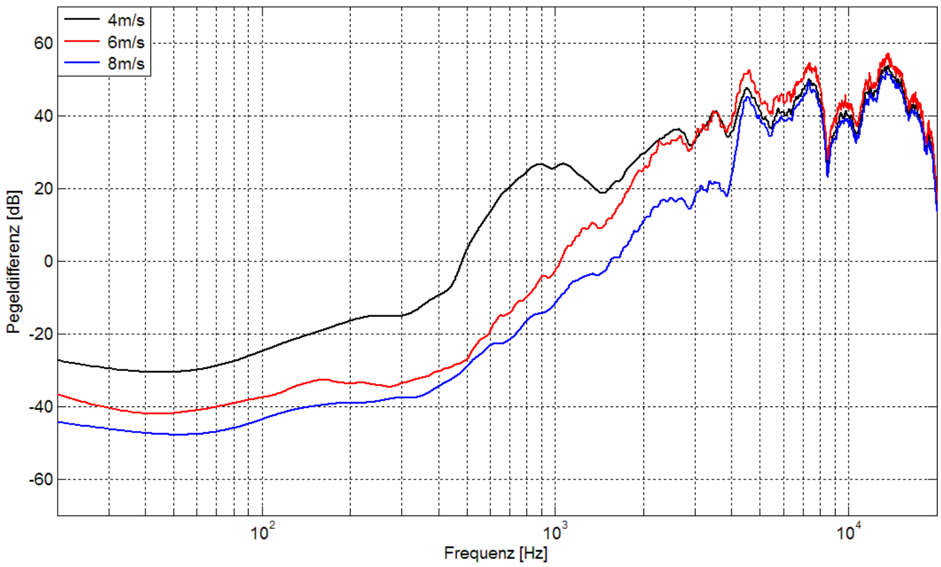

Dynamic of eH150 at 45° wind attack

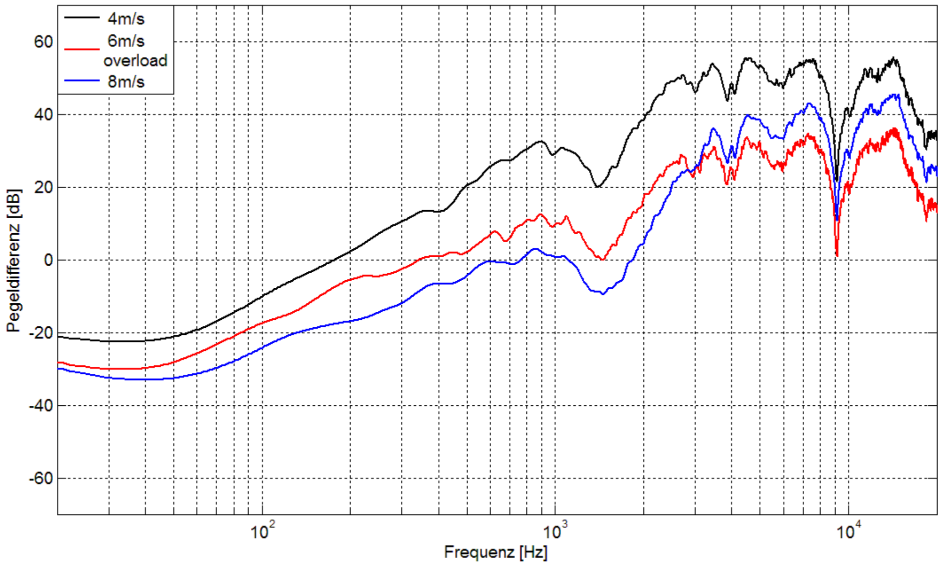

Dynamic of HD457 at 0° wind attack

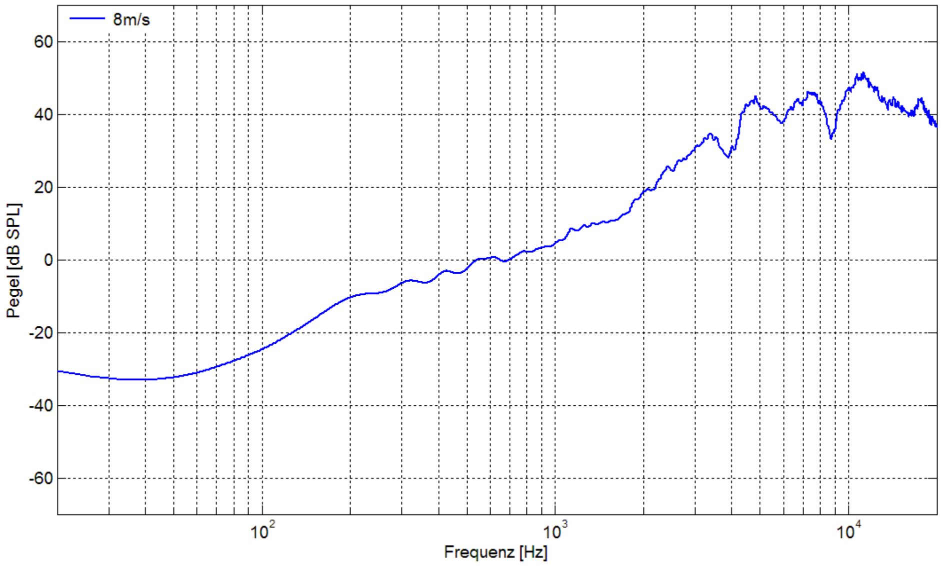

Dynamic of HD457 at 45° wind attack (due to overload only 8 m/s depicted)

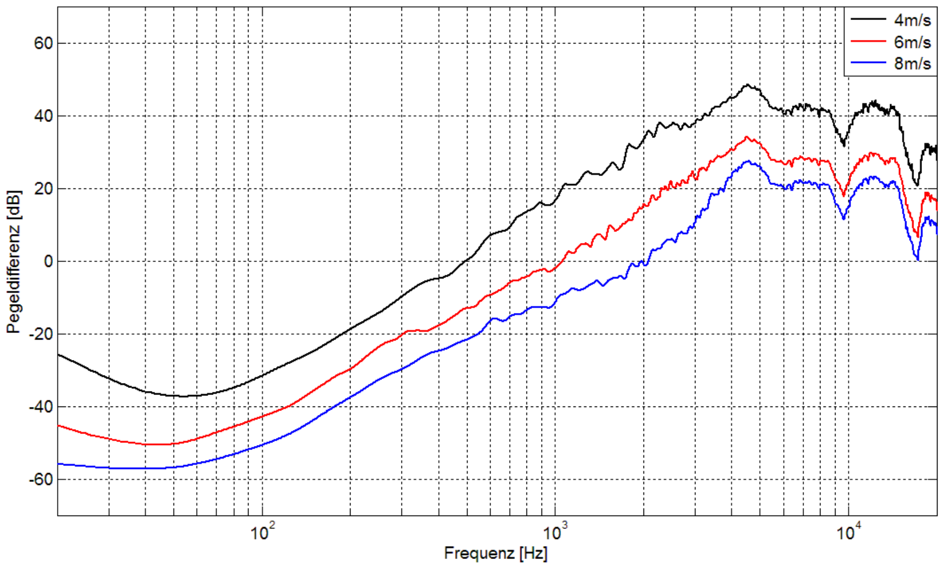

Dynamic of LX70 at 0° wind attack

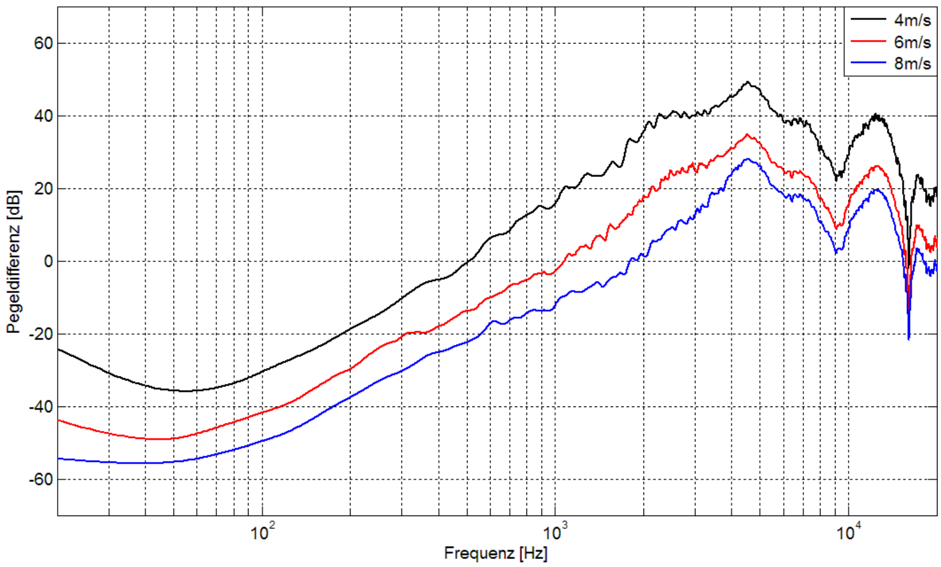

Dynamic of LX70 at 0° wind attack with a "tight-fit" condition

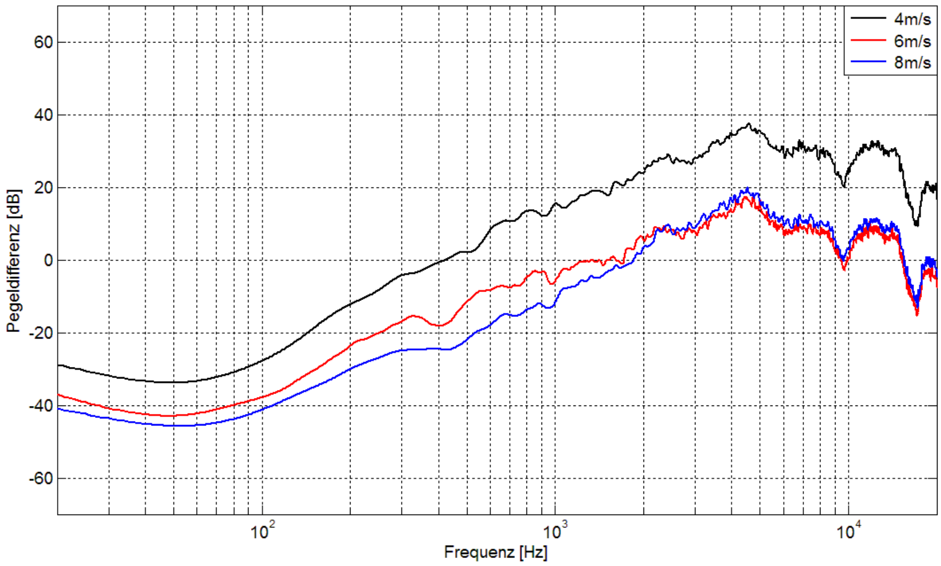

Dynamic of LX70 at 45° wind attack

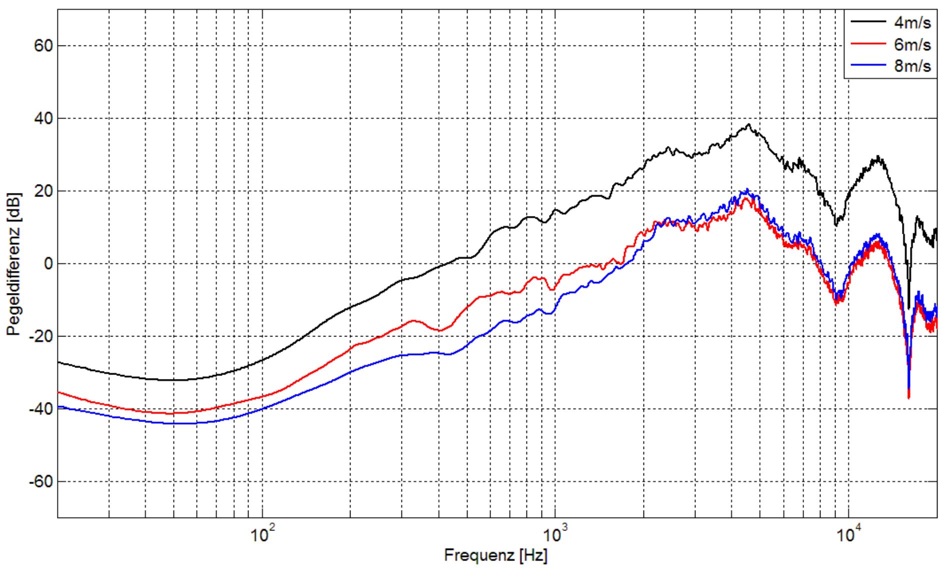

Dynamic of LX70 at 45° wind attack with a "tight-fit" condition

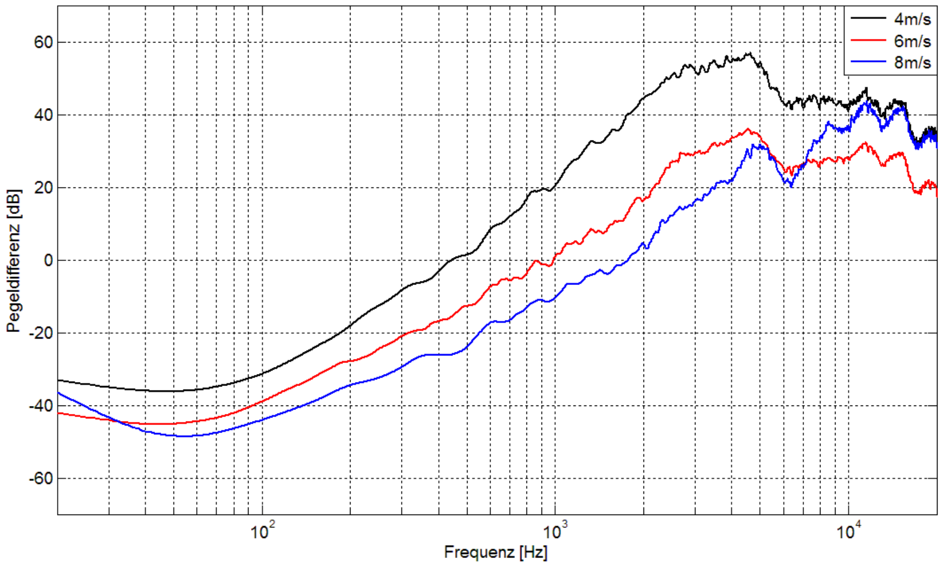

Dynamic of MX75 at 0° wind attack

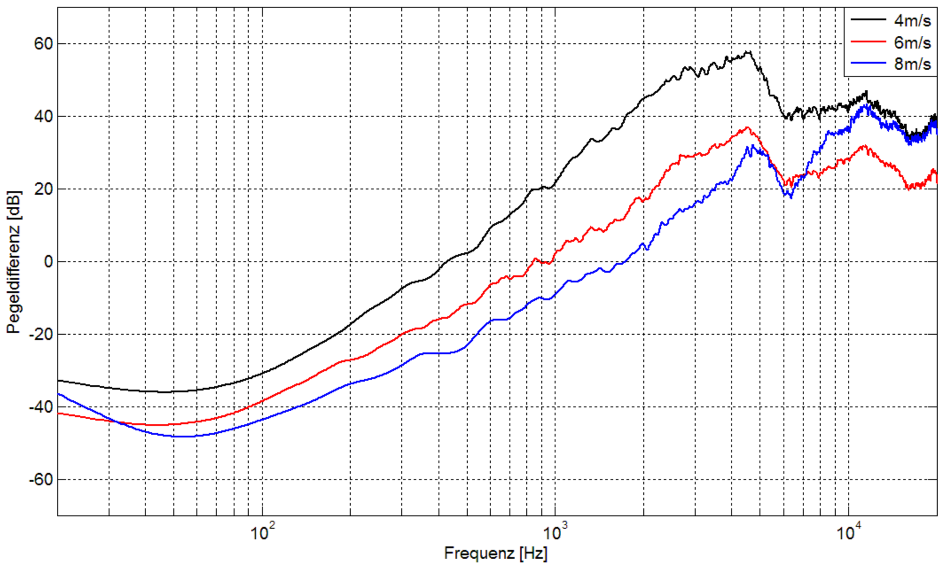

Dynamic of MX75 at 0° wind attack with a "tight-fit" condition

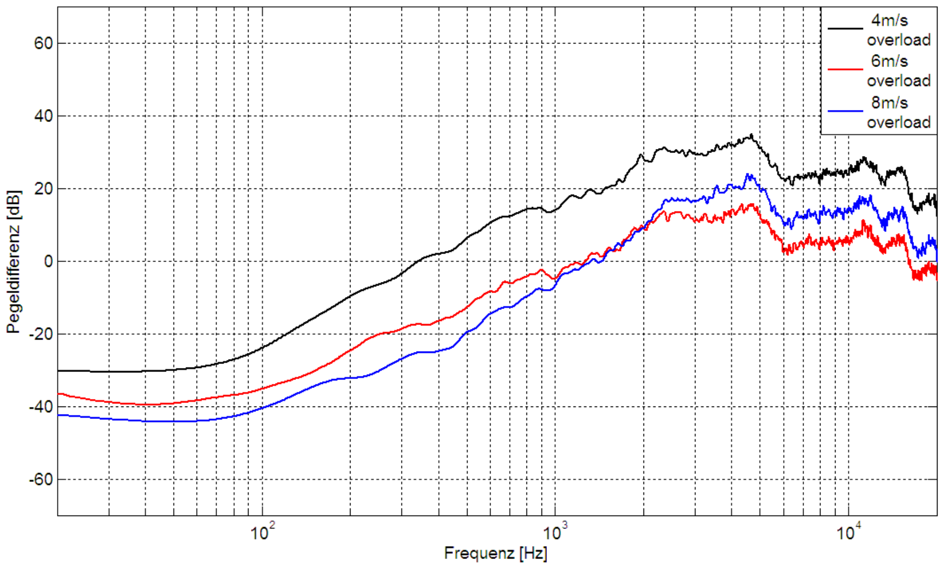

Dynamic of MX75 at 45° wind attack

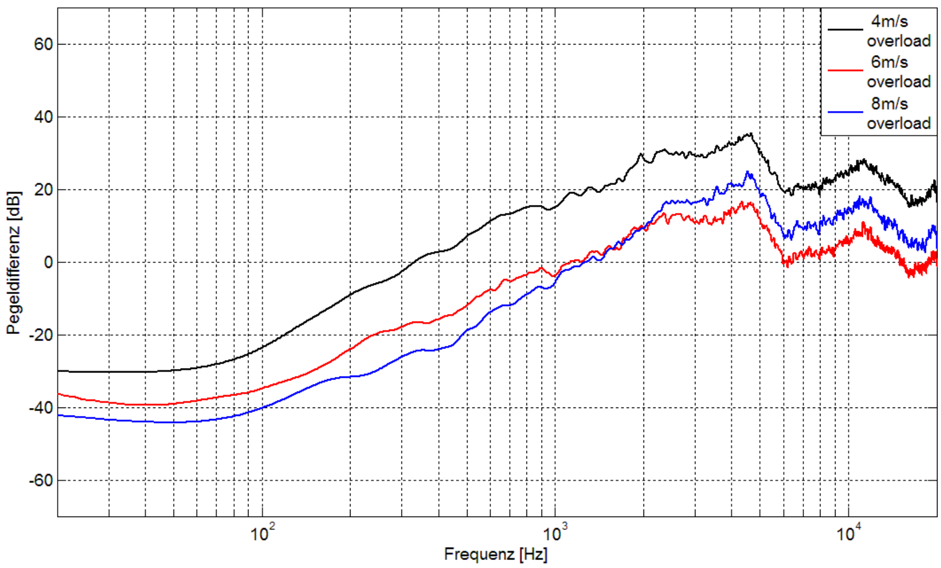

Dynamic of MX75 at 45° wind attack with a "tight-fit" condition

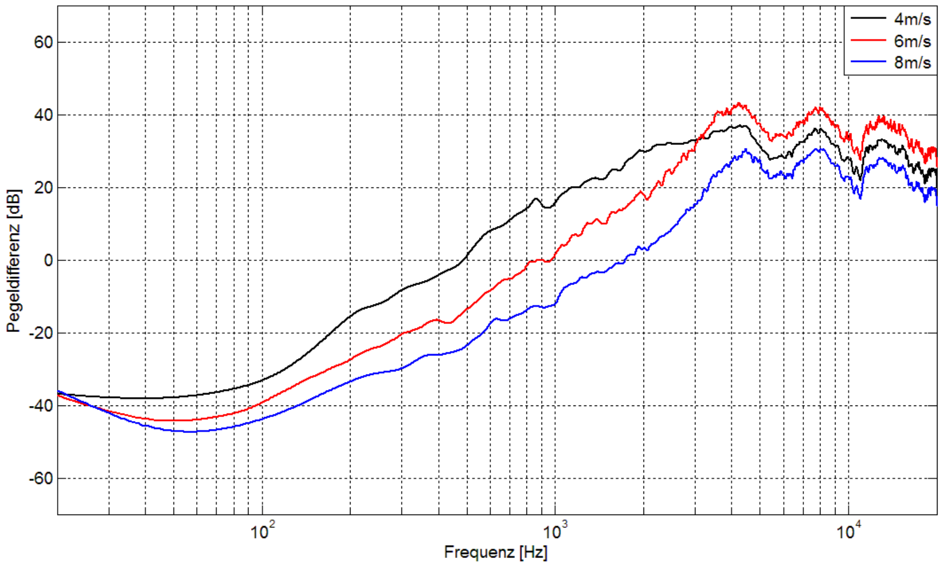

Dynamic of MX260 at 0° wind attack

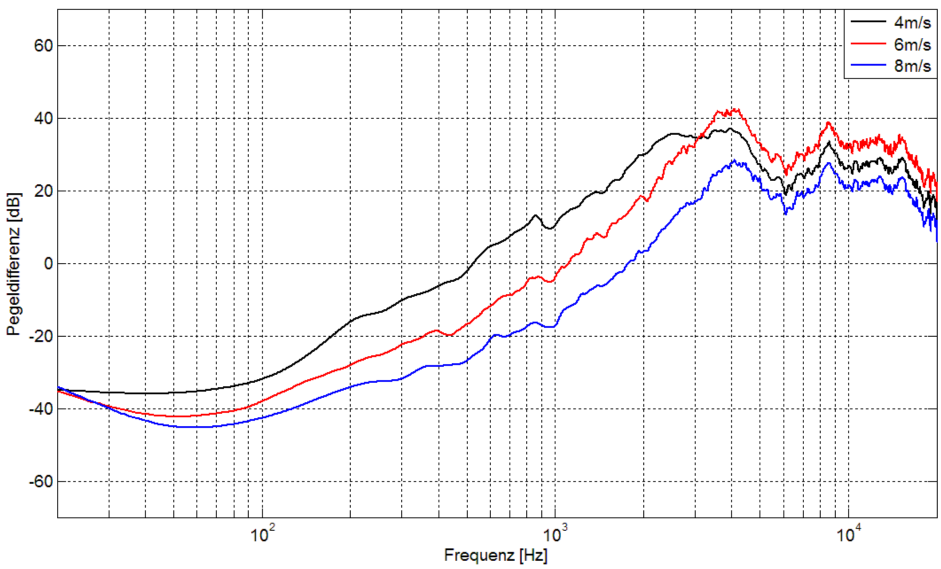

Dynamic of MX260 at 0° wind attack with a "tight-fit" condition

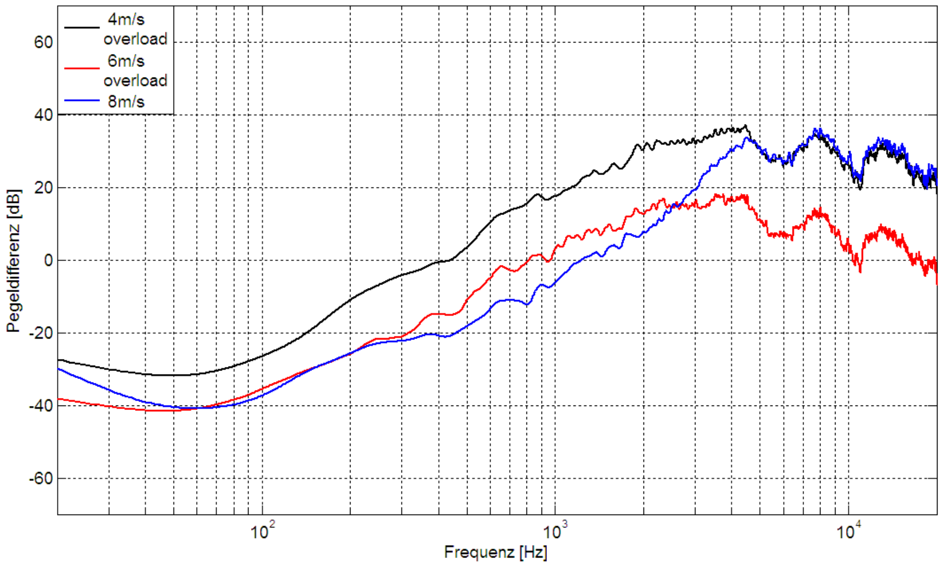

Dynamic of MX260 at 45° wind attack

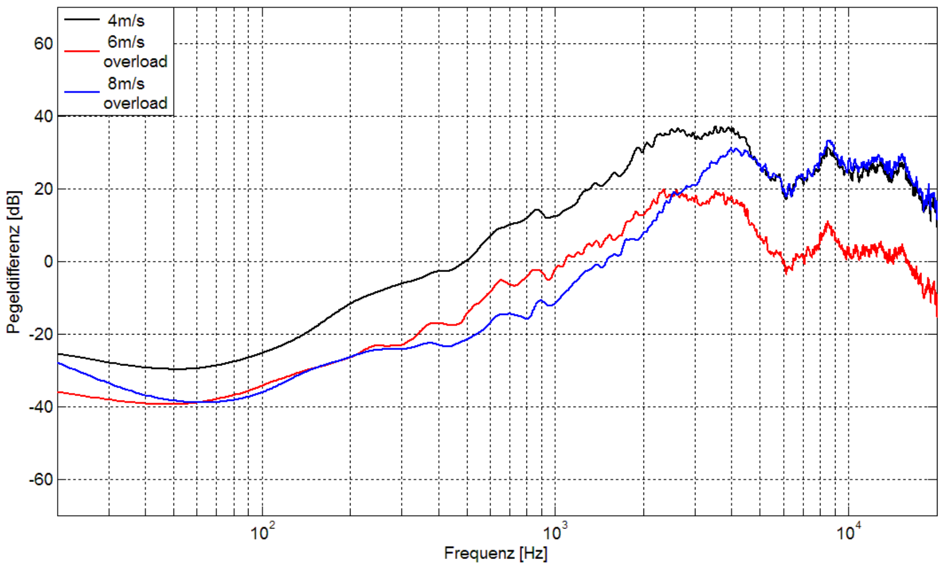

Dynamic of MX260 at 45° wind attack with a "tight-fit" condition

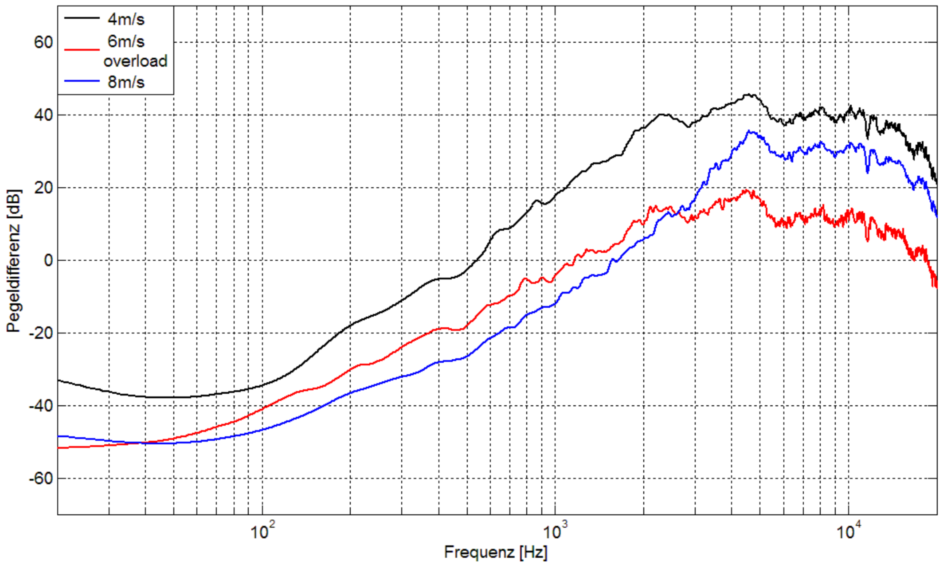

Dynamic of MX660 at 0° wind attack

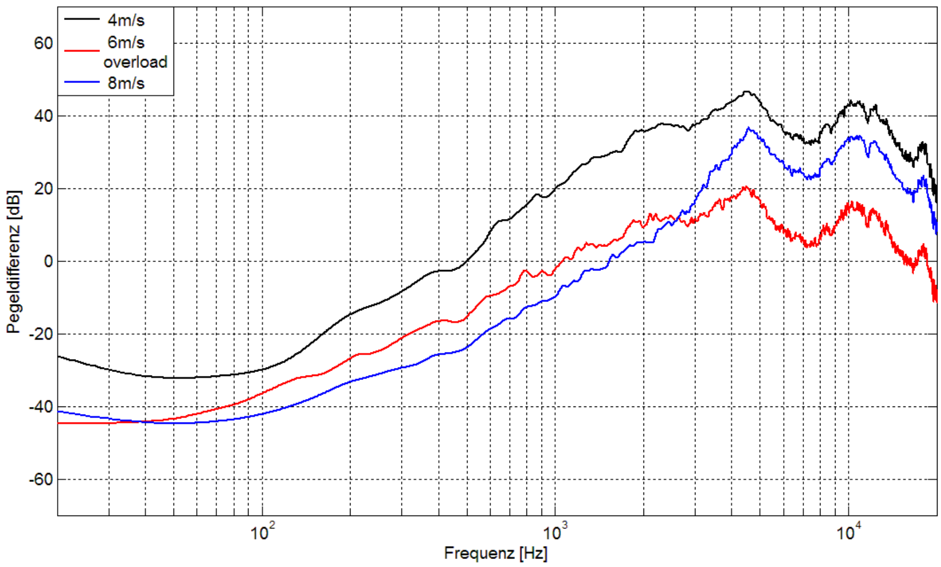

Dynamic of MX660 at 0° wind attack with a "tight-fit" condition

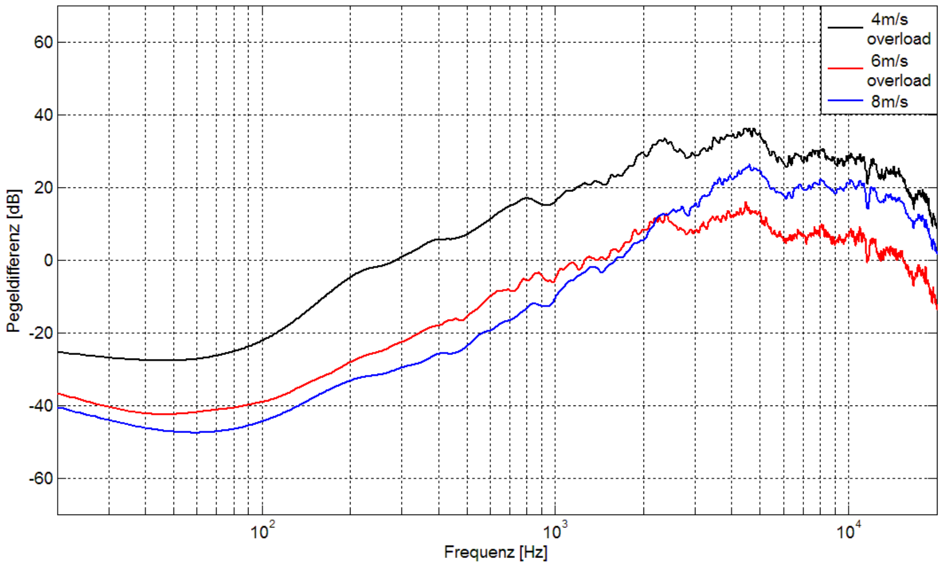

Dynamic of MX660 at 45° wind attack

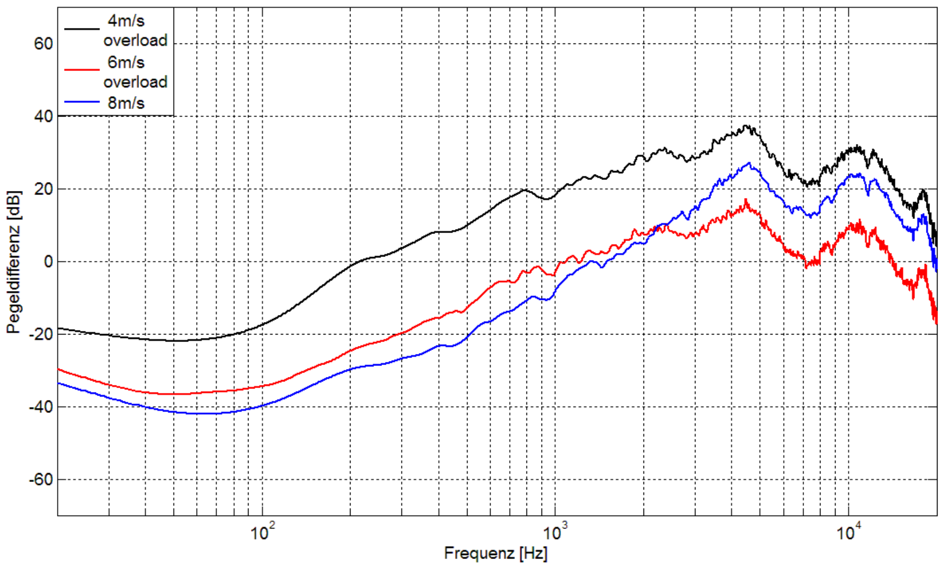

Dynamic of MX660 at 45° wind attack with a "tight-fit" condition

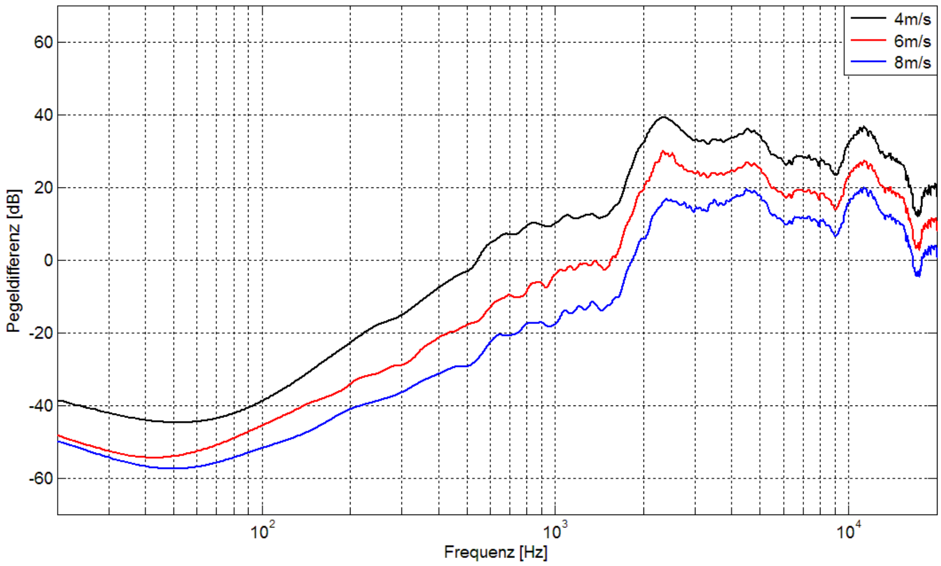

Dynamic of MXL70 at 0° wind attack

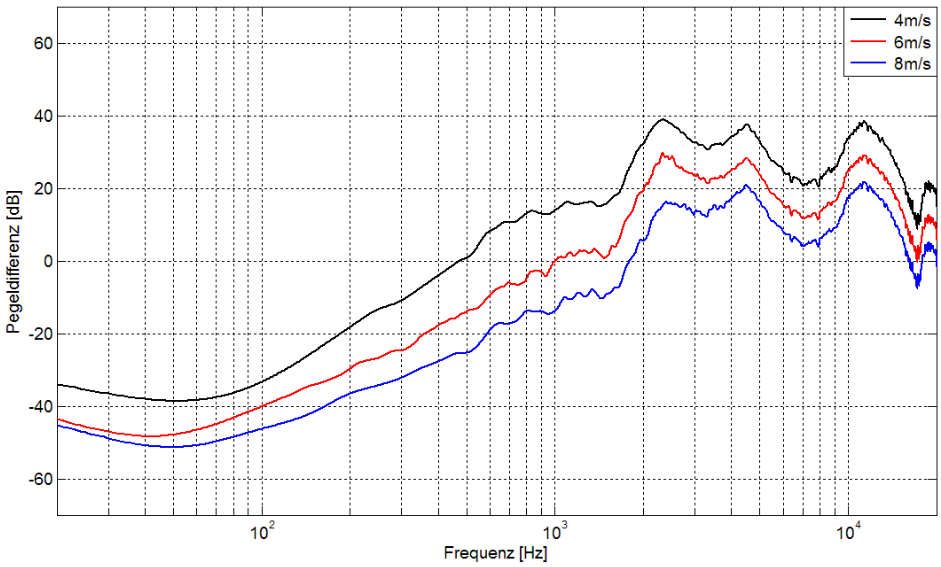

Dynamic of MXL70 at 0° wind attack with a "tight-fit" condition

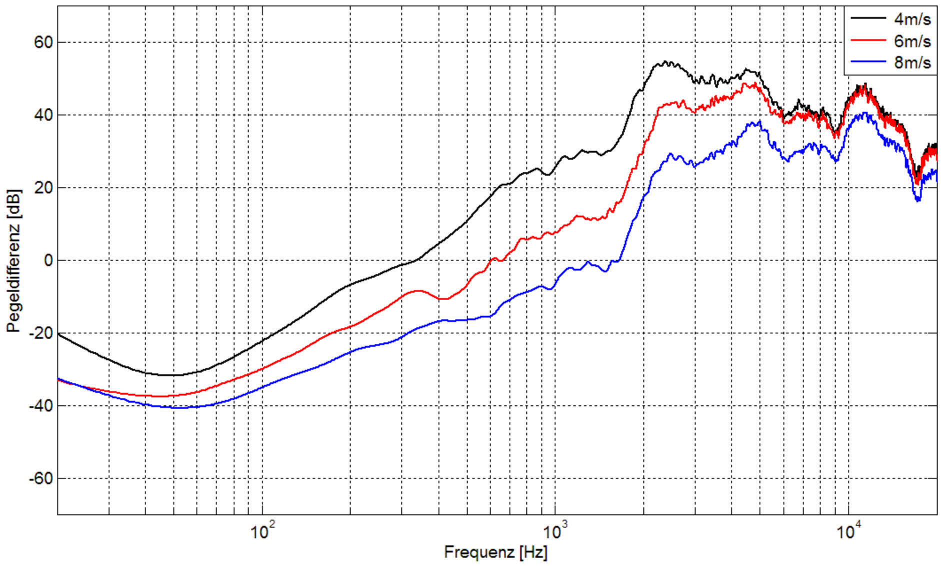

Dynamic of MXL70 at 45° wind attack

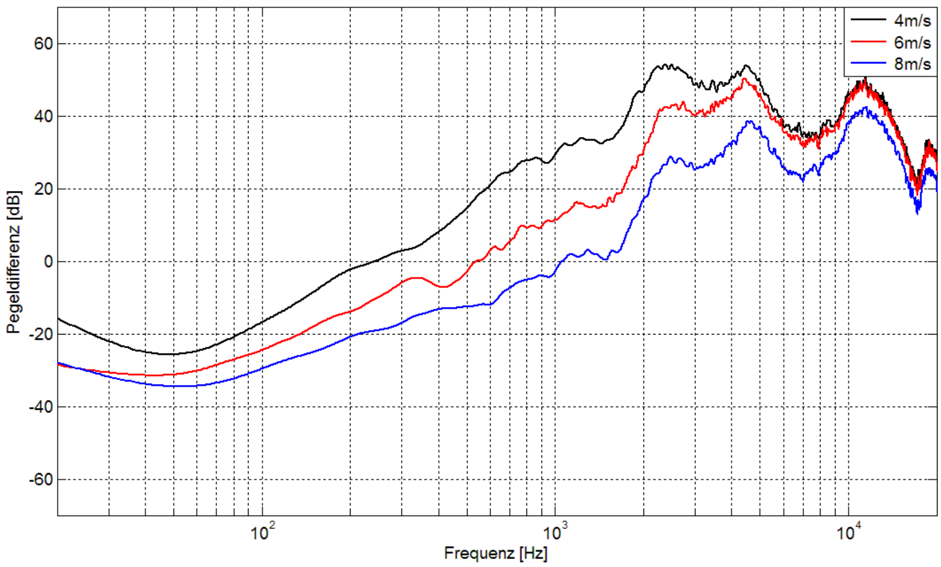

Dynamic of MXL70 at 45° wind attack with a "tight-fit" condition

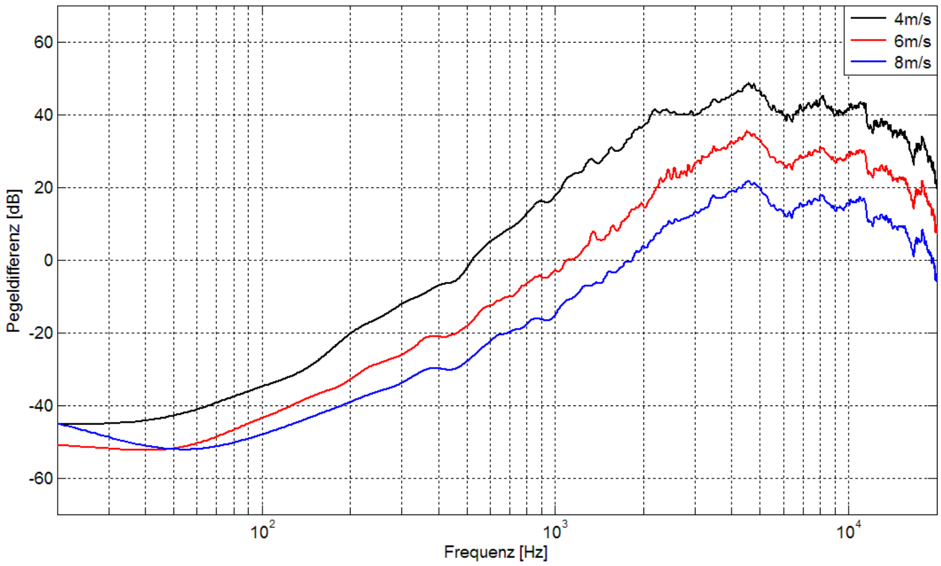

Dynamic of MXL560 at 0° wind attack

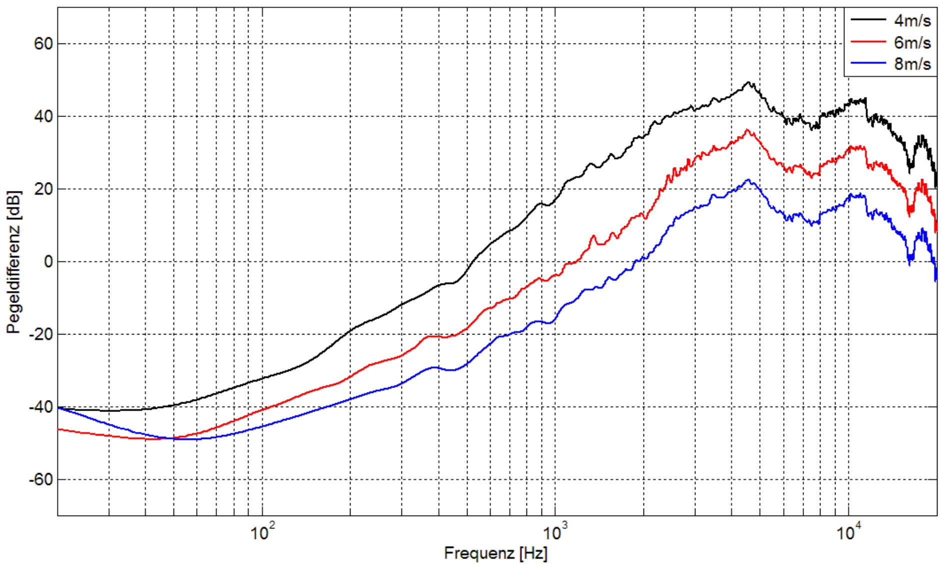

Dynamic of MXL560 at 0° wind attack with a "tight-fit" condition

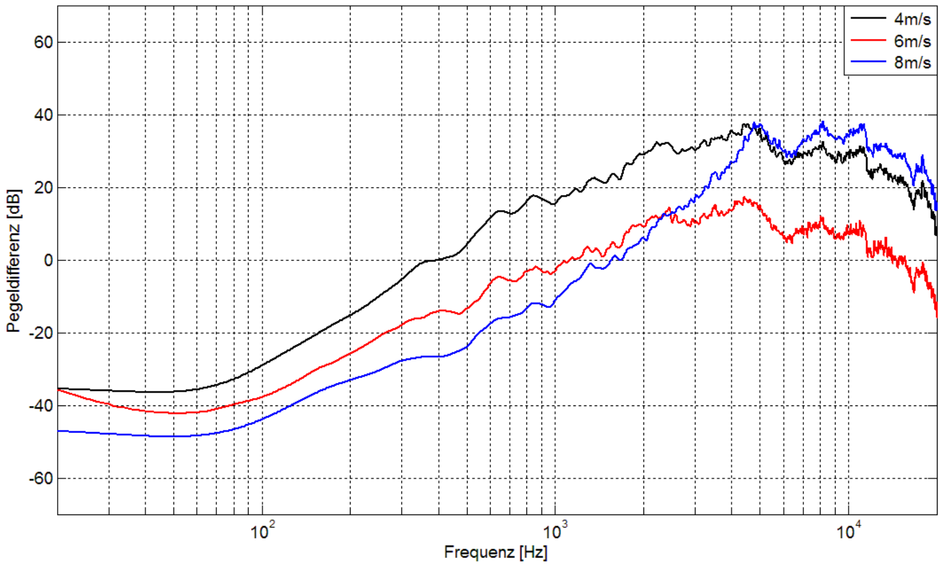

Dynamic of MXL560 at 45° wind attack

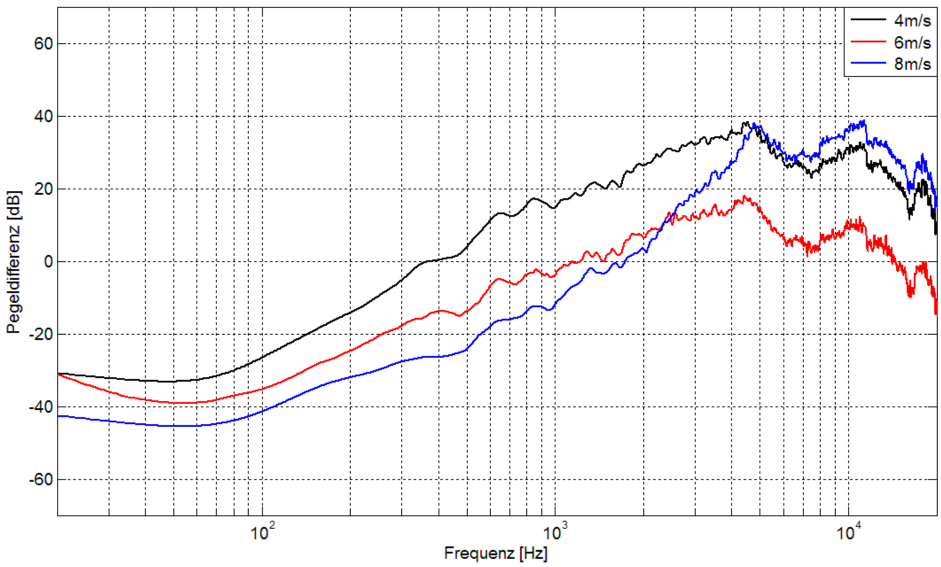

Dynamic of MXL560 at 45° wind attack with a "tight-fit" condition

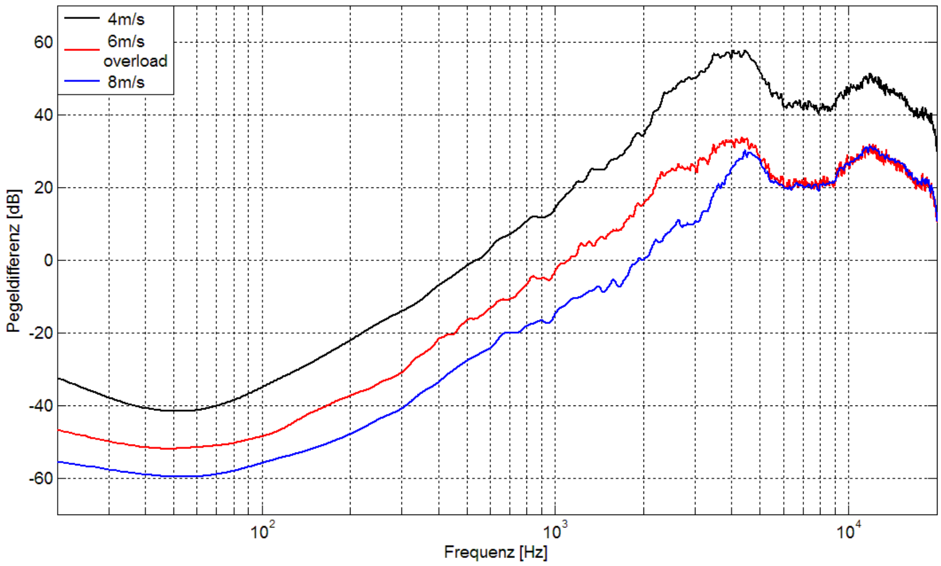

Dynamic of OMX70 at 0° wind attack

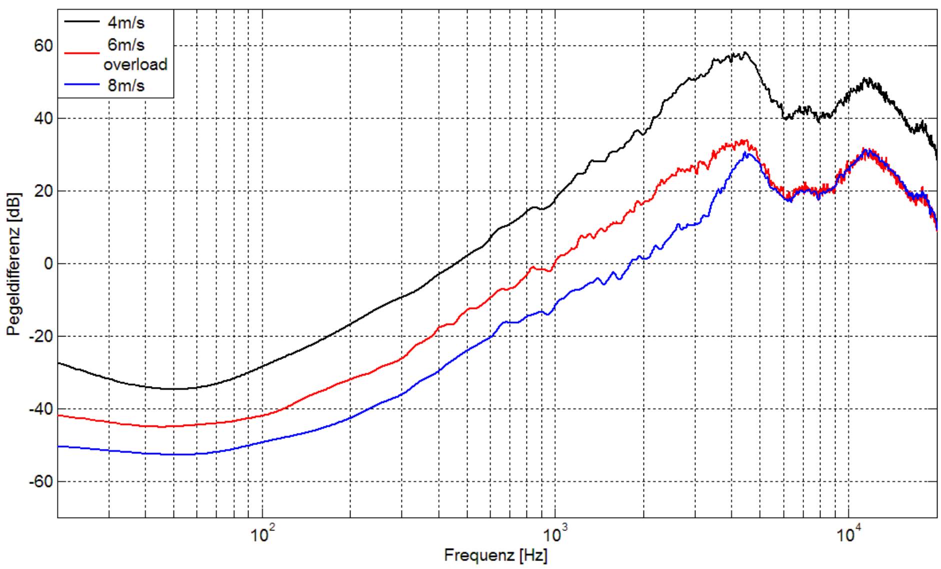

Dynamic of OMX70 at 0° wind attack with a "tight-fit" condition

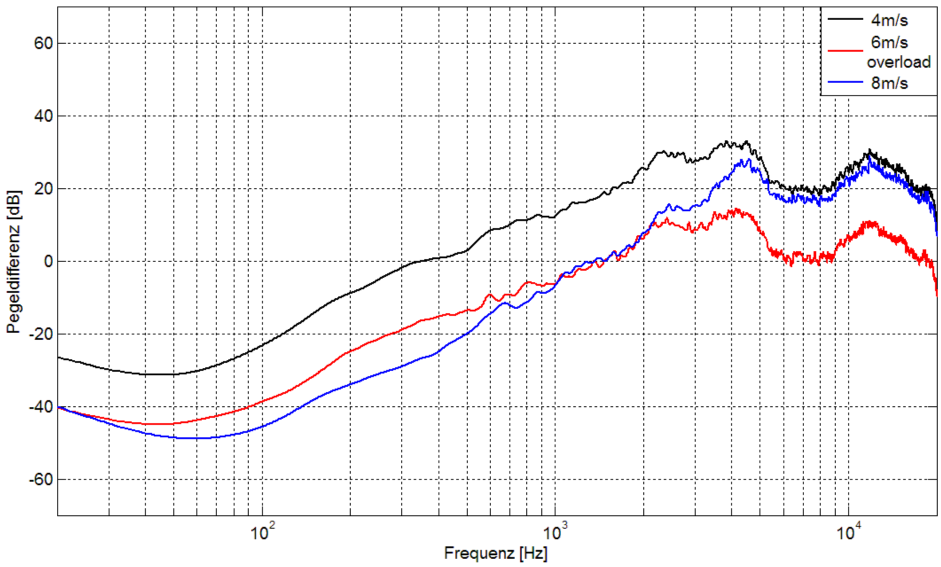

Dynamic of OMX70 at 45° wind attack

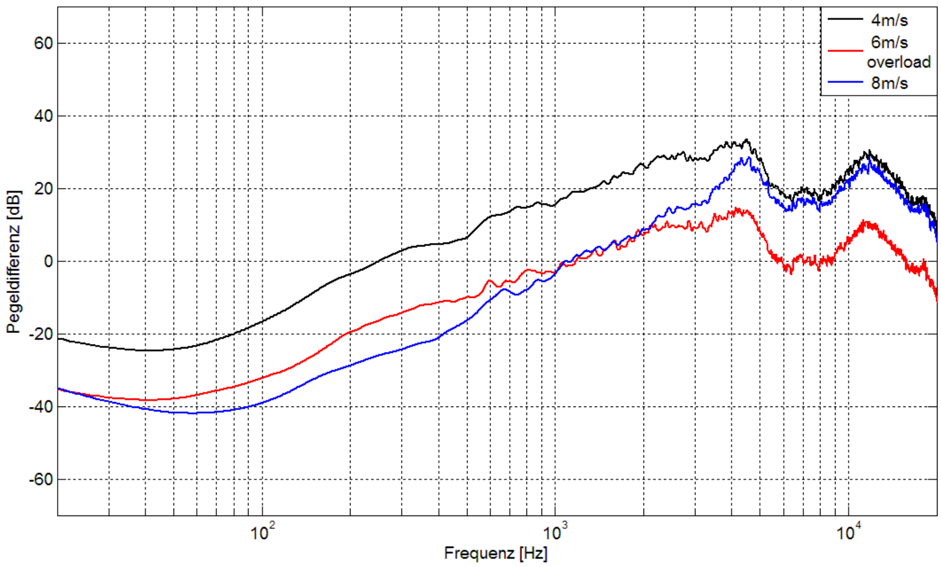

Dynamic of OMX70 at 45° wind attack with a "tight-fit" condition

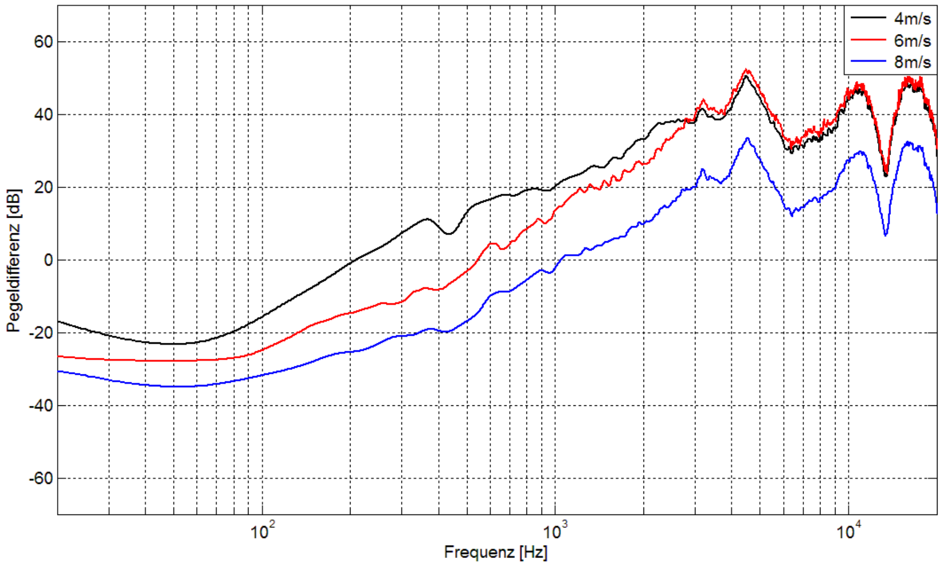

Dynamic of PX100 at 0° wind attack

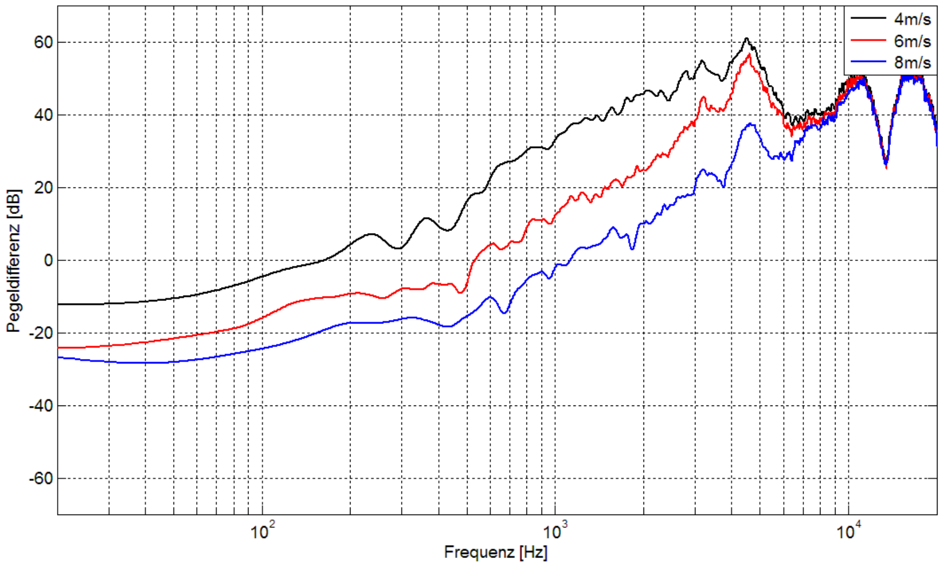

Dynamic of PX100 at 45° wind attack

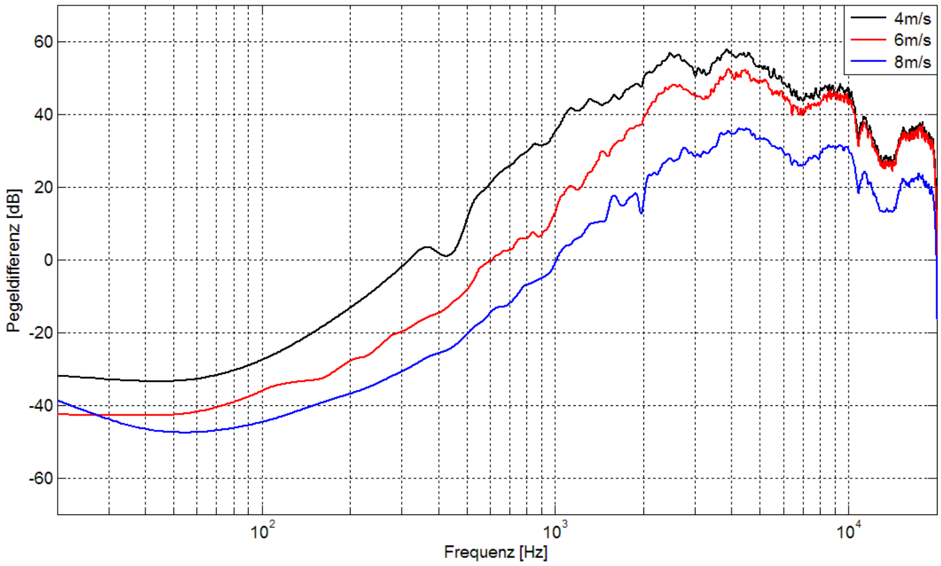

Dynamic of PXC150 at 0° wind attack

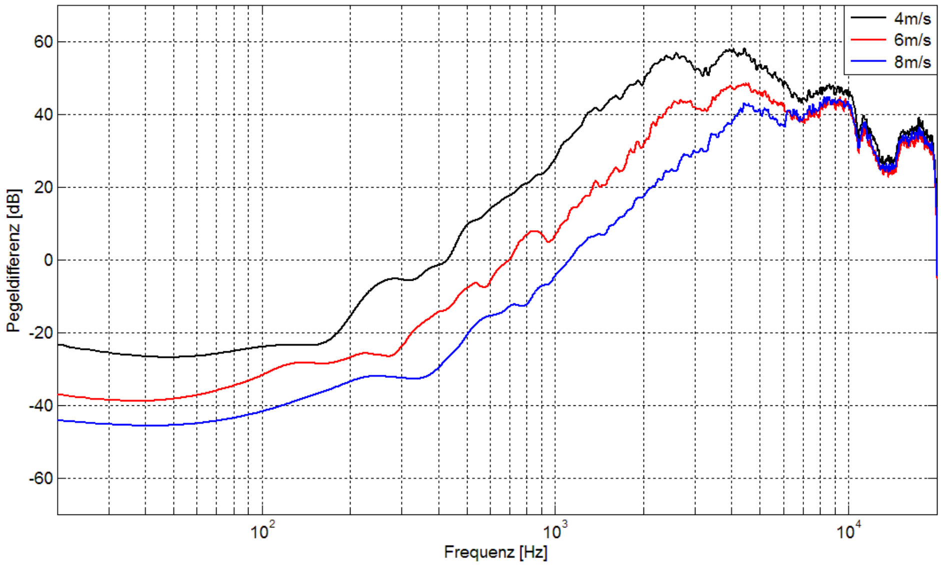

Dynamic of PXC150 at 45° wind attack

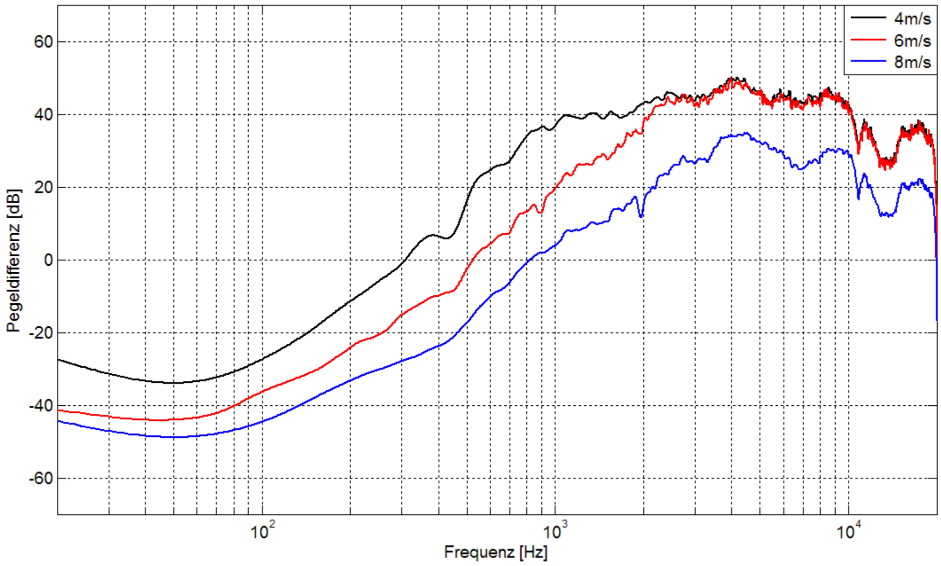

Dynamic of PXC150 with ANC, at 0° wind attack

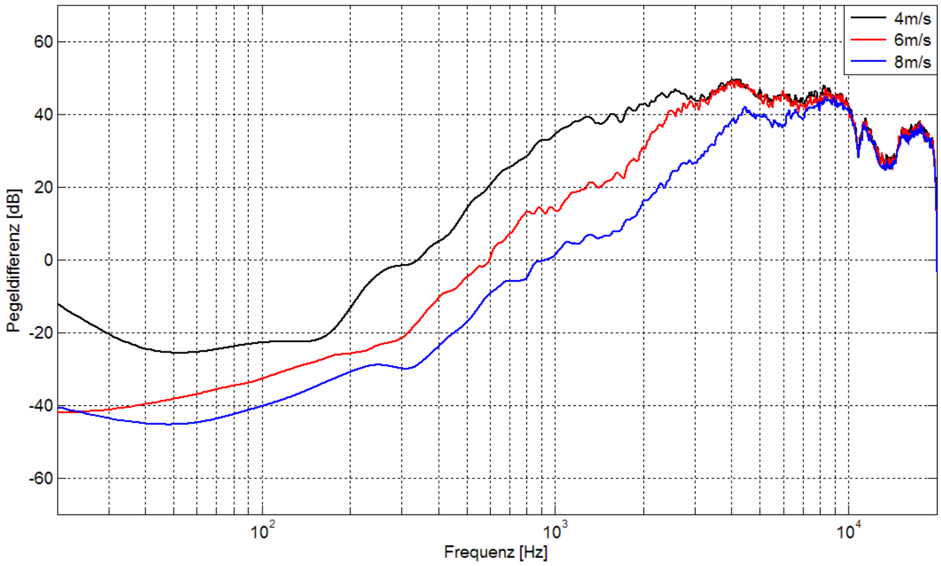

Dynamic of PXC150 with ANC, at 45° wind attack